# IMPROVING THE RELIABILITY OF RWANDA'S ELECTRICITY GRID WITH SOLAR PV MICRO-GRIDS AND BATTERY ENERGY STORAGE SUPPORT

**A THESIS SUBMITTED TO**
**GRADUATE SCHOOL OF NATURAL AND APPLIED SCIENCES**
**OF**
**KOCAELI UNIVERSITY**
**BY**

**OBED NKURIYINGOMA**

**IN PARTIAL FULFILLMENT OF THE REQUIREMENTS**
**FOR**
**THE DEGREE OF DOCTOR OF PHILOSOPHY**
**IN**
**ENERGY SYSTEMS ENGINEERING**

**KOCAELİ 2024**

# IMPROVING THE RELIABILITY OF RWANDA'S ELECTRICITY GRID WITH SOLAR PV MICRO-GRIDS AND BATTERY ENERGY STORAGE SUPPORT

**A THESIS SUBMITTED TO**
**GRADUATE SCHOOL OF NATURAL AND APPLIED SCIENCES**
**OF**
**KOCAELI UNIVERSITY**

**BY**

**OBED NKURIYINGOMA**

**IN PARTIAL FULFILLMENT OF THE REQUIREMENTS**
**FOR**
**THE DEGREE OF DOCTOR OF PHILOSOPHY**
**IN**
**ENERGY SYSTEMS ENGINEERING**

**Prof. Dr. Engin ÖZDEMİR**
**Supervisor, Kocaeli University** ……..

**Asst. Prof. Dr. Serkan SEZEN**
**Jury member, Kocaeli University** ……..

**Asst. Prof. Dr. Mehmet UÇAR**
**Jury member, Düzce University** ……..

**Assoc. Prof. Murat AYAZ**
**Jury member, Kocaeli University** ……..

**Assoc. Prof. Fatih Mehmet NUROĞLU**
**Jury member, Karadeniz Technical University** ……..

**Thesis Defense Date: 15.10.2024**

## ETHICAL STATEMENT AND RESEARCH FUND SUPPORT

In this thesis/project study, which I prepared in accordance with the thesis writing rules of Kocaeli University Graduate School of Natural and Applied Sciences,

I declare that,

- This thesis/project is my own and an original work,
- I act in accordance with scientific ethical principles and rules at all stages of my study, including preparation, data collection, analysis, and presentation of information,
- I have cited all data and information obtained within the scope of this study and that I have included these sources in the bibliography,
- This study complies with the similarity criteria determined by the Graduate School of Natural and Applied Sciences of Kocaeli University in terms of the plagiarism software to which Kocaeli University is subscribed,
- I have not done any falsification of the data used,
- I have not submitted any part of this thesis/project as another thesis/project work at this university or another university.

■ Any stage of this thesis/project work has not been provided any financial/infrastructural support by any institution/organization.

☐ The data and information produced within the scope of this thesis/project work were carried out by ……with the financial/infrastructure support within the scope of the project no of …… .

I declare that I accept all the moral and legal consequences at any time that may arise regarding my work in the event of situation contrary to this statement.

…….....

Obed NKURIYINGOMA

**PUBLISHING AND INTELLECTUAL PROPERTY RIGHTS**

I declare that I have given Kocaeli University the permission to archive all, or any part of my graduate thesis/project approved by the Graduate School of Natural and Applied Sciences, in printed and electronic format, and make it available for use at the conditions specified as follows. Within this permission, all intellectual property rights except for the usage rights granted by Kocaeli University will remain with me and the usage rights of all or a part of my thesis/project in future studies such as articles, books, communiqués, licenses, patents is my own on condition both that the name of my advisor is reserved and within the knowledge of both parties. I declare and undertake that the thesis/project is my own original work, that I have not violated the rights of others and that I am the only authorized owner of my thesis/project. I undertake to use the copyrighted texts in my thesis, which must be used with written permission from their owners, with written permission, and to submit copies of them to the University when requested.

Within the scope of the **"Directive on Collecting, Organizing and Making Access to Graduate Theses in Electronic Environment"** published by the Council of Higher Education (CoHE), my thesis is made available in the CoHE National Thesis Center / Kocaeli University Libraries Open Access System, except for the conditions stated below.

☐ With the decision of the institute board of directors, the opening of my thesis/project to access has been postponed for 2 years from the date of graduation.
☐ With the reasoned decision of the institute board of directors, the opening of my thesis/project to access has been postponed for 6 months from the date of graduation.
■ No confidentiality decision has been made regarding my thesis/project.

……

OBED NKURIYINGOMA

**ACKNOWLEDGEMENTS**

My sincere gratitude and thankful to Almighty God the most gracious. Then, I want to take this opportunity to acknowledge my deep gratitude and appreciation to my advisor, Prof. Dr. Engin ÖZDEMİR, for the unlimited support, direction, feedback, and assistance provided to me throughout my research. Without my advisor, this thesis would not have been possible. Furthermore, I want to express my gratitude to the members of my thesis monitoring committee, Asst. Prof. Dr. Serkan SEZEN and Asst. Prof. Dr. Mehmet UÇAR for their constructive support, comments, and recommendations.

In addition, I am grateful to the staff members of Energy Systems Engineering Department at Kocaeli University for their commitment to academic excellence and their dedication to teaching and research have inspired me to pursue my own scholarly endeavors.

My thankful and appreciation to my parents, my wife, and my beloved children for their unlimited support, understanding, and priceless efforts during my whole life that have gave me a lovely environment and motivations.
I want also to express my appreciation for the great support from the Turkish Government Scholarship Council (YTB).

To all who have contributed to my success, thank you for your invaluable support and contributions.

October - 2024 Obed NKURIYINGOMA

**TABLE OF CONTENTS**

**LIST OF FIGURES**

## LIST OF TABLES

## INDEX OF SYMBOLS AND ABBREVIATIONS

| | |
|---|---|
| ° | : Degree |
| °C | : Degree Celsius |
| $\alpha_T$ | : Absolute Temperature Coefficient |
| $\alpha'_T$ | : Relative Short Circuit Current Temperature Coefficient |
| $\beta_T$ | : Open Circuit Voltage Temperature Coefficient |
| 1/(a*km) | : per Year Kilometer |
| 1/a | : per Year |
| 1/A/a | : per Customer per Year |
| 1/C/a | : per Customer per Year |
| 1/Ca | : per Customer Year |
| A | : Ampere |
| $A_i$ | : Number of Affected Customers for an Interruption at Load Point i |
| A/K | : Ampere per Degree Kelvin |
| V/K | : Volt per Degree Kelvin |
| B | : Exponential Capacity |
| C/a | : Customer per Year |
| Ch/a | : Customer Hour per Year |
| CH4 | : Methane Gas |
| $C_i$ | : Number of Customers Supplied by Load Point i |
| CO2 | : Carbon Dioxide |
| cos φ | : Power Factor |
| $C_p$ | : Polarization Capacitance |
| D | : Diode |
| $E_g$ | : Band Gap Energy |
| eV | : Electron Volt |
| $Fr_{ko}$ | : Frequency of Occurrence of Contingency ko |
| $frac_{i,ko}$ | : Fraction of the Load which Lost at Load Point i, for Contingency ko |
| G | : Solar irradiance |
| h | : Hour |
| h/a | : Hour per Year |
| h/C/a | : Hour per Customer per Year |
| h/Ca | : Hour per Customer Year |
| i | : Load Point Index |
| I | : Current |
| I-V | : Current-Voltage |
| $I_b$ | : Battery Discharging Current |
| $I_{bat}$* | : Battery Reference Current |
| $I_{ph}$ | : Photo Current |
| $I_d$ | : Diode Current |
| $I_{mp}$ | : Maximum Point Current |
| $I_o$ | : Diode Reverse Saturation Current |
| $I_{SC}$ | : Short Circuit Current |
| j | : Element in MCS |
| ko | : Contingency Index |

| | |
|---|---|
| k | : Boltzmann Constant |
| K | : Degree Kelvin |
| km | : Kilometer |
| $Km^2$ | : Square Kilometer |
| kV | : Kilovolt |
| kVA | : Kilovolt Ampere |
| kW | : Kilowatt |
| $kW/m^2$ | : Kilowatt per Square Meter |
| kWh | : Kilowatt Hour |
| kWh/kWp | : Kilowatt Hour per Kilowatt Peak |
| $kWh/m^2$ | : Kilowatt Hour per Square Meter |
| kWh/Year | : Kilowatt Hour per Year |
| kWp | : Kilowatt Peak |
| $L_m$ | : Total Connected Power Interrupted for each Interruption Event |
| $L_T$ | : Total Connected Power Supplied |
| m | : Meter |
| $m^2$ | : Square Meter |
| $m^3$ | : Cubic Meter |
| $m^3/s$ | : Cubic Meter per Second |
| MW | : Megawatt |
| MW/a | : Megawatt per Year |
| MWh | : Megawatt Hour |
| MWh/a | : Megawatt Hour per Yeah |
| MWh/Ca | : Megawatt Hour per Customer Yeah |
| MWp | : Megawatt Peak |
| MWh/Year | : Megawatt Hour per Yeah |
| mΩ | : Milliohms |
| n | : Ideality Factor |
| $N_i$ | : Number of Sample |
| $N_p$ | : Number Parallel Strings |
| $N_s$ | : Number of Cells in Series |
| P | : Power |
| P-V | : Power-Voltage |
| $P_b$ | : Battery Power |
| $pc_i$ | : Contracted Active Power at Load Point i |
| $pd_i$ | : Weighted Average Amount of Power Disconnected at Load Point i |
| $P_L$ | : Power to Load |
| $P_{net}$ | : Net Power |
| $P_{PV}$ | : Power from PV |
| $Pr_{ko}$ | : Probability of Occurrence of Contingency ko |
| $ps_i$ | : Weighted Average Amount of Power Shed at Load Point i |
| q | : Electron Charge |
| Q | : Battery Capacity |
| $R_b$ | : Internal Resistance of Battery |
| RC | : Resistance-Capacitance |
| $r_m$ | : Duration of each Interruption Event |
| $R_o$ | : Circuit Ohmic Resistance |

| | |
|---|---|
| $R_p$ | : Shunt Resistance |
| $R_{po}$ | : Polarization Resistor |
| $R_s$ | : Series Resistance |
| t | : Time |
| T | : Temperature |
| $T_{amb}$ | : Ambient Temperature |
| Tc | : Operating Temperature |
| TWh | : Terawatt Hour |
| US$/kWp | : United State Dollars per Kilowatt Peak |
| US$/kWh | : United State Dollars per Kilowatt Hour |
| V | : Voltage |
| Vex | : Exponential Voltage |
| $V_{mp}$ | : Maximum Point Voltage |
| $V_{OC}$ | : Open Circuit Voltage |
| $V_{po}$ | : Polarization Voltage |
| $V_t$ | : Terminal Voltage |
| W | : Watt |
| $W/m^2$ | : Watt per Square Metter |
| X | : Stochastic Variable |
| y | : Realization in MCS |

**Abbreviations**

| | |
|---|---|
| AC | : Alternating Current |
| ACS | : Addis Centre Substation |
| ACCI | : Average Customer Curtailment Index |
| ACIF | : Average Customer Interruption Frequency |
| ACIT | : Average Customer Interruption Time |
| AID | : Average Interruption Duration |
| AENS | : Average Energy Not Supplied |
| ANN | : Artificial Neural Network |
| ASAI | : Average Service Availability Index |
| ASIDI | : Average System Interruption Duration Index |
| ASIFI | : Average System Interruption Frequency Index |
| ASUI | : Average Service Unavailability Index |
| BDEW | : Bundesverband der Energie- und Wasserwirtschaft (Association of the German Energy and Water Industries) |
| BESS | : Battery Energy Storage System |
| CAIDI | : Customer Average Interruption Duration Index |
| CAIFI | : Customer Average Interruption Frequency Index |
| CSI | : Current Source Inverter |
| DC | : Direct Current |
| DER | : Distributed Energy Resource |
| DG | : Distributed Generation |
| DRC | : Democratic Republic of the Congo |
| ECOST | : Expected Interruption Cost Index |
| EENS | : Expected Energy Not Supplied |

ELP : Estimated Load Profile
EMS : Energy Management System
ESS : Energy Storage Systems
FEA : Failure effect analysis
FLC : Fuzzy Logic Controller
GFL : Grid Following Inverter
GFM : Grid Forming Inverter
HC : Hill Climbing
HLI : Hierarchical Level I
HLII : Hierarchical Level II
HLIII : Hierarchical Level III
HV : High Voltage
IBPS : Inverter-Based Power Sources
IEAR : Interrupted Energy Assessment Rate Index
INC : Incremental Conductance
KCL : Kirchhoff's Current Law
L-COM : Commercial Load
L-IND : Industrial Load
L-RES : Residential Load
L-SIND : Semi-Industrial Load
LP : Load Point
LPENS : Load Point Energy Not Supplied
LPES : Load Point Energy Shed
LPIC : Load Point Interruption Cost
LPIF : Load Point Interruption Frequency
LPIT : Load Point Interruption Time
LV : Low Voltage
MCS : Monte Carlo Simulation
MLD : Maximum Load Demand
MMCS : Modified Monte Carlo Simulation
MG : Microgrid
MPP : Maximum Power Points
MPPT : Maximum Power Point Tracking
MV : Medium Voltage
NOCT : Nominal operating temperature
NST : National Strategy for Transformation
P&O : Perturb and Observe
PCC : Point of Common Coupling
PLL : Phase Locked Loop
PV : Photovoltaics
RBTS : Roy Billinton Test System
RES : Renewable Energy Source
SAIDI : System Average Interruption Duration Index
SAIFI : System Average Interruption Frequency Index
SDG : Sustainable Development Goal
SLP : Standard Load Profile
SOC : State of Charge
STC : Standard Test Condition

| | |
|---|---|
| TCIF | : Total Customer Interruption Frequency |
| TLOC | : Total Loss of Continuity |
| TPCONTIF | : Total Contracted Power Interruption Frequency |
| TPCONTIT | : Total Contracted Power Interruption Time |
| WTG | : Wind Turbine Generator |

## GÜNEŞ FOTOVOLTAİK MİKRO ŞEBEKE VE BATARYA ENERJİ DEPOLAMA DESTEĞİ İLE RUANDA ELEKTRİK ŞEBEKESİNİN GÜVENİLİRLİĞİNİN ARTIRILMASI

## ÖZET

Modern dünyada enerjinin önemi ve ihtiyacı her geçen gün artmaya devam etmektedir. Enerji talebi artışı, enerji güvenilirliği ve sürekliliği zorunluluğunu yer almaktadır. Ancak geleneksel enerji kaynaklarından enerji üretiminin artması, çevresel ve küresel ısınma sorunlarını da arttırmaktadır. Geleneksel enerji kaynakların olumsuz etkilerinin üstesinden gelmek için yenilenebilir enerji kaynakları (YEK) gibi çevre dostu alternatif enerji kaynakları, çevresel faydaları ve bulunabilirlikleri nedeniyle teşvik edilmekte ve kullanılmaktadır. Yenilenebilir enerji kaynaklarından enerji hasadı, enerji sürdürülebilirliğinin çözümlerinden biridir. Ancak YEK'in doğası gereği kesintili olması nedeniyle, batarya enerji depolama sistemleri (BEDS) gibi Enerji Depolama Sistemleri (EDS) kullanılmaktadır. Ayrıca YEK, güç sisteminin güvenilirliğinin arttırılmasına olumlu katkıda bulunur. Diğer bir taraftan, gelişmekte olan ülkelerde özellikle küçük yerleşim bölgelerinde dağıtım şebekelerinin yetersizliği nedeniyle şebekenin sağladığı elektrik enerjisinde sık sık kesintiler yaşanmaktadır. Bu sorun, bölgelerde yaşayan insanların yaşam kalitesini ve verimliliğini olumsuz yönde etkilemektedir. BEDS destekli yenilenebilir enerji kaynaklarının dağıtım sistemine entegre edilmesiyle bu sorunun üstesinden gelinebilir. Özellikle Ruanda'da radyal dağıtım şebekesi için elektrik arzındaki güvenilirliğin iyileştirilmesinde, iletim, dağıtım sistemi de dahil olmak üzere güç sistemi altyapısının düzeltilmesini ve enerji üretim kapasitesinin artırılmasını gerektirmektedir. Bu çalışmada Ruanda elektrik şebekesinin güvenilirliğini artırmak için fotovoltaik sistemleri ve BEDS, Gatumba ve Ntongwe fiderlerine entegre edildi. Yapılan çalışmalardan elde edilen sonuçlar, Ruanda'daki güneş enerjisi potansiyelinin, %86,65'e varan performans oranıyla %64,38'e varan kendi kendine yeterlilik düzeyinde yük sağlama yeteneğine sahip olduğunu göstermiştir. Güneş fotovoltaic sistemi ve BEDS ile entegre edilen besleyicilerde şebeke güvenilirliğini artırmak için, şebekenin devre dışı olduğu durumlarda yük talebinin fotovoltaic sistemi ve BEDS tarafından karşılanmasına olanak tanıyan koruma anahtarları yapılandırılmıştır, böylece enerji talebi karşılanır ve kesinti sıklığı ve süresi azaltılır. DigSILENT ve PV*SOL simülasyon araçlarını kullanarak, elde edilen simülasyon sonuçları, batarya destekli güneş PV sistemler ile güç sistemi güvenilirliğinin, sistem ortalama kesinti sıklığı ve süresi için sırasıyla %71,6 ve %95,5 oranında iyileştiğini göstermektedir.

**Anahtar Kelimeler:** Batarya Enerji Depolama Sistemi (BEDS), DigSILENT PowerFactory, Enerji Güvenilirliği, Güneş PV Sistemi, PV*SOL.

## IMPROVING THE RELIABILITY OF RWANDA'S ELECTRICITY GRID WITH SOLAR PV MICRO-GRIDS AND BATTERY ENERGY STORAGE SUPPORT


## ABSTRACT

The importance and need for energy in the modern world continue to increase daily. This increase in energy demand goes with the necessity of its reliability and continuity of its supply. However, increasing energy use from conventional sources raises environmental and global warming issues. To mitigate the traditional energy sources' negative impacts, environment-friendly renewable energy sources (RES) have been promoted and used due to their environmental benefits and availability. Energy harvesting from RESs plays an essential role toward energy sustainability. To achieve the continuity of energy supply, given the intermittent nature of RES, Energy Storage Systems (ESS) such as Battery Energy Storage Systems (BESS) must be integrated with RESs. Furthermore, integrating RES into power systems has the capability to upgrade the system's reliability. In many developing countries, including small residential areas, the inadequacy of distribution networks often leads to frequent interruptions in grid-supplied electrical energy. This situation significantly impacts the life quality and productivity of the local population. However, this challenge can be addressed by introducing RESs and BESS in the distribution network to ensure a reliable and energy supply continuity. Particularly in Rwanda, for radial distribution network, the reliability improvement in electricity supply requires rectifications of power system infrastructure, including transmission, distribution system, and an increase in energy generation capacity. To assess the influence of RES on Rwanda's electricity grid reliability, solar photovoltaic (PV) systems with BESS are integrated into Gatumba and Ntongwe feeders. The results from conducted studies showed that the potential of solar energy can achieve a level of self-sufficiency of up to 64.38% and a performance ratio of up to 86.65%. To enhance the grid's reliability at the feeders integrated with solar PV system and BESS, protection switches are configured to allow the load demand to be supplied by PV system and BESS when the grid is unavailable thereby supplying the energy demand and reducing interruption frequency and duration. Simulation results from DigSILENT and PV*SOL simulation tools showed that by integrating solar PV systems with BESS to Gatumaba and Ntongwe feeders, the system reliability ameliorates by 71.6% and 95.5% for system average interruption frequency and duration, respectively.



**Keywords:** Battery Energy Storage System (BESS), DigSILENT PowerFactory, Energy Reliability, Solar PV System, PV*SOL.

# 1. INTRODUCTION

The increase in electricity load demand, the expansion of infrastructure, and the integration of new technology into daily life require electricity to be supplied as reliably and uninterruptible as possible. Electricity is generated predominantly from conventional energy sources (fossil fuel and coal). They are exhaustible, and their reserves are being depleted, and cause high levels of environmental pollution. Renewable Energy Sources (RES) provide alternative solutions to the disadvantages associated with conventional energy sources. RES will not run out, and they are replenished continuously. They present enormous environmental benefits, such as little to no greenhouses or pollutant emissions. Being available locally, RES provides solutions to political and regional disputes related to fossil fuels (Ahmad et al., 2020). In recent years, the use of renewable energy sources (RES) such as wind and solar for energy generation has been significantly increased. However, the intermittent nature of RES's remains a critical issue when integrated into the existing grid system.

Solar Photovoltaics (PV) system provides electricity directly from the sunlight. It has several advantages compared to other RES such as availability, flexibility and no moving part involved in the power generation process. To address the intermittent nature of solar energy and to ensure the continuity of energy supply, Battery Energy Storage Systems (BESS) store excess generated energy during peak sunlight hours for use during periods of low or no sunlight. Batteries increase solar PV system reliability and allows the system be more independent (Abdin & Noussan, 2018; Jasuan et al., 2018; Jiang et al., 2021). The PV system integration presents challenges related to generated power prediction, voltage stability, frequency response, reactive power support, power quality, etc. To overcome these challenges, systematical solutions such as grid codes and policies, advanced control, and Energy Storage Systems (ESS) must be developed (Shafiullah et al., 2022). On the other hand, grid-connected solar PV systems are used to enhance the grid's reliability and this is achieved by optimum system sizing and location (Mohamed et al., 2019; Ostovar et al., 2021).

# 2. LITERATURE REVIEW

## 2.1. Rwanda Energy Overview

Rwanda is located in the Eastern African region. It has a total land with surface of 26,338 square kilometers and over 13 million of population. The Rwandan government aims to transform Rwanda from a developing country to a middle-income country by 2035 through the National Strategy for Transformation (NST1). To achieve this goal of access to affordable and clean energy in line with the seventh sustainable development goal (SDG), the government of Rwanda targets universal electricity access by 2024 from 18% in 2014 (J. de D. K. Hakizimana et al., 2016).

### 2.1.1. Electric Power Generation

In Rwanda, electricity is generated from different sources (hydro, methane gas, peat, thermal, and solar). By the end of June 2023, the total installed capacity is 353.4MW. The estimated access rate as of June 2023 is 71.9% (53.6% on-grid and 18.3% off-grid), and the target is to achieve 556MW by 2024 (URL-1). Table 2.1 shows a list of existing power plants for different sources and their respective installed capacity, and Figure 2.1 shows the electricity generation mix (URL-1; E. Hakizimana et al., 2020).

Table 2.1. Rwanda's installed generation capacity as by June 2023

| | Type | Installed Power Capacity (MW) | Generation Mix Percentage |
|---|---|---|---|
| 1 | Hydropower | 109.662 | 31.03% |
| 2 | Peat Fired PP | 85 | 24.05% |
| 3 | Thermal Power | 58.8 | 16.64% |
| 4 | Import | 46.1 | 13.04% |
| 5 | Methane Gas | 29.79 | 8.43% |
| 6 | Solar Power | 12.05 | 3.41% |
| 7 | Shared | 12 | 3.40% |
| 8 | **Total** | **353.402** | **100%** |

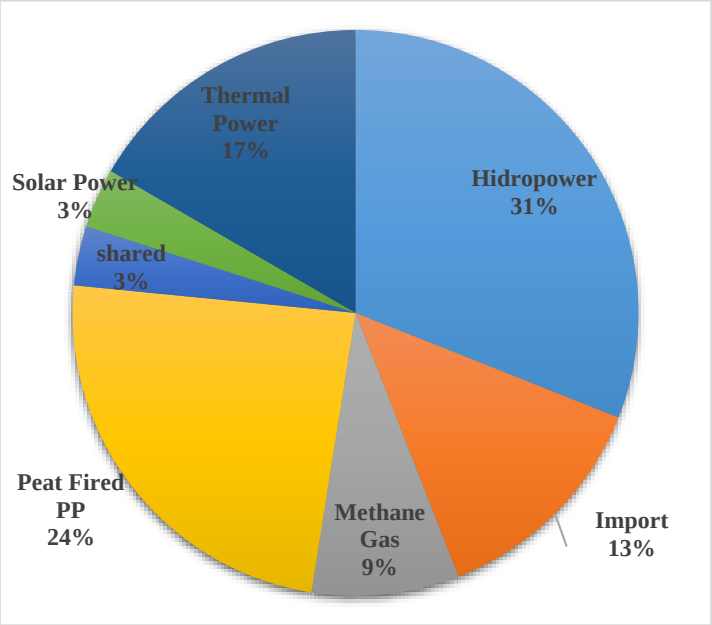


Figure 2.1. Rwanda's electricity generation mix installed capacity

### 2.1.2. Transmission and Distribution Network

The transmission system is composed of high voltage (HV) lines with 220kV, 110kV, and 70kV voltage levels and medium voltage (MV) of 30kV, 15kV, 17.32kV, and 5.5kV voltage levels. By the end of June 2023, the length of HV transmission lines was about 1158km, and other transmission projects were in progress. For region interconnection purposes, 220kV transmission lines are used. Rwanda's electricity network is interconnected with Uganda in the north, Burundi in the south, and Democratic Republic of the Congo (DRC) in the west (Bimenyimana et al., 2018; URL-1). In total, 33 substations around the country are operational for HV to MV power transformation. The electricity is distributed at MV and low voltage (LV). The distribution network is covered by 10,520km of MV and 18,465.7km of LV distribution lines (URL-2).

### 2.1.3. Energy Resources and Potentials

Energy resource identification is the first step in energy supply services. The availability of energy resources and their corresponding potentials for a particular country plays a significant role in sustainable, affordable, and accessible energy services. Rwanda's most dominant natural energy resources are water, solar radiation, methane gas, geothermal, and peat reserves (Gasore et al., 2021; E. Hakizimana et al., 2020).

Solar Energy

Rwanda's geographical location is well-suited for solar energy production and utilization, with the solar irradiation intensity ranging from 4 to 5.4kWh/m² and about 5 hours of peak sun per day, as illustrated in Figure 2.2. The estimated total annual solar energy potential is estimated to be 66.8TWh. Daily practical PV output potential between 3.7 and 4.29kWh/kWp. Currently, there are three grid-connected solar PV plants with a combined installed capacity of 12.05MW, accounting for 3.41% of the total electricity production (E. Hakizimana et al., 2020).

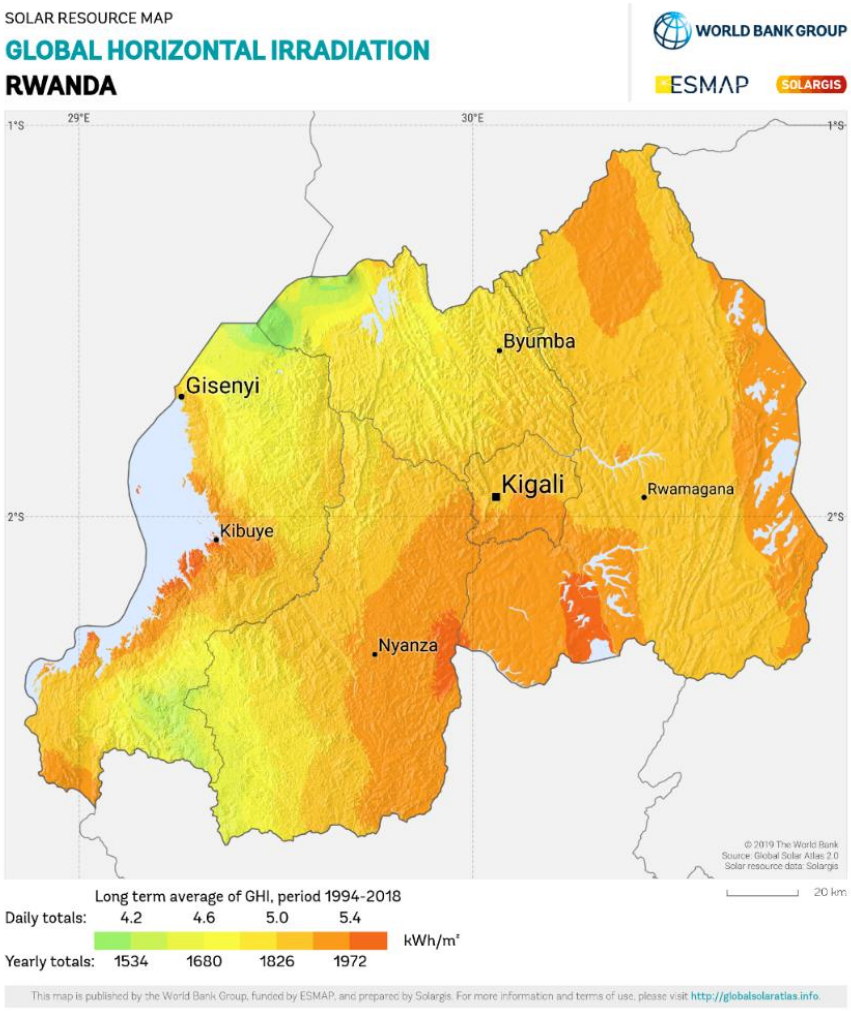


Figure 2.2. Rwanda global solar irradiation

## Hydropower

Hydropower exploits the energy from water's gravitational force and movement, known as potential and kinetic energy, to generate electricity. Hydropower resources can be used for electricity generation or other purposes such as irrigation, freshwater supply, flood control, and recreation. In Rwanda, the hydropower resources are primarily composed of rivers with flow rates that are relatively low ($0.05m^3/s$ to $7.14m^3/s$ in the rainseason) and limited storage capacity which potentials depend on the available hydrological fluctuations of the site. Currently, 333 potential sites for hydropower have been identified, and the majority have a potential generation capacity below 5MW (Ituze et al., 2017).

## Geothermal Energy

The geothermal resources in Rwanda, categorized into four main prospect areas, Karisimbi, Kinigi, Gisenyi and Bugarama, are all within the belt along Lake Kivu. These areas are associated with volcanoes in the western and with earthquakes in the southwestern regions. Exploration studies have estimated that the geothermal potential for electricity generation could contribute 300MW for long term and 20MW for short term. However, the resource's precise size has yet to be confirmed, highlighting the need for further research and determination after the exploratory drilling is completed. From the available information, it is evident that Rwanda possesses regions with low-temperature geothermal resources suitable for producing electricity and for direct industrial purposes (URL-3).

## Methane Gas

Methane gas is present in Lake Kivu, which is situated between Rwanda and the Democratic Republic of the Congo (DRC) in the Eastern African Rift Zone. Both countries equally share the resources. The lake, which covers an area $2,400km^2$, holds significant amounts of methane (CH4) and carbon dioxide (CO2) gases that are naturally occurred with a capacity estimated at 55 billion $m^3$ and 300 billion $m^3$, respectively; and around 70% are economically exploitable. The gases are most concentrated at depths between 270 meters and 500 meters. Rwanda began using this resource for methane-to-power electricity generation projects, other industrial uses, and fertilizer applications

(URL-3). The methane gas in Lake Kivu has the power generation potential of 700MW for around 55 years, providing a sustainable energy source for the region. Rwanda's potential electricity generation capacity from methane gas is estimated at around 350MW, while the rest belongs to the DRC (Bolson et al., 2021).

Peat Energy

Rwanda recently completed a research on its peat reserves, indicating that the peat bogs in the country cover 50,000 hectares in total and hold dry peat of approximately 155 million tons. The research found that approximately 77% of these peat deposits are located close to the Nyabarongo and Akanyaru rivers, and in the Rwabusoro Plains. Additionally, the study highlighted the electricity generation potential from these peat reserves to be estimated at 150MW by using sod peat application and 117MW with milled peat application over a 30-year operational period. Currently, Rwanda has two peat-to-power projects in progress: The Gishoma peat-to-power project in the Rusizi district and the Hakan project in the Gisagara district. These projects aim to develop 15MW and 80MW of power, respectively (Bolson et al., 2021; J. de D. K. Hakizimana et al., 2016; URL-3).

## 2.2. Electricity Grid Reliability Assessment

System reliability is composed of two important elements: system security and system adequacy. System adequacy ensures that the system can meet customers' energy needs by maintaining sufficient infrastructure for distribution, transmission, and generation. On the other hand, system security guarantees the system's capability to manage disturbances and maintain quality and power supply continuity. (Gautam, 2018). These two elements are the backbone of a power system’s reliability, that defines its capacity to meet peak demand, adapt to demand and generation fluctuations, and maintain stable frequency and voltage within acceptable limits across the network (URL-4). The system's reliability is determined by factors such electric interruptions frequency (including customers and connected loads), interrupted power, and duration of the interruptions (Wadi, 2017). Improving the reliability of a system involves reducing one or all of these factors.

The reliability evaluation is realized at different operational parts of a power system known as hierarchical levels, as presented in Figure 2.3. Hierarchical level I (HLI) assesses the sufficiency of generation facilities and is called ‘‘reliability evaluation for generation capacity’’. Hierarchical level II (HLII) assesses both transmission and generation facilities and is called ‘‘composite system or bulk system reliability evaluation’’. Hierarchical level III (HLIII) assesses all three parts of the operations of a power system and evaluates the individual load point levels reliability (Gautam, 2018; Heidari, 2015).

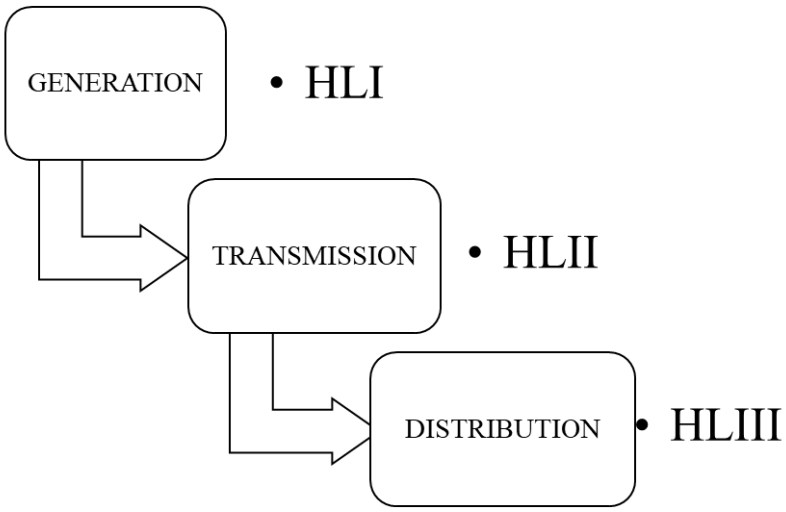


Figure 2.3. Parts of operation of power system and reliability assessment hierarchical levels

## 2.3. Reliability Indices

The reliability indices are classified as load points (LP) or system-level indices. The evaluation of reliability of a power system consists of determining the load interruption within an operating period. A bus bar, terminal, or load can be defined as a load point. The load point reliability indices indicate the reliability of the power system at each load point and are necessary to evaluate the weak points in the system. On the other hand, system indices are a combination of all load point indices. Furthermore, reliability indices are separated by frequency or expectance, energy, and interruption costs indices. Each category offers distinct insights into different aspects of the system's reliability, providing a comprehensive understanding of its performance.

### 2.3.1. Load Point Reliability Indices

The reliability indices at load points are defined by the following parameters: Average Customer Interruption Time (ACIT), Average Customer Interruption Frequency (ACIF), Load Point Interruption Time (LPIT), Load Point Interruption Frequency (LPIF), Load Average Interruption Duration (AID), Load Point Interruption Costs (LPIC), Total Customer Interruption Frequency (TCIF), Total Contracted Power Interruption Time (TPCONTIT), Total Contracted Power Interruption Frequency (TPCONTIF), Load Point Energy Shed (LPES), and Load Point Energy Not Supplied (LPENS). The expressions for Load Point Reliability Indices are as Equation (2.1) to (2.12)

$$\mathrm{ACIF_i} = \sum_{\mathrm{ko}} \mathrm{Fr_{ko}} \,.\, \mathrm{frac_{i,ko}} \quad \text{Unit: } {}^{1}/_{\mathrm{a}} \tag{2.1}$$

$$ACIT_i = \sum_{ko} 8760 \,.\, Pr_{ko} \,.\, frac_{i,ko} \quad Unit: {}^{h}/_{a} \tag{2.2}$$

$$ACIT_i = \sum_{ko} 8760 \,.\, Pr_{ko} \,.\, frac_{i,ko} \quad Unit: {}^{h}/_{a} \tag{2.3}$$

$$LPIF_i = \sum_{ko} Fr_{ko} \quad Unit: {}^{1}/_{a} \tag{2.4}$$

$$LPIT_i = \sum_{ko} 8760 \,.\, Pr_{ko} \quad Unit: {}^{h}/_{a} \tag{2.5}$$

$$AID_i = \frac{ACIT_i}{ACIF_i} \quad Unit: h \tag{2.6}$$

$$TCIF_i = ACIF_i \,.\, C_i \quad Unit: {}^{C}/_{a} \tag{2.7}$$

$$TCIT_i = ACIT_i \,.\, C_i \quad Unit: {}^{Ch}/_{a} \tag{2.8}$$

$$TPCONTIF_i = \sum_{ko} 8760 \,.\, Fr_{ko} \,.\, frac_{i,ko} \,.\, Pc_i \quad Unit: {}^{MW}/_{a} \tag{2.9}$$

$$TPCONTIT_i = \sum_{ko} 8760 \,.\, Pr_{ko} \,.\, frac_{i,ko} \,.\, Pc_i \quad Unit: {}^{MWh}/_{a} \tag{2.10}$$

$$LPENS_i = ACIT_i \,.\, (pd_i + ps_i) \quad Unit: {}^{MWh}/_{a} \tag{2.11}$$

$$LPES_i = ACIT_i \,.\, ps_i \quad Unit: {}^{MWh}/_{a} \tag{2.12}$$

Where:

$i$ is the load point index.

$ko$ is the contingency index

$C_i$ is the number of customers supplied by load point $i$.

$Fr_{ko}$ is the frequency of occurrence of contingency $ko$.

$Pr_{ko}$ is the probability of occurrence of contingency $ko$.

$frac_{i,ko}$ is the fraction of the load which is lost at load point $i$, for contingency $k$.

For unsupplied loads, or for loads that are shed completely, $frac_{i,ko} = 1.0$.

For loads that are partially shed, $0.0 \leq frac_{i,ko} < 1.0$.

$Pc_i$ is the contracted active power at load point *i*.

$Pd_i$ is the weighted average amount of power disconnected at load point *i*.

$Ps_i$ is the weighted average amount of power shed at load point *i*.

### 2.3.2. System Reliability Indices

The System Average Interruption Frequency Index (SAIFI) that measures how repeatedly power interruptions are experienced by the customers over a defined period of time. The Customer Average Interruption Frequency Index (CAIFI) indicates the average frequency of interruptions experienced by affected customers. The Average System Interruption Frequency Index (ASIFI) is based on load rather than the number of customers affected, revealing the distribution performance for systems serving industrial or commercial customers. The System Average Interruption Duration Index (SAIDI) shows the total interruption duration experienced by customers during a specified period. The Customer Average Interruption Duration Index (CAIDI) is a metric that calculates the average time needed to reinstate service for customers. The Average System Interruption Duration Index (ASIDI) indicates the total duration of interruptions based on load during a specified period. The Average Service Availability Index (ASAI) represents the fraction of time that customers remain connected during a specified period. Average Service Unavailability Index (ASUI) shows the probability of all loads being supplied. Lastly the Energy Not Supplied (ENS), the Average Energy Not Supplied (AENS), and the Average Customer Curtailment Index (ACCI) are the indices related to the amount of energy not supplied. The expressions for System Reliability Indices are as Equation (2.13) to (2.23)

$$SAIFI = \frac{\sum ACIF_i . C_i}{\sum C_i} \quad Unit: {}^{1}/_{C/a} \tag{2.13}$$

$$CAIFI = \frac{\sum ACIF_i . C_i}{\sum A_i} \quad Unit: {}^{1}/_{A/a} \tag{2.14}$$

$$SAIDI = \frac{\sum ACIT_i . C_i}{\sum C_i} \quad Unit: {}^{h}/_{C/a} \tag{2.15}$$

$$CAIDI = \frac{SAIDI}{SAIFI} \quad Unit: h \tag{2.16}$$

$$ASUI = \frac{\sum ACIT_i . C_i}{8760 . \sum C_i} \tag{2.17}$$

$$ASAI = 1 - ASUI \quad (2.18)$$

$$ASIDI = \frac{\sum(r_{m} * L_{m})}{L_T} \quad Unit: {}^{h}/_{a} \quad (2.19)$$

$$ASIFI = \frac{\sum L_m}{L_T} \quad Unit: {}^{1}/_{a} \quad (2.20)$$

$$ENS = \sum LPENS_i \quad Unit: {}^{MWh}/_{a} \quad (2.21)$$

$$AENS = \frac{ENS}{\sum C_i} \quad Unit: {}^{MWh}/_{Ca} \quad (2.22)$$

$$ACCI = \frac{ENS}{\sum A_i} \quad Unit: {}^{MWh}/_{Ca} \quad (2.23)$$

Where:

$C_i$ is the number of customers supplied by load point *i*.

$A_i$ is the Number of affected customers for an interruption at load point *i*.

*A* is the number of affected customers.

*C* is the number of customers.

$L_m$ is the total connected power interrupted, for each interruption event.

*LT* is the total connected power supplied.

$R_m$ is the duration of each interruption event.

## 2.4. Review of Related Studies

Exploring the assessment of power system reliability has been a focal point in literature, with numerous research studies employing diverse methods and algorithms. These studies frequently utilized specialized programs or software to facilitate their analyses.

(Wadi, 2017) evaluated the dependability of a closed-loop distribution system by employing an analytical approach that relied on the Modified Monte Carlo Simulation (MMCS) and Total Loss of Continuity (TLOC) method. The study indicates that the distribution network cover over 80% of operational failures in a power system. As a result, there is a significant focus on assessing and improving the distribution network reliability. The study compared the effectiveness of two new techniques for assessing the reliability of a distribution system in Istanbul, Turkey. These techniques were tested using actual data provided by the Bosphorus Electric Distribution Company and were compared with the results obtained through Monte Carlo Simulation (MCS) method. The comparison revealed the practicality and adaptability of the two new techniques based on their results.

(Saeedi, 2016) studied the effects on the reliability of distribution system by integration of distributed generations (DG). To meet the growing needs of customers, utility companies are advised to enhance both non-renewable and renewable distributed generations (DGs). The study uses the MCS algorithm to evaluate the reliability of a distribution network incorporating distributed generators with battery storage systems. The reliability indices used for evaluation were Expected Energy Not Supplied (EENS), SAIFI, and SAIDI. The simulation consisted of two distinct phases. The first phase consisted of the distribution network reliability assessment in the absence of DGs. The second phase involved an evaluation of network reliability by considering the integration of DGs. Thus, reliability improvement was observed by inserting DGs into the network.

(Gautam, 2018) conducted reliability studies on distribution system incorporated with energy storage. ESS possess potential solutions to address system reliability for RES utilization in distribution network integrated with DGs. In this work, by using MCS algorithm, a novel reliability model for ESS to integrate developed ESS with DGs and time-dependent load were presented.

(Heidari, 2015) examined the dependability of the power distribution system when DG units are present. The presence of DGs can enhance network reliability by decreasing the frequency and length of outages, although this is contingent on the operating mode. Therefore, the islanding mode of operation of DGs presents a solution to reduce the frequency of interruption of selected loads. In this work, a new sub-islanding approach based on two algorithms that detect exact location of DG units and to identify fault location, a mixed-integer sectionalizing switches optimal placement linear programming model, and a new mixed-integer sectionalizing and protective switches optimum number and location nonlinear programing model are presented. Finally, a contingency-based analytical technique for reliability assessment is adopted.

(Teshome, 2016) presented a study on DG in improving power system reliability at Addis Centre Substation (ACS). The main causes of reliability problems at the ACS substation and a solution for improving them were investigated and proposed. In this study, Power Factory simulations for reliability assessment, before and after integrating DGs in the system, were conducted. The proposed solutions showed the capability of improving reliability at the ACS substation.

(Koyi, 2019) studied the improvement of the reliability of electricity grid with introduction of renewable microgrids (MG) in Nigeria. In the study, Nigeria's grid was modelled in Power Factory and different scenarios to increase electricity availability were studied by connecting DGs and ESS to the appropriate position to meet the load demand.

(Adefarati & Bansal, 2017b) conducted a study on reliability assessment of distribution systems integrated with renewable DG. The study's objectives were to reduce the expected interruption cost index (ECOST) and minimize the EENS. As results, SAIFI index was improved by 16.46%, while SAIDI index showed an 11.22% improvement. Also, CAIDI exhibited a 6.24% increase, and the average energy not supplied (AENS) improved by 12.5%. Additionally, the system interrupted energy assessment rate index (IEAR) experienced a 2.43% enhancement, while the EENS and ECOST indices realized improvements of 11.97% and 9.84%, respectively.

The introduction of DGs, mostly solar PV and wind sources, into a power system changed the single power flow into a bidirectional power flow. DGs also contribute to the power systems' reliability by outages number reduction in radial systems and by increasing generation capacity. Many studies have presented the contribution of DGs to improving the reliability of electric power systems. (Adefarati & Bansal, 2017a) studied the economic and reliability assessment of a power system integrated with RES based MGs. In the study, wind turbine generators (WTG), PV, and BESS were used as DGs. (Harker Steele et al., 2021) studied the effects of variable energy resources on the reliability of power system. (Dadfar et al., 2017) studied the reliability evaluation of a 20kW solar power station in grid-connected mode. (Wei et al., 2011) studied the reliability evaluation of MG with PV and WTG hybrid systems.

Numerous methods for assessing and evaluating reliability have been developed and utilized in various research studies to serve specific purposes. Such methods are markov model (Adefarati & Bansal, 2017a, 2017b; Gautam, 2018; W. Li et al., 2014; Teshome, 2016; Wu et al., 2017), Monte Carlo simulation (MCS) (Ali Kadhem et al., 2017; Dongmei et al., 2014; Guo-hua et al., 2011; Saeedi, 2016; Teshome, 2016; Wang et al., 2014), modified Monte Carlo (Wadi et al., 2018), continuous-time Markov chain (Dadfar et al., 2017), reliable block diagram (Bousshoua & Elmaouhab, 2019), variance reduction

(Ali Kadhem et al., 2017), and new mixed-integer nonlinear programming model (Heidari, 2015).

Continuity of power supply improvement, voltage stability, power quality improvement, reactive power compensation, and load demand satisfaction, etc., are the object topics of many studies related to the positive impacts associated with the integration of RES on the distribution network level (Luo et al., 2018; Nwaigwe et al., 2019; Panigrahi et al., 2020). On the other hand, proper sizing of the capacity of RES and ESS, control techniques, planning, protection, optimal location, and profitability of the integration of such systems were the object topics of many conducted studies (Luo et al., 2018; Ehsan & Yang, 2018; Razavi et al., 2019; Y. Li et al., 2018; Valencia et al., 2021).

## 2.5. Monte Carlo Simulation Methods

The reliability evaluation can be done based on two methods named as historical method and predictive method. Historical method is based on the system historical failure data. Predictive method is classified as analytical analysis that uses simplified mathematical model to calculate reliability indices and simulation analysis that uses the system random behavior for simulate the series of real experiment for reliability indices estimation.

Monte Carlo Simulation Method (MCS) is a predictive method also known as multiple probability simulation that produces random failures for each unit of a power system (Garip et al., 2022). Specifically, MCS method is the most suitable method used for large and complex system with high level of uncertainty (Garip et al., 2022; Hashish et al., 2023).

For random generated $N_i$ samples, for $X$ stochastic variables with their respective marginal probability density function, the reliability analysis flow chart is shown by Figure 2.4 for each realization $y$, element $j$, and time step $t$ for stochastic variable $X^{y,j,t}$ (Pol et al., 2023).

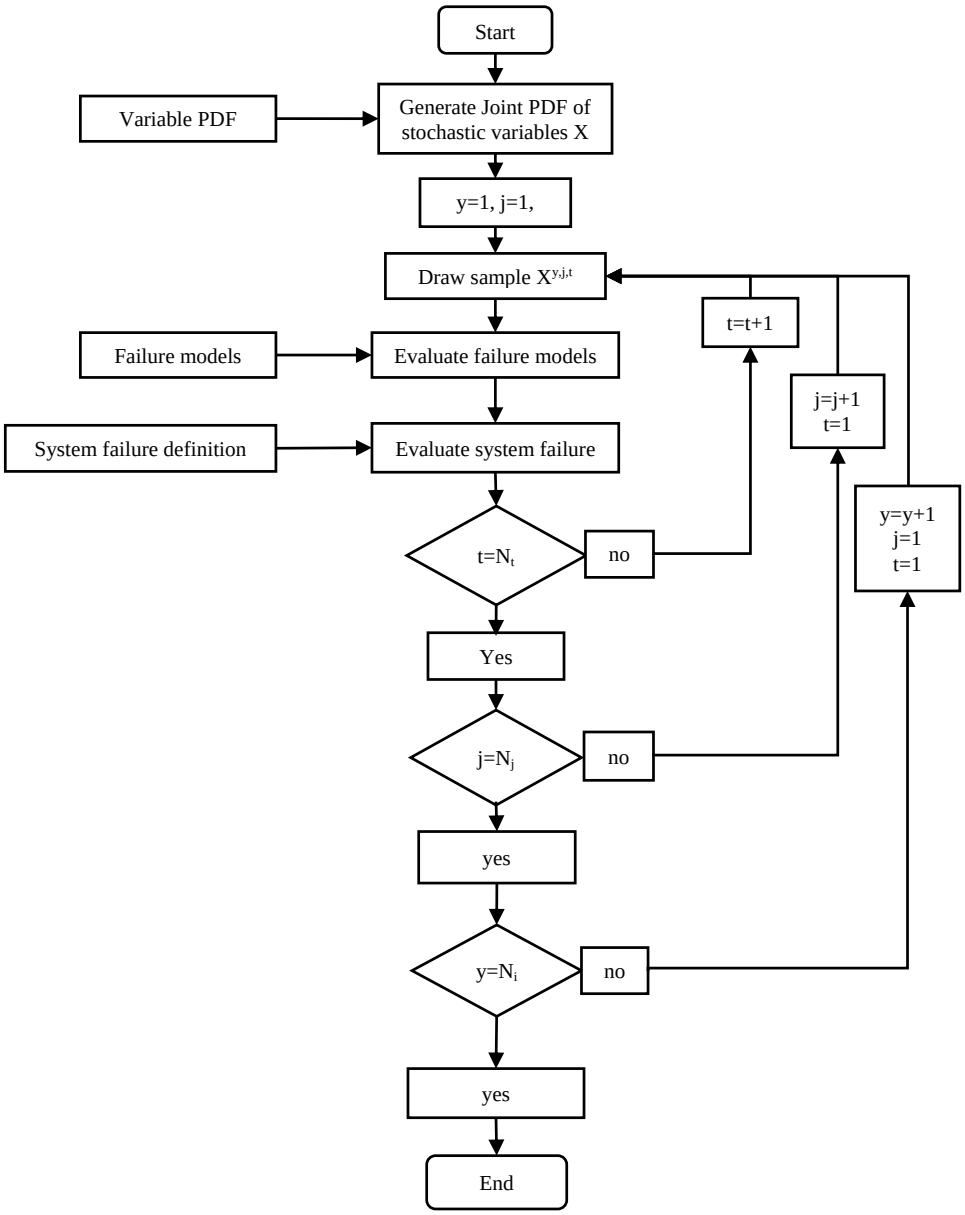


Figure 2.4. Flow chart for reliability analysis based on MCS method

# 3. RENEWABLE ENERGY SOURCES AND DISTRIBUTED GENERATION CONCEPT

Multiple technologies for renewable energy sources (RES) are in existence, with each providing significant environmental benefits. Solar photovoltaic (PV) technology transforms solar radiation into electricity, lowering carbon emissions by reducing dependence on fossil fuels. Solar thermal systems harness solar radiation to create heat and steam, aiding the shift to cleaner energy. Wind turbines convert kinetic energy of the wind to produce electricity. Additionally, hydropower plants and biomass systems also have crucial roles in reducing our carbon footprint.

## 3.1. Distributed Generation

Distributed generation (DG), also known as decentralized or embedded generation, involves generating electricity near where it will be used, as opposed to traditional centralized power plants located far away from consumers, which require extensive transmission networks. DG power plants are typically smaller in scale, with a capacity of less than 10MW, and they are connected to the local distribution network. These plants can generate and store electrical energy and are often referred to as distributed energy resources (DER), as shown in Figure 3.1.

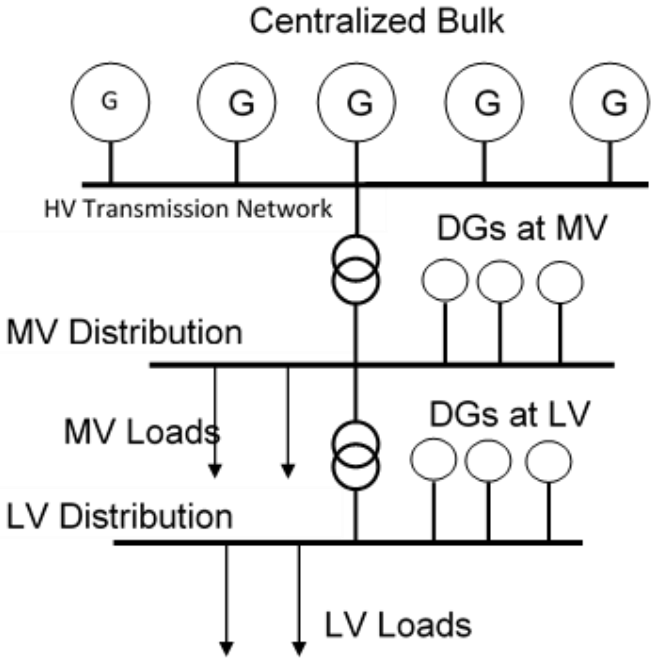


Figure 3.1. Electric grid with distributed generation

The renewable energy generation plants are smaller in generation capacity (50MW - 100MW) and geographically widely spread. As DGs, renewable energy plants are integrated to the existing distribution system. The distributed generation concept promotes the generation of electric power from RES. However, the high degree of penetration of distributed and renewable generation has an unfortunate consequence on the stability of the electric grid. Renewable energy generation plants must also contribute to system stability control by providing ancillary services such as synchronous generators. Some countries have devised grid codes for power system operation, while these codes are encouraged in other nations. This enables distributed generators (DGs) to offer the required support for system operation, thus minimizing and eradicating the adverse effects of high penetration of RES (Shahzad & Asgarpoor, 2017).

Distributed Generators (DGs) have different impacts on various parts of the power system. In distribution networks, DGs have the potential to improve voltage levels and power quality, and to enhance protection (Shahzad & Asgarpoor, 2017). They also help reduce system losses on transmission networks by supplying energy from the distribution system close to consumers, thus decreasing the need for extensive transmission infrastructure. Additionally, the average output power of centralized generators is affected by DGs, as they provide additional power. However, DGs also introduce uncertainty in generated power caused by the intermittent nature of RESs and leads to the need for additional reserve plants.

### 3.2. Battery Energy Storage System

The challenge introduced by the intermittent nature of RES is addressed by energy storage systems (ESS). ESS within the grid serves various purposes and applications for functions like black start, voltage and frequency control, network reinforcement deferral, backup power, peak shaving, renewable energy self-consumption, off-grid systems, and correction of forecasting inaccuracy for wholesale market participants (Kim et al., 2018).

Batteries store energy in chemical form and can be utilized later when required. Battery energy systems encompass battery energy management, which is shown Figure 3.2. Thus, with BESS, electric power is smoothly supplied in a power system where RESs are used. Reliability improvement, stability, power quality improvement, fast response, and

uninterrupted power supply are examples of BESS uses in an MG (Rosewater et al., 2019; Yang et al., 2018; Kim et al., 2018).

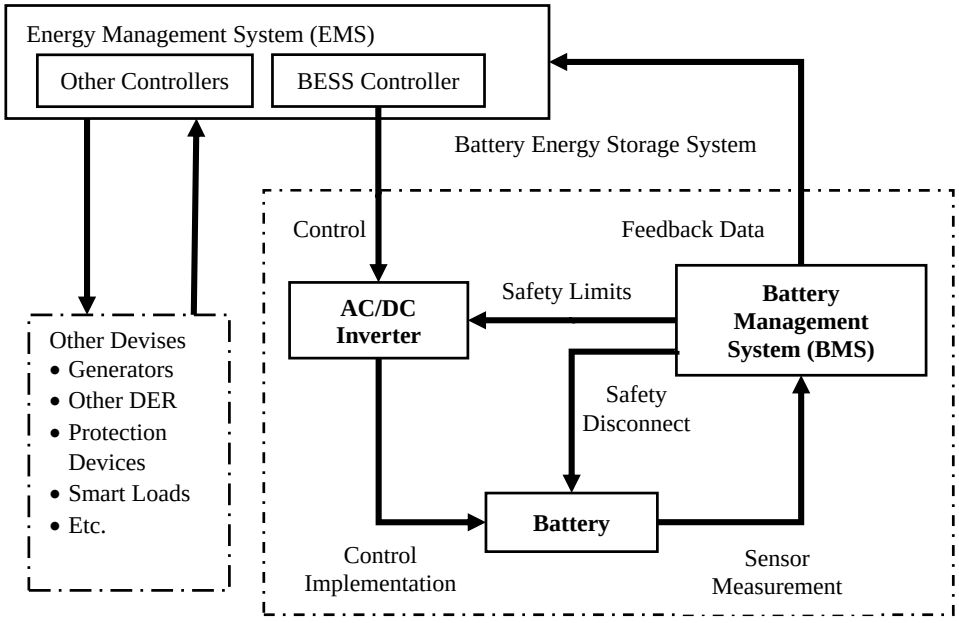


Figure 3.2. BESS Layout with Energy Management System

## 3.3. Microgrids

A microgrid (MG) is a clearly defined electrical limits composed by a set of loads and DGs that act as a single controllable entity and can operate either disconnected or connected to the main electric grid's distribution system (grid-connected or islanding mode) (Kim et al., 2018).

Distributed energy sources (DER) and loads that can be defined as critical and controllable loads are interconnected and systematically controlled within a MG. DGs in the form of an MG system can improve energy supply's power quality, reliability, and security in a distribution system. MG layout is composed of different DGs types and loads and connected to the main grid through the point of common coupling (PCC) as shown in Figure 3.3. Furthermore, MGs are classified depending on their configurations, applications, and the technology structure's complexity. According to the applications, MGs can be classified as commercial and industrial MGs for commercial centers and industrial zones, utility MGs for different purposes such as reliability of critical

infrastructure and achieving emission targets, public institution MGs, critical MGs, and rural and remote MGs.

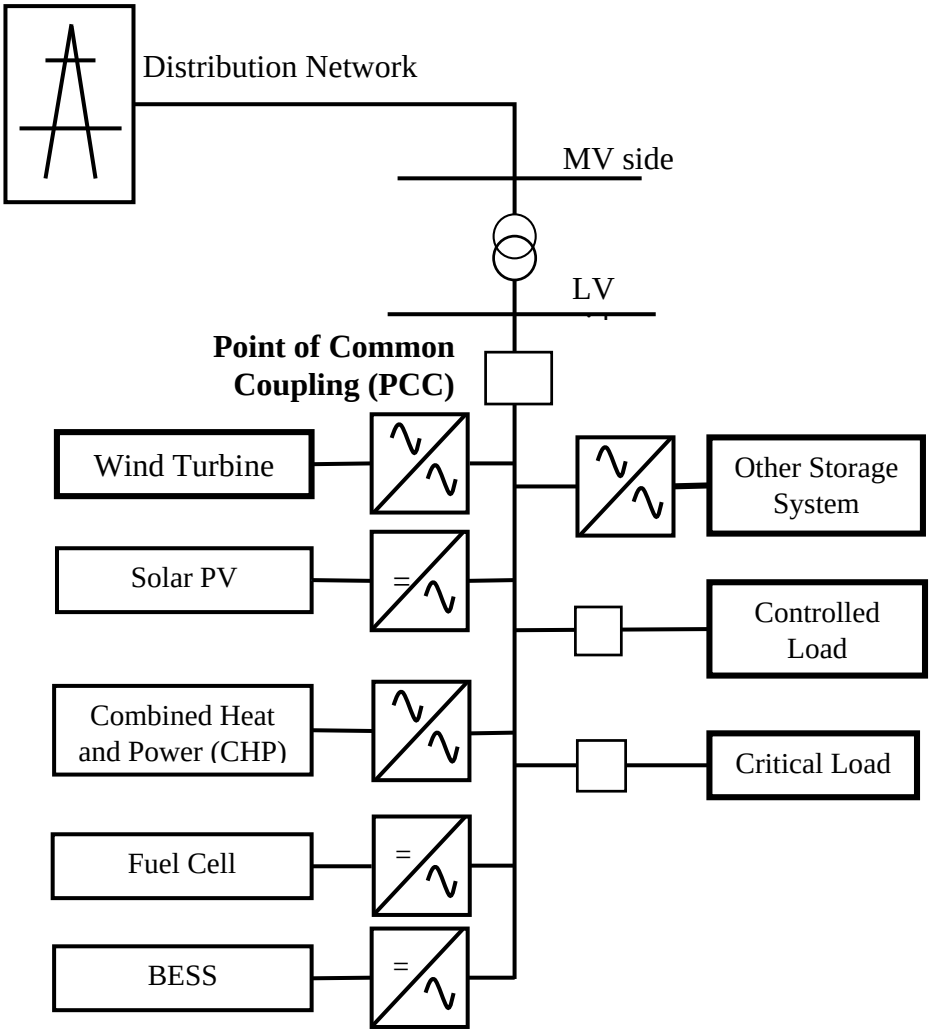


Figure 3.3. Microgrid layout

### 3.4. Solar PV and BESS based Microgrid

The introduction of the MG system into an electrical power system promotes the use of RES. As shown in Figure 3.3, solar PV and BESS-based MG is an MG composed of solar PV as a distrıbuted generator, BESS, controlled load, and critical load. Solar PV is the DG unity and source of direct current (DC) power in the MG. Solar PV is connected to the alternating current (AC) buss bar through DC - AC inverter. A bidirectional DC-AC inverter is used as a link between the BESS and the other components of MG. The system is composed of controlled loads and critical loads. Under normal conditions, both load types are supplied by solar PV, BESS, and imported energy from the main grid. Under

islanding operation mode, when the available power is not enough to supply the whole load, only the critical load is supplied through solar PV and BESS. The operation scenarios in an MG are controlled by systematic control of different components within the MG. Solar PV and BESS-based MGs perform different functions, such as harmonics mitigation, reactive power compensation, maximum power extraction from PV arrays, balancing grid current, and seamless transition from grid-connected mode to islanding mode of operation (Narayanan et al., 2020).

# 4. MODELLING OF SOLAR PV ELECTRIC POWER PRODUCTION SYSTEM INCLUDING BATTERY ENERGY STORAGE

Solar PV generates electricity directly from solar radiation, making it the simplest way to generate usable electricity. Solar PVs can generate electricity ranging from small-scale for household applications to utility-scale power plants of more than 10MWp capacity.

Out of power generation technologies, solar PV is more popular, more cost-effective, and more realistic for solving energy's associated challenges. PV power plants generate electricity depending on the quantity of availability of sunlight. In order to ensure a continuous supply of power, solar PV systems must use ESS. Solar PV systems are frequently combined with BESS to provide a continuous power supply (Cui et al., 2018; Mbungu et al., 2020). Using BESS alongside PV power generation allows optimal performance of PV power applications.

## 4.1. Off-Grid Photovoltaic (PV) System

The off-grid solar PV system is a way of generating electrical power independently. Off-grid solar PV systems are primarily used in remote areas where access to the utility grid is practically impossible or when the power consumer needs to be independent. The extra-generated energy is stored in batteries for late use when the sun's light is unavailable. Off-grid solar systems must be sized correctly to generate sufficient power and must have adequate battery capacity to meet load demand all year round.

A typical off-grid solar PV system comprises four parts, including solar panels, solar charge controller, off-grid inverter, and batteries, as shown in Figure 4.1.

Depending on the installation, an off-grid PV system can only provide DC power for DC loads or, with the help of an inverter, to provide AC power for AC loads. When the BESS and inverter are used in the same system, the DC or AC bus systems can be used for the system configuration where the arrays are connected through a charge controller to BESS, and to AC side via PV inverter.

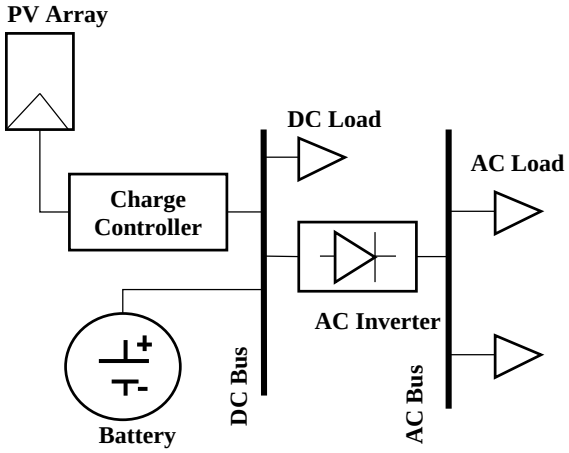


Figure 4.1. Off-Grid solar PV system elements

## 4.2. Grid-Connected PV System

A grid-connected PV system is connected to the utility grid and varies from small rooftop installations for businesses and homes to large solar power stations. Contrary to stand-alone power systems, the energy generated by grid-connected system is usually directly supplied to the grid and the system rarely includes BESS.

System configurations of grid integration of PV modules is classified as PV inverters without DC/DC converter (Single-Stage) and PV inverters with DC/DC converter (Double-Stage) and Figure 4.2 shows a typical grid-connected PV system basic elements.

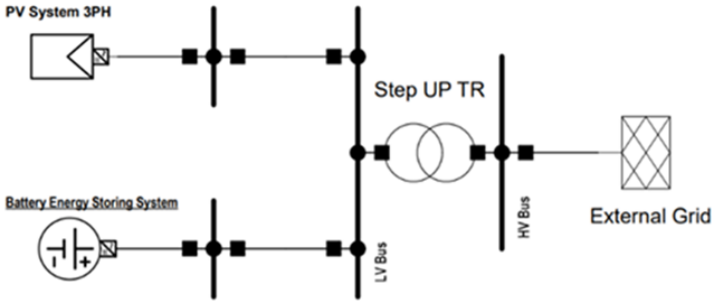


Figure 4.2. Grid-Connected PV system basic elements

## 4.3. Solar PV Cell Model

The PV cell electrical models are shown in Figure 4.3 and are classified as a single diode (or five parameter) and two diode models (Bellia, 2019; Jena & Ramana, 2015; Soto et al., 2006; Yuan et al., 2014).

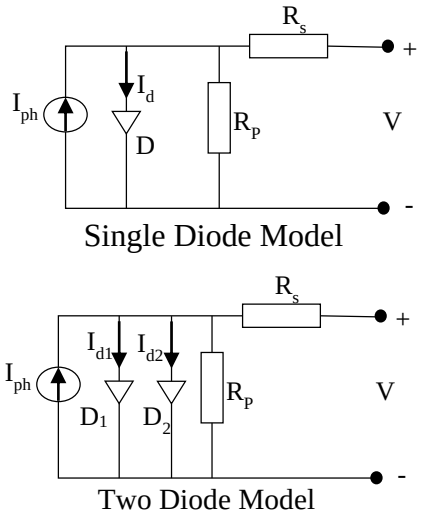


Figure 4.3. Electrical model of solar PV cell

By applying Kirchhoff's Current Law (KCL) in Single Diode model, the expression of the current at the output is given by Equation (4.1) and (4.2);

$$I = I_{ph} - I_d - I_{sh} \tag{4.1}$$

$$I = I_{ph} - I_o \left[ exp \frac{q(V + IR_s)}{nkT} - 1 \right] - \frac{V + IR_s}{R_p} \tag{4.2}$$

The single diode model five electrical parameters are shunt resistance ($R_p$), series resistance ($R_s$), reverse saturation current of diode ($I_o$), photo current ($I_{ph}$), and diode ideality factor ($n$).

In Two Diode Model by applying KCL, the expression of output current is given by Equation (4.3);

$$I = I_{ph} - I_{o1} \left[ exp \frac{q(V+IR_s)}{n_1 kT} - 1 \right] - I_{o2} \left[ exp \frac{q(V+IR_s)}{n_2 kT} - 1 \right] - \frac{V+IR_s}{R_p} \tag{4.3}$$

As shown in Equation (4.3), two diode model has more parameters that make it a complex model than single diode model (Jena & Ramana, 2015).

### 4.4. PV Array Model

Parallel and/or series connection of PV cells form PV modules; and parallel and/or series connection of PV modules form PV arrays, as shown in Figure 4.4.

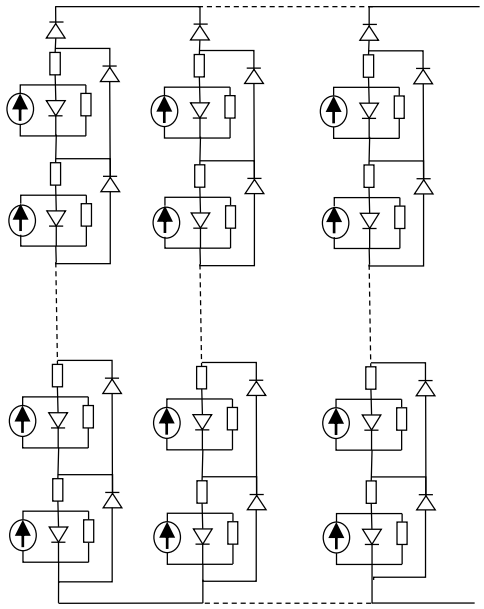

Figure 4.4. PV module equivalent circuit model

The relationship between output voltage ($V_t$) and current ($I_t$) of PV module with $N_s$ series and $N_p$ parallel connection of PV cells are derived from single solar cell relationship and is given by Equation (4.4);

$$I_t = N_p I_{ph} - N_p I_o \left[ exp \frac{q\left(V_t + I_t \frac{N_s}{N_p} R_s\right)}{N_s nkT} - 1 \right] - \frac{V_t + I_t \frac{N_s}{N_p} R_s}{\frac{N_s}{N_p} R_p} \tag{4.4}$$

If supposed that: $N_p I_{ph} = I'_{ph}$ , $N_p I_o = I'_o$ , $\frac{N_s}{N_p} R_s = R'_s$ and $\frac{N_s}{N_p} R_p = R'_p$ the Equation (4.4) becomes;

$$I_t = I'_{ph} - I'_o \left[ exp \frac{q(V_t + I_t R'_s)}{N_s nkT} - 1 \right] - \frac{V_t + I_t R'_s}{R'_p} \tag{4.5}$$

The current - voltage relationship given by Equations (4.2) and (4.5) are similar. Thus, for PV array and single solar cell, current-voltage relationship is similar. Therefore, PV array and single PV solar cell can be modelled in the same way.

## 4.5. PV Model Parameters Identification

Six unknown PV model parameters are found in Equation (4.2), those parameters define voltage and current relationship for PV cell and are different from one cell to another

depending on the material and technologies the cell is made of and the environmental condition. The PV model parameters are:

- Photo Current ($I_{ph}$)
- Ideality Factor (n)
- Temperature of cell (T)
- Diode saturation current ($I_o$)
- Shunt resistance ($R_p$)
- Series Resistance ($R_s$)

Ideality Factor (n)

The ideality factor ($n$) is related only to the material of the solar cell and independent of solar irradiation and temperature. The value of $n$ compared to the value of $n_{ref}$ at Standard Test Condition (STC) is given by $n = n_{ref}$ at STC $G_{ref} = 1000\frac{W}{m^2}$ and $T_{ref} = 298K$ (Soto et al., 2006; Tian et al., 2012).

Photo Current ($I_{ph}$)

The photo current ($I_{ph}$) is a function of on the cell Temperature ($T$) and the solar irradiance ($G$) and is given by Equation (4.6) (Tian et al., 2012);

$$I_{ph} = I_{ph,ref}\left(\frac{G}{G_{ref}}\right)\left[1 + \alpha'_T\left(T - T_{ref}\right)\right] \quad (4.6)$$

Where $I_{ph,ref}$ is Photo current at STC, $\alpha'_T$ is the relative short-circuit current temperature coefficient and $\alpha'_T = \frac{\alpha_T}{I_{ph,ref}}$, and $\alpha_T$ is the absolute temperature coefficient.

Diode Saturation Current ($I_o$)

$I_o$ is primarily dependent on the temperature of the cell and the Equation (4.7) gives its relationship between with temperature as (Soto et al., 2006; Tian et al., 2012);

$$I_o = I_{o,ref}\left[\frac{T}{T_{ref}}\right]^3 exp\left[\frac{E_{g,ref}}{kT_{ref}} - \frac{E_g}{kT}\right] \quad (4.7)$$

Where $I_{o,ref}$ is diode saturation current at STC, $E_{g,ref}$ is band gap energy at STC, and $E_g$ is band gap energy and $E_g = 1.16 - 7.02 \times 14^{-4}\left(\frac{T^2}{T-1108}\right)$.

Temperature of cell (T)

The change in temperature of cell exists due to change in the insolation and the ambient temperature and the Equation (4.8) describes the change in ambient temperature;

$$T = T_{amb} + \left(\frac{NOCT - 20°}{0.8}\right)G \tag{4.8}$$

$NOCT$ is the cell nominal operating temperature given by the manufacturer and $T_{amb}$ is the ambient temperature.

Shunt resistance ($R_p$)

Approximately, the shunt resistance is given by Equation (4.9):

$$R_p > \frac{10V_{oc}}{I_{sc}} \tag{4.9}$$

$R_p$ is shunt resistance, $I_{sc}$ is short circuit current, and $V_{oc}$ is open circuit voltage at operating condition and shunt resistance ($R_{p,ref}$) at STC are related as shown by Equation (4.10) (Soto et al., 2006);

$$\frac{R_p}{R_{p,ref}} = \frac{G}{G_{ref}} \tag{4.10}$$

Series Resistance ($Rs$)

As an approximation, the series resistance is given by Equation (4.11):

$$R_s < \frac{0.1V_{oc}}{I_{sc}} \tag{4.11}$$

The series resistance is independent of irradiation and temperature at both STC and operating conditions and it is assumed to be constant as shown by Equation (4.12) (Soto et al., 2006);

$$R_s = R_{s,ref} \tag{4.12}$$

Reference parameters

A solar PV cell's reference parameters are obtained at the STC under which a solar panel is tested. At STC, the solar Irradiance is 1000 Watts per square meter, the temperature of the cell is 25°C, and the mass of the air is 1.5.

PV manufacturers provide open circuit voltage (*Voc,ref*), short circuit current (*Isc,ref*), voltage (*Vmp,ref*), and current (*Imp,ref*) for maximum power of a PV panel at STC (Tian et al., 2012). At STC the unknown reference parameters $I_{ph,ref}$, $I_{o,ref}$, $n_{ref}$, $R_{p,ref}$, and $R_{s,ref}$ and are obtained by using the following relationships from Equation (4.13) to (4.17);

- At open circuit condition:

$$0 = I_{ph,ref} - I_{o,ref}\left[exp\frac{q\left(V_{oc,ref}\right)}{n_{ref}kT_{ref}} - 1\right] - \frac{V_{oc,ref}}{R_{p,ref}} \tag{4.13}$$

- At short circuit condition:

$$I_{sc,ref} = I_{ph,ref} - I_{o,ref}\left[exp\frac{q\left(I_{sc,ref}R_{s,ref}\right)}{n_{ref}kT_{ref}} - 1\right] - \frac{I_{sc,ref}R_{s,ref}}{R_{p,ref}} \tag{4.14}$$

- At maximum power:

$$I_{mp,ref} = I_{ph,ref} - I_{o,ref}\left[exp\frac{q\left(V_{mp,ref}+I_{mp,ref}R_{s,ref}\right)}{n_{ref}kT_{ref}} - 1\right] - \frac{V_{mp,ref}+I_{mp,ref}R_{s,ref}}{R_{p,ref}} \tag{4.15}$$

The derivative with respect to voltage of power at maximum power point is zero:

$$\frac{I_{mp,ref}}{V_{mp,ref}} = \frac{\frac{1}{R_{p,ref}} + \frac{I_{O,ref}q}{n_{ref}kT_{ref}}\left[exp\frac{q\left(V_{mp,ref}+I_{mp,ref}R_{s,ref}\right)}{n_{ref}kT_{ref}}\right]}{1 + \frac{R_{s,ref}}{R_{p,ref}} + \frac{I_{O,ref}qR_{s,ref}}{n_{ref}kT_{ref}}\left[exp\frac{q\left(V_{mp,ref}+I_{mp,ref}R_{s,ref}\right)}{n_{ref}kT_{ref}}\right]} \tag{4.16}$$

- The open circuit voltage temperature coefficient at *Gref* is given by:

$$\beta_T = \frac{V_{oc,ref} - V_{oc,Tc}}{T_{ref} - T_c} \tag{4.17}$$

$Tc = Tref \pm 10K$, cell operating temperature. From Equation (4.17), at the operating temperature $Tc$ , the open circuit voltage can be derived. The fifth equation is obtained by substituting the expressions in Equation (4.6), (4.7), (4.10), and (4.13) into equation (4.4) where the values are related to the temperature *Tc*.

For different irradiation levels at temperature of 25ºC, Figure 4.5 and Figure 4.6 show the *P-V* characteristics and *I-V* characteristics of solar PV panel. The solar PV panel is modeled in Matlab and fsolver function is used for reference parameters identification. The electrical parameters of a single crystalline solar PV panel at reference condition were obtained from reference (Soto et al., 2006) and the values are 4.37A for short circuit current, 42.93V for open circuit voltage, 33.68V for voltage at maximum power, 3.96A for current at maximum power, -0.1523 V/K for temperature coefficient at open circuit voltage, 0.00175A/K for temperature coefficient at short circuit current, 72 cells connected series, and 1.12eV for band gap energy.

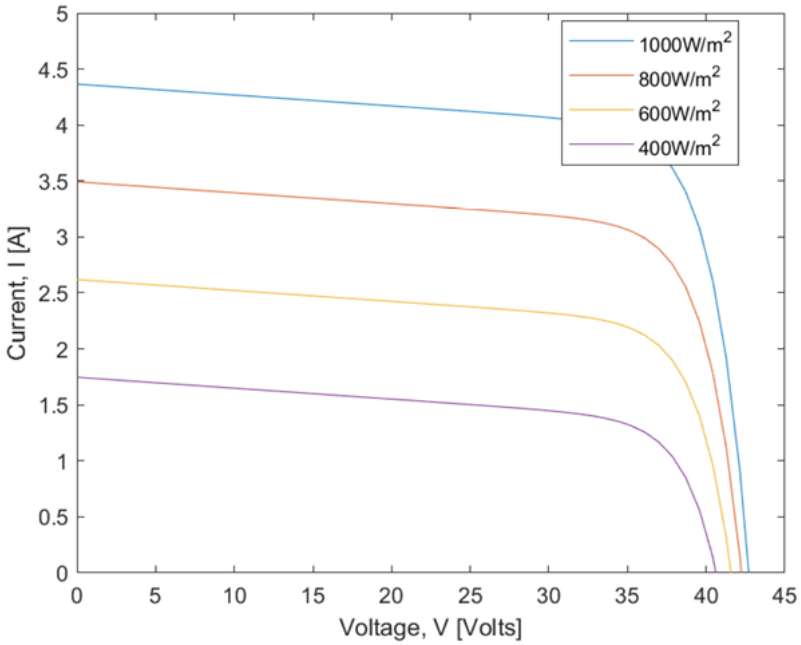


Figure 4.5. Single crystalline PV panel I-V characteristics at 25°C constant cell temperature

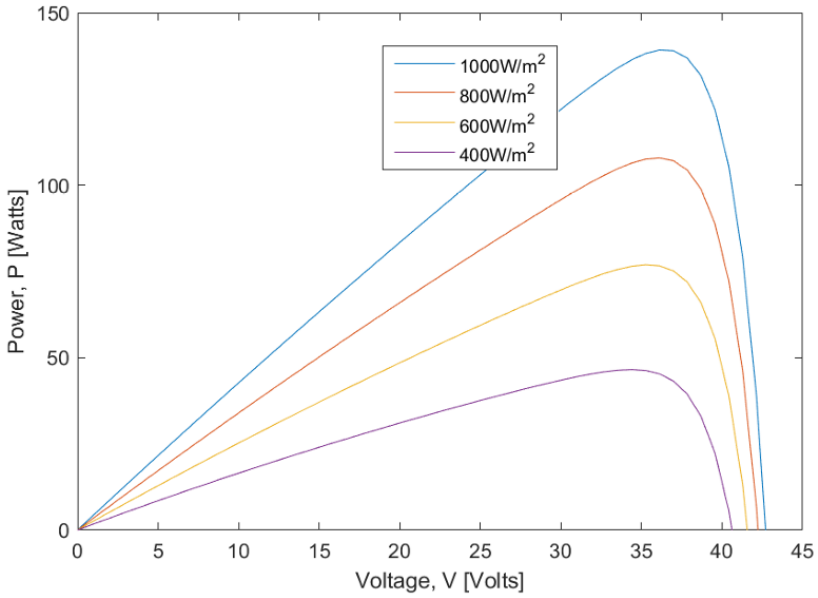


Figure 4.6. Single crystalline PV panel P-V characteristics at 25°C constant cell

The temperature effect on solar PV panels was verified by changing the temperature and keeping the solar radiation constant and Figure 4.7 and Figure 4.8 show the I-V and P-V characteristics.

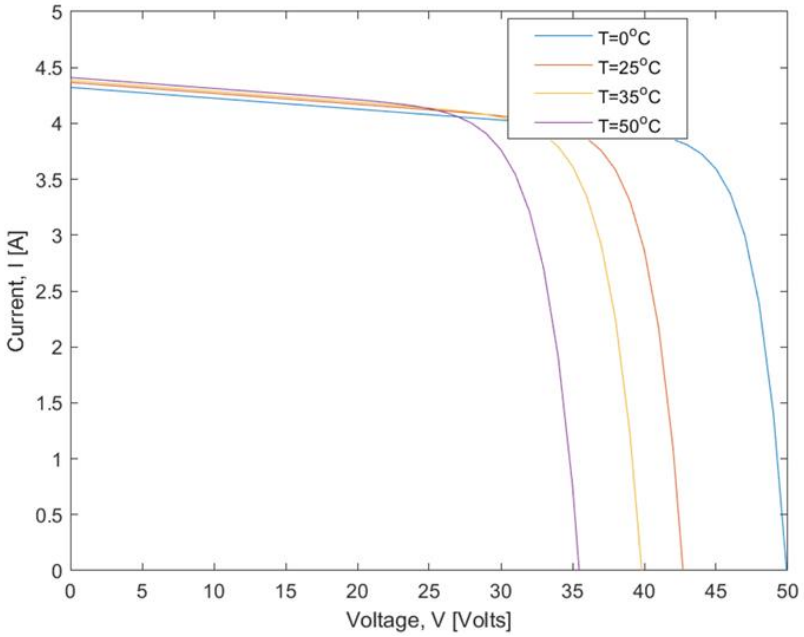


Figure 4.7. Single crystalline panel I-V characteristics at1000W/m$^2$ constant irradiation level

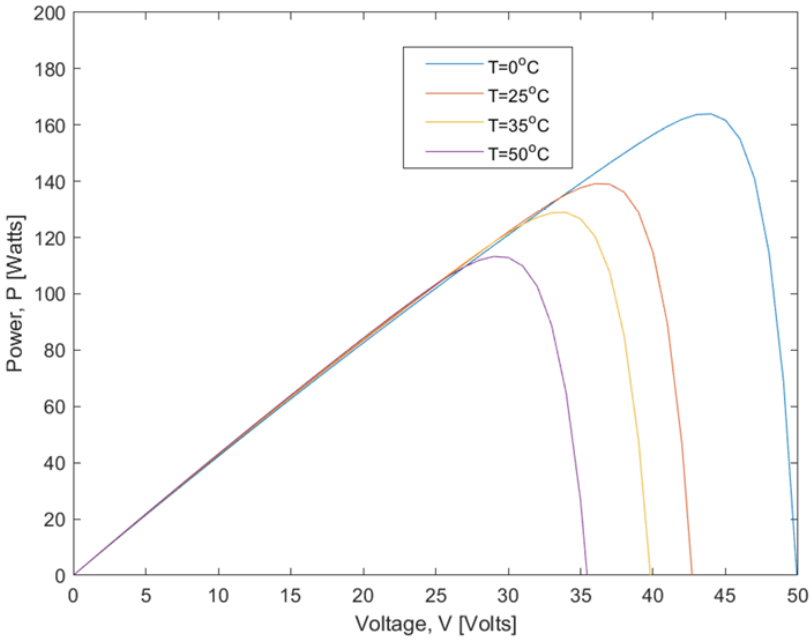


Figure 4.8. Single crystalline panel P-V characteristics at 1000W/m$^2$ constant irradiation level

## 4.6. Battery Energy Storage Model

### 4.6.1. Thevenin-based Battery Model

The model consists of an open-circuit voltage ($V_{oc}$), resistance-capacitance (RC) loop composed by a polarization resistor ($R_{po}$) and a polarization capacitance ($C_p$), and circuit ohmic resistance ($R_o$). The RC loop circuit reflect the influence of battery polarization. The circuit model of the thevenin-based battery model is shown in Figure 4.9.

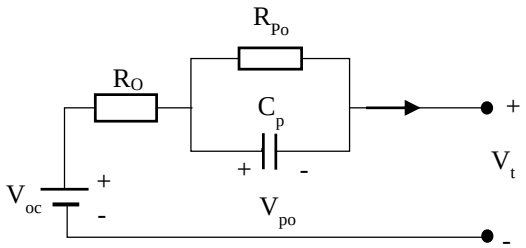


Figure 4.9. Thevenin-based battery model

The terminal voltage ($V_t$) and current (I) are obtained by using KCL as in Equation (4.18) and (4.19);

$$V_t = V_{oc} - IR_o - V_{po} \tag{4.18}$$

and

$$C_p \frac{dV_{po}}{dt} + \frac{V_{po}}{R_{po}} = I \tag{4.19}$$

### 4.6.2. Generic Battery Model

The model is composed by a resistance and a controlled voltage source, as shown in Figure 4.10. The model parameters can be provided by the discharge curve from the manufacturer, and dynamic simulation software like Matlab/Simulink can be used to simulate a specific type of battery. Terminal voltage ($V_t$) and state of charge (SOC) are the two important parameters that represent a battery.

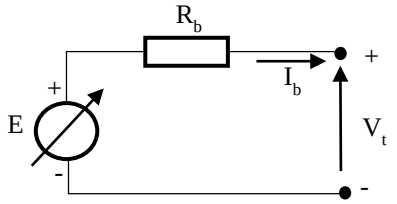


Figure 4.10. Genetic battery model

The terminal voltage ($V_t$) and state of charge (SOC) of a battery are determined by using the following relationships in Equation (4.20) and (4.21);

$$V_t = V_{oc} - R_b I_b - V_{po} \frac{Q}{Q - \int I_b \, dt} + V_{ex} e^{(-B \int I_b \, dt)} \tag{4.20}$$

and

$$SOC = 100\left(1 - \frac{\int I_b \, dt}{Q}\right) \tag{4.21}$$

Here, $V_{oc}$ is the open circuit voltage of the battery, $R_b$ is internal resistance of the battery, $V_{po}$ is polarization voltage, $I_b$ is battery discharging current, $V_{ex}$ is exponential voltage, $B$ is exponential capacity, and $Q$ is battery capacity.

## 4.7. Energy Management System (EMS)

The energy flow of a PV power station integrated with BESS needs to be controlled in order to determine whether the battery will be charged and discharged according to the available energy. The set of algorithms for controlling the flow of energy flow in a PV-Battery system are shown in Figure 4.11.

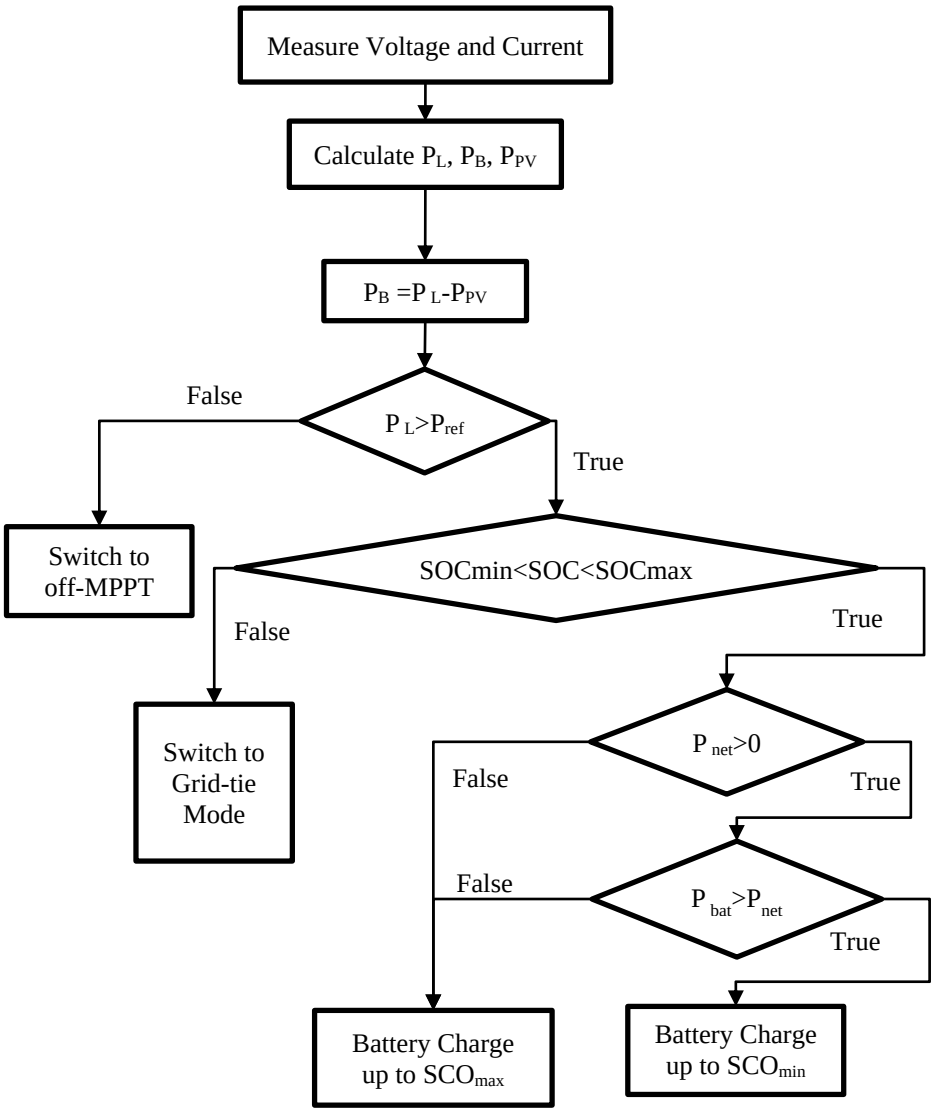


Figure 4.11. Energy management system flow chart

- Maximum Power Point Tracking (MPPT) switches its state from on to off when load power is below the Maximum Power Point (MPP) power limit.
- For grid-tied mode with BESS, PV and Battery work together to compliment the energy vacant, or to store the excessive power. Only if the load demand exceeds the capacity of PV and battery, the grid takes control.
- For islanding mode, the reference current for battery, $I_{bat}* = (P_L - P_{PV})/V_{bat}$, where $V_{bat}$ is the battery voltage. The battery goes to charging mode when PV generates excessive power, and to discharging mode when PV produces insufficient power.

# 5. PV SYSTEM COMBINED WITH BESS FOR SMALL HOUSEHOLDS APPLICATION

This study uses PV*SOL simulation software to provide a techno-economic assessment of a grid-connected solar PV system with a battery energy storage system (BESS) for a residential community in the Shyogwe sector, Muhanga district, Rwanda. The system meets the load demand for a collective of 100 households and supports a water-pumping system for farming activities using the solar PV system generated energy. According to the results from the simulations, with a peak load demand of 30.4kW, the annual energy demand is 82.34MWh. The simulations also demonstrated that a 57.33kWp PV system combined with 89.2kWh BESS can supply 68.65% of its own power, and can achieve 86.05% performance ratio of and 64.38% self-sufficiency level of when the target desired ratio to consumption is 110% annually. The financial analysis revealed 9.65 years of amortization period and 9.14% return on assets.

Large-scale PV plants connected to electric grid primarily supply the generated electricity to the grid. For residential and commercial purposes, small-scale PV system can also be connected to the grid (Ahmad et al., 2020; Jasuan et al., 2018). In off-grid systems, batteries are essential as they significantly improve the availability and reliability of electricity. They store excess energy generated by solar PV systems, ensuring a continuous power supply even when sunlight is not able to meet the load demand, such as during the night. This role of batteries increases the solar PV system's both the reliability and self-sufficiency (Jiang et al., 2021). Furthermore, BESS can be combined with grid-connected PV system for commercial, residential, or community uses (with grid access) to reduce grid dependence and improve self-consumption levels (Dorahaki et al., 2022). If the available energy from solar PV and BESS is not enough to satisfy the load demand, in such case, power is taken from the grid only. For a more optimized system, the grid's energy is only used for load demand support when necessary, and to make the overall system more cost-effective, batteries are charged exclusively from the solar PV systems.

The combination of BESS with Solar PV offer techno-economic solutions to high PV penetration related challenges at distribution networks. Energy storage integrated with RES provides solutions including curtailing or storing generated energy, discharging

stored energy, and load demand flexibility (Hargreaves & Jones, 2020). BESS offers energy solutions for PV energy timeshift, controlling of PV energy flow, and upgrading distribution transformers. These solutions are essential for effectively managing the integration of high levels of PV generation into distribution networks (Tercan & Elma, 2022). One of the strategies to make PV and BESS more cost-efficient is establishing a community ESS to decrease individual capital expenditure (Segundo Sevilla et al., 2018).

Multiple simulation tools are available for researchers to conduct in-depth studies on solar photovoltaic (PV) systems, and their selection is function of the study objectives and nature. These tools include PVsyst (Alnoosani1 et al., 2018; Jagadale et al., 2022; Kumar et al., 2020; Rout & Kulkarni, 2020), INSEL (Nigam & Sharma, 2020; Ram et al., 2022), TRNSYS (Cao et al., 2022; Rafał et al., 2020; Sekhar et al., 2017), PV*SOL (Dondariya et al., 2018; Mrehel, 2020; Nhau et al., 2021; Pushpavalli et al., 2021), SOLARPRO (Alsadi & Khatib, 2018; Lee et al., 2021), HOMER (Al et al., 2018; Khalil et al., 2021; Morad, 2018), Solar Advisor Model (Chennaif et al., 2022; Panjwani & Khan, 2021; Umar et al., 2018).

This chapter highlights the significance of grid-connected PV systems for electricity reliability enhancement and accessibility. The system's design enables to receive electric grid support when the energy from the PV and battery energy storage systems (BESS) is inadequate to meet the power demand.

## 5.1. Methodology

### 5.1.1. PV System Simulating Tools Selection

In addition to sunlight, other factors need to be considered when designing a solar power system in a specific location, including solar intensity potential and weather patterns. They have a significant role in designing and implementing an efficient solar power system for its techno-economical capabilities and feasibility. Thus, it is essential to carefully analyze and simulate the solar power system's output to ensure its successfully optimal performance. Table 5.1 provides a summary of PV system simulation software tools associated advantages and disadvantages. After evaluation for simulating tools, PV*SOL Software is selected for a PV system with Battery Energy Storage Systems

(BESS) simulation and designing. This decision is based on the fact that PV*SOL is a leading PV system simulation and designing tool used by energy planners, engineers, technicians, installers, and architects worldwide. PV*SOL's capabilities extend to designing and simulating different types of modern PV systems, ranging from small-scale rooftop installations to large-scale PV power plants up to 100,000 modules (URL-5).

Table 5.1. Summary of advantages and disadvantages of PV system simulation tools

| SNO | Simulation Tools | ADVANTAGES | LIMITATIONS |
|---|---|---|---|
| 1. | PVsyst (Mrehel, 2020; Rout & Kulkarni, 2020; Segundo Sevilla et al., 2018; Tercan & Elma, 2022) | 1. It holds a vast database of meteorological data<br>2. Grid-connected, off-grid, and offshore solar photovoltaic (PV) systems applications<br>3. Support in system configuration and design<br>4. Market available PV-components database | 1. Collector configuration sizing restrictions<br>2. There is no connection with other software tools |
| 2. | INSEL (Jagadale et al., 2022; Kumar et al., 2020) | 1. Create block diagrams to simulate electrical components, meteorological data, and heat/thermal energy<br>2. Grid-connected and off-grid systems applications<br>3. Simulations that involves sun-tracking system and shading analysis | 1. Limited settings for system configuration<br>2. Economic analysis feature is not available |
| 3. | TRNSYS (Nigam & Sharma, 2020; Ram et al., 2022; Sekhar et al., 2017) | 1. Analysis of HRES<br>2. Solar thermal energy<br>3. Adding mathematical models to a system or project can be achieved easily<br>4. Ability integrate with other simulation software programs<br>5. Uses METEONORM database as weather database<br>6. Load profile analysis | 1. For hybrid RES, biofuel and hydropower are excluded<br>2. Estimation of CO2 emission not available in the basic version |
| 4. | PV*SOL(Cao et al., 2022; Dondariya et al., 2018; Nhau et al., 2021; Rafał et al., 2020) | 1. System sizing and electrical parameters<br>2. Grid-connected and standalone PV system<br>3. PV panel orientation<br>4. Load profile and consumption<br>5. PV systems with BESS<br>6. Geographical location and meteorological profile<br>7. Inverter configuration optimization<br>8. Shading effect analysis<br>9. Economic analysis | 1. Only PV systems are simulated<br>2. There is no connection with other software tools |

Table 5.1. (Continue) Summary of advantages and disadvantages of PV system simulation tools

| SNO | Simulation Tools | ADVANTAGES | LIMITATIONS |
|---|---|---|---|
| 5. | SOLARPRO (Mrehel, 2020; Pushpavalli et al., 2021) | 1. Calculating the effects of shading on energy output<br>2. Field measured data<br>3. Economic analysis<br>4. Provide output in terms of I-V Curve | 1. Only PV systems are simulated |
| 6. | HOMER(Al et al., 2018; Alsadi & Khatib, 2018; Lee et al., 2021) | 1. Analysis of hybrid RES<br>2. Grid-connected system and off-grid system<br>3. Economic analysis | 1. No thermal system<br>2. Some daily variables are not considered |
| 7. | Solar Advisor Model (Khalil et al., 2021; Morad, 2018; Panjwani & Khan, 2021) | 1. Real-time simulations analysis<br>2. Grit-tie storage system<br>3. Economic analysis<br>4. Different types of RES and hybrid system simulation | 1. 3 D shading modeling is not supported<br>2. Unavailability weather database for some locations |

## 5.2. Location

When selecting a site for a solar PV system, various factors must be considered. The solar PV modules must be oriented to capture as much sunlight as possible effectively, and efforts should be made to minimize shading losses on the panels (Kayhan et al., 2015).

An ideal site close to the customers is selected to install a photovoltaic (PV) system in Shyogwe Sector of Muhanga District, Southern Province, Rwanda, with coordinates of -2°5’7” latitude and 29°46’23” longitude. The specified area is located in the equatorial zone. From geographical standpoint, the equatorial region receives more significant of solar radiation amount than other areas. The yearly global irradiation is 1,853kW/m$^2$ with an average temperature of 19.9°C. The PV system exploits the high solar potential in the selected location and minimizes the high temperatures drawbacks. The solar PV system produces electricity to power residential loads in the vicinity of a wetland valley and water pumping systems for agricultural purposes. The PV*SOL software features a climate database derived from MeteoNorm by the Swiss climate and weather data specialists at Meteotest (URL-6). Figure 5.1 shows the outside temperature values and the amount of irradiance onto horizontal for the first week of June.

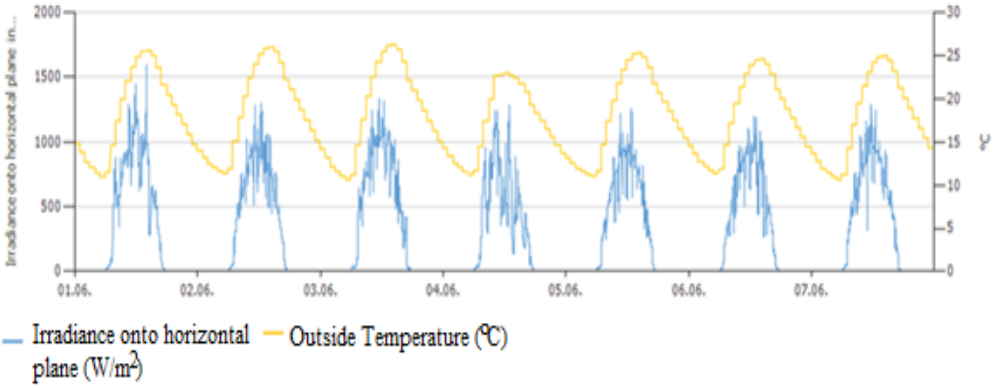


Figure 5.1. Outside temperature and irradiance amount onto horizontal surface for the first week of June

## 5.3. Load Profile

The load profile for residential refers to household electricity usage and is typically represented using hourly demand data or assumptions (Elma & Selamogullari, 2012).

In this study, the consumers mainly belong to Rwanda's middle social class. These households typically reside in small houses consisting of three bedrooms, a living room, and an outside adjacent small kitchen. While some of these households have access to the electrical grid, those that are grid-connected primarily use electricity for lighting, powering household appliances such as radios and television sets, and charging mobile phones. In this study, we are exploring the potential additional applications of electricity to benefit the local community. The energy produced by PV system can be used for agriculture water pumping systems, leading to increased agricultural productivity and improved quality of life for the community.

Table 5.2 shows the daily data for load estimation and consumption. After consulting the power ratings of the most commonly used home appliances in 20 households (20% of the total load), the load profile was calculated. It was assumed that the remaining houses would have a similar load demand. The specific load profile data has been inputted into the PV*SOL software.

To summarize, the total calculated values for yearly energy consumption and peak load demand are 82.34MWh and 30.4kW, respectively.

Table 5.2. Daily load consumption for 100 households estimation

| Type of load | Type of Appliances | Total Number of Appliances | Power Ratings in W | Total power in kW | Time of Use in Hours | | Daily Consumption in kWh | | |
|---|---|---|---|---|---|---|---|---|---|
| | | | | | Day Time | Night Time | Day Time | Night Time | Total Energy |
| House | Incandescent Lamp in the bedroom | 300 | 15 | 4.5 | | 6 | | 27 | 27 |
| | Incandescent Lamp in kitchen and sitting room | 200 | 15 | 3 | | 3 | | 9 | 9 |
| | Incandescent Lamp in hallways | 100 | 15 | 1.5 | 2 | 4 | 3 | 6 | 9 |
| | Incandescent Lamp for external light | 200 | 15 | 3 | | 12 | | 36 | 36 |
| | Radios | 100 | 60 | 6 | 5 | 4 | 30 | 24 | 54 |
| | TV set | 100 | 80 | 8 | 2 | 6 | 16 | 48 | 64 |
| | Phone Charging | 200 | 6 | 1.2 | 3 | | 3.6 | | 3.6 |
| Irrigation | Water Pump | 2 | 2200 | 4.4 | 4 | 2 | 17.6 | 8.8 | 26.4 |
| | | | | | | Total | 70.2 | 158.8 | 229 |

## 5.4. System Configuration

### 5.4.1. PV Modules

The PV*SOL software database contains a comprehensive list of PV modules currently available. Users can manually select modules from this list, following which PV*SOL will suggest the most appropriate one to use. Monocrystalline modules from various producers were selected, and PV*SOL picked out the most suitable modules based on the location and load profile.

Factors like shading, module degradation, and the desired consumption ratio influence the number of modules needed. The number of modules can also be adjusted as monthly or annual consumption percentage. The desired ratio to consumption has two parameters: the reference period and the desired ratio to consumption (consumption margin). The reference period refers to the specific time of the year that PV*SOL uses as a basis for sizing the PV modules to meet the energy demand over the entire year.

During this research, the module's shading factor was set to 5%, and its degradation was set to 1% over a year. Various values ranging from 90% to 120% were selected for the target desired ratio to consumption, and the outcomes are compared.

### 5.4.2. Inverters and Battery System

Various types of inverters with varying configurations database is available in PV*SOL. The various type of inverters are selecting from a list of inverter and PV*SOL software analyzes and optimizes the compatibility from selected inverters and identifies suitable inverter configurations for the PV system. The identical process is used when selecting the BESS. Figure 5.2 illustrates the single-line diagram circuit of the system under consideration. Details about the system's components are provided at the bottom. The electrical parameters of the PV module and BESS at standard test conditions (STC) are presented in Table 5.3. Table 5.4 contains the technical parameters utilized in PV*SOL software for designing and simulating the PV system with BESS.

Table 5.3. PV panel and battery electrical data at STC

| **PV Panel Electrical Data** | |
|---|---|
| Model | Q.PEAK DUO XL-G9.3 455 |
| Manufacturer | Hanwha Q.CELLS |
| Cell Type | Si monocrystalline |
| Nominal Output Power | 455W |
| MPP Current | 10.2A |
| MPP Voltage | 44.61V |
| Short-Circuit Current | 10.67A |
| Open Circuit Voltage | 53.22V |
| Efficiency | 20.42% |
| Fill Factor | 80.13% |
| **Battery Electrical Data** | |
| Type | Lithium iron – Lithium iron phosphate |
| Manufacturer | Sonnen GmbH |
| Model | sonnenBatterie 10 / 99kWh - 27.6kW |
| Cells Number | 32 |
| Nominal Voltage | 102.4V |
| Self-Discharge | 2% per Month |
| Internal Resistance | 13mΩ |

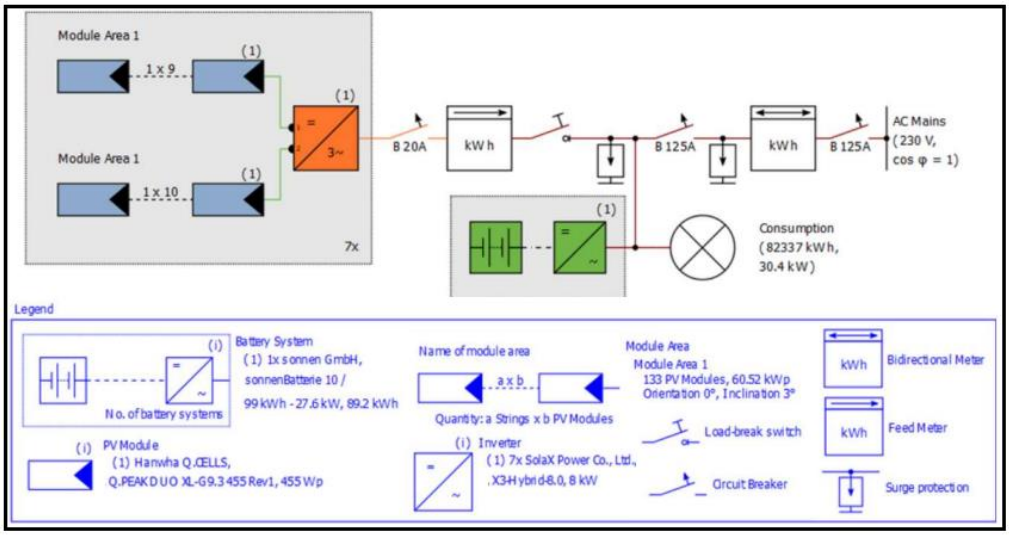


Figure 5.2. PV system and BESS proposed single line diagram

Table 5.4. PV system technical parameters

| **Configuration: Grid-Connected PV System with Electrical Appliances and Battery Systems** | | |
|---|---|---|
| **Climate Data:** | County: Rwanda,<br>Location: Shyogwe | Latitude: -2º5'7"<br>Longitude: 29º46'23" |
| **AC Mains** | Voltage (N-L1): 230V<br>Number of Phases: 3-Phase | |
| **Model for Irradiation on the Inclined Plane**: Hay & Davies<br>**Model for Diffuse Irradiation**: Hofmann | | |
| **Load** | Peak Load: 30.4kW<br>Annual Consumption: 82337kWh | |
| **Shading and Degradation of PV Modules** | Shading Percentage Value: 5%<br>Degradation of Module | Linear (straight-line)<br>Remaining power after 20 years: 80% |
| **Desired Ratio to Consumption** | Desired Ratio: 90% - 120% | Reference Period: Year and Worst Month |
| **Installation Type** | Fix Mounted – Open Space | |
| **Inclination** | 3º | |
| **Orientation** | 0º | |

## 5.5. Financial Analysis

Determining the necessary investment for implementing the planned PV system is a key aspect of financial analysis. This involves collecting information on the return on investment, amortization period, and cost of installation and production, operating and maintenance expenses. Financial analysis plays an important role in deciding the feasibility of investing in a solar PV system. PV*SOL software allows for the input of various financial parameters, as well as the sold electricity price to a third party, feed-in

concept, energy balance, the energy price inflation rate, and net-metering tariffs. In this particular study, the PV system under consideration is being analyzed over a 20-year period. The parameters for financial analysis are detailed in Table 5.5.

Table 5.5. Financial analysis parameters

| Parameter | Description |
|---|---|
| **Evaluation Period** | 20 years |
| **Installation Cost** | 2,240 US$/kWp |
| **Net Metering Tariffs** | Consumption type: Residential (0.24 US$/kWh) |
| **Expenses for Operation and Maintenance** | 1% of investment |
| **Energy prices Inflation Rate** | 2.9 %/Year |

## 5.6. Simulation Results

This study is carried out simulation and design of a grid-connected solar PV system with BESS for a community of 100 households in the Shyogwe Sector of the Muhanga District, Southern Province, Rwanda.

In order to achieve the system's independence from the grid different desired ratios were considered (90%, 100%, 110%, and 120%). The simulation was conducted for the entire year, and the worst month (month with the lowest solar radiation levels at the location). This is essential in optimizing the appropriate the desired ratio to consumption parameter to achieve greater self-sufficiency in meeting the yearly load demand. To examine the impact of shading, for each reference period and desired ratio to consumption combination, shading values of 0%, 5%, 10%, and 15% were evaluated and the values across different shading levels were recorded. Overall, eight cases were investigated. Table 5.6 gives the simulation results summary report from different cases.

The results of various scenarios are evaluated by grading them on a scale from 100% to 60% based on each parameter best and worst outcomes. The considered parameters were the performance ratio, return on assets, level of self-sufficiency, payback energy ratio, and amortization period. In Table 5.7 the performance analysis results summary are presented.

Technically and financially, the case with the desired ratio of 110% with the year as a reference period was chosen as the best scenario for this study. The performance ratio,

level of self-sufficiency, payback energy ratio, and direct power consumption are 86.05%, 64.38%, 89.14%, and 68.65%, respectively. The amortization period for all scenarios ranged from 9.55 years to 10.87 years. The PV system, BESS, or Grid directly provide the power. The BESS primarily is charged from the PV system and occasionally from the grid. Energy consumption and energy flow graph are shown in Figure 5.3 and Figure 5.4, respectively. The financial analysis indicates a 9.14% return on assets of the system and 9.65 years as the amortization period. The accrued cash flow is demonstrated in Figure 5.5.

Table 5.6. PV*SOL simulation results summary

| **Desired Factor** | **90%** | | **100%** | | **110%** | | **120%** | |
|---|---|---|---|---|---|---|---|---|
| **Reference Period** | **Year** | **Worst Month** | **Year** | **Worst Month** | **Year** | **Worst Month** | **Year** | **Worst Month** |
| PV Output Power (kWp) | 46.98 | 48.8 | 52.1 | 53.81 | 57.33 | 59.27 | 62.68 | 64.61 |
| PV Modules Area ($m^2$) | 230.05 | 238.95 | 255.12 | 263.45 | 280.72 | 290.15 | 306.87 | 316.35 |
| Modules Number | 103 | 107 | 114 | 118 | 126 | 130 | 138 | 142 |
| PV Energy (MWh/Year) | 68.16 | 71.11 | 75.84 | 77.92 | 83.41 | 85.96 | 91.43 | 93.77 |
| Grid Feed-in (MWh/Year) | 14.53 | 16.66 | 20.12 | 21.71 | 26.17 | 28.37 | 32.97 | 35.00 |
| Battery Charger from PV System (MWh/Year) | 29.57 | 30.10 | 30.95 | 31.26 | 31.94 | 32.17 | 32.65 | 32.83 |
| Battery Charger from Grid (kWh/Year) | 0.75 | 0 | 0 | 0.75 | 0.75 | 1.75 | 1.75 | 1.5 |
| Direct Own Use (MWh/Year) | 24.06 | 24.34 | 24.77 | 24.95 | 25.31 | 25.46 | 25.83 | 25.94 |
| Consumption from Grid (MWh/Year) | 32.55 | 31.76 | 30.69 | 30.26 | 29.35 | 29.01 | 28.21 | 28.00 |
| Consumption from Battery (MWh/Year) | 25.71 | 26.21 | 26.91 | 27.17 | 27.71 | 27.91 | 28.31 | 28.46 |
| Own Power Consumption | 78.68 % | 76.55% | 73.48 % | 72.15% | 68.65 % | 67.05% | 63.95% | 62.70% |
| Level of Self Sufficient | 60.60 % | 61.38% | 62.80 % | 63.28% | 64.38 % | 64.78% | 65.78% | 66.05% |
| Performance Ratio | 85.78 % | 86.15% | 86.03 % | 85.63% | 86.05 % | 85.78% | 86.25% | 85.83% |
| Return on Assets | 9.39% | 9.27% | 9.26% | 9.19% | 9.14% | 8.69% | 7.94% | 7.54% |
| Amortization Period (Years) | 9.6 | 9.55 | 9.57 | 9.62 | 9.65 | 9.97 | 10.55 | 10.87 |
| Payback Energy Ratio | 44.64 % | 52.47% | 65.57 % | 71.75% | 89.14 % | 97.65% | 116.81 % | 125.02% |

Table 5.7. PV*SOL simulation results performance analysis

| Desired Factor | Reference Period | Payback Energy | Level of Self Sufficient | Return On Assets | Performance Ratio | Amortization Period | Total Average |
|---|---|---|---|---|---|---|---|
| 90% | Year Worst | 60% | 60% | 100% | 70% | 100% | 78% |
| 90% | Month | 60% | 70% | 100% | 95% | 100% | 85% |
| 100% | Year Worst | 75% | 80% | 100% | 90% | 100% | 89% |
| 100% | Month | 75% | 80% | 100% | 60% | 100% | 83% |
| 110% | Year Worst | 85% | 90% | 95% | 90% | 100% | 92% |
| 110% | Month | 90% | 95% | 85% | 70% | 85% | 85% |
| 120% | Year Worst | 100% | 100% | 70% | 100% | 70% | 88% |
| 120% | Month | 100% | 100% | 60% | 75% | 60% | 79% |

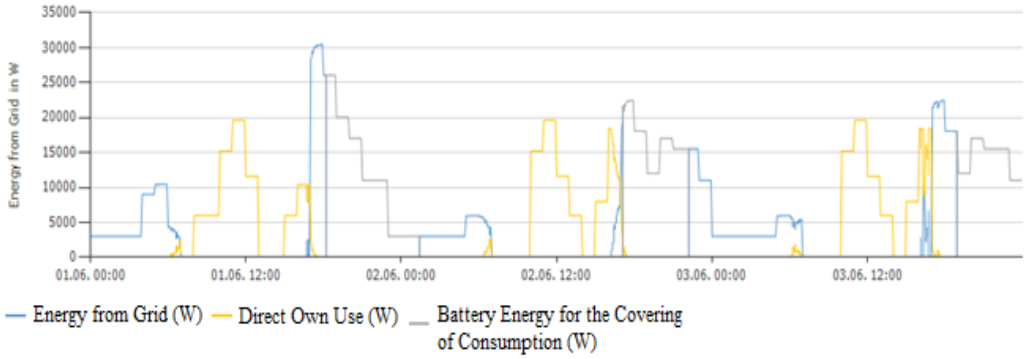


Figure 5.3. Direct Own Use, energy supplied from the grid, and energy sourced from BESS (consumption between 1-3 June)

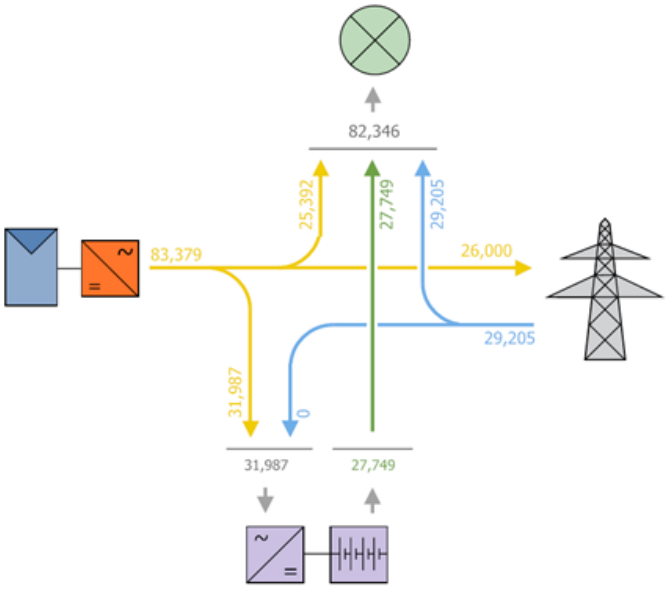


Figure 5.4. Annual energy flow graph in kWh for 110% desired ratio and year as reference period

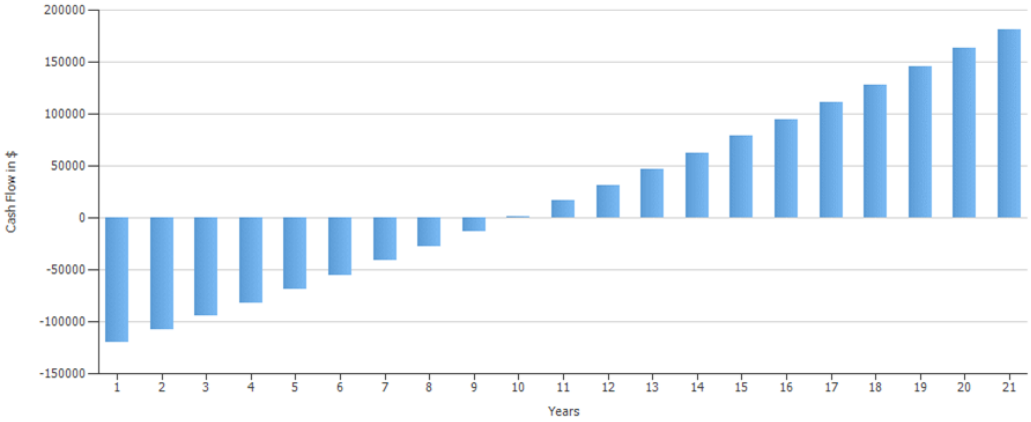


Figure 5.5. Accrued cash flow (cash balance)

## 5.7. Conclusion

A grid-connected solar PV system with a BESS using PV*SOL is designed and simulated. The initial step involved establishing the load profile and designing the PV system. This includes selecting the solar-related parameters such as module degradation, desired ratio to consumption, load profile, shading value, and choosing the location. The chosen location is in the Shyogwe sector of the Muhanga district in Rwanda. The yearly consumption was determined to be 82.34MWh with a peak load of 30.4kW. The obtained simulation results proved that grid-connected solar PV system with a BESS could meet the load requirements with 64.38% self-sufficiency level, 68.65% direct power consumption, 89.14% energy payback ratio, and 86.05% performance ratio. The financial analysis revealed 9.14% return on assets, and 9.65 years of amortization period. This study highlights the vital role and techno-economic feasibility of PV systems with BESS in developing countries in decreasing grid dependency while enhancing the availability and reliability of electricity.

# 6. INVERTERS CONFIGURATION AND CHARGE CONTROLLER FOR SOLAR PV AND BESS INTEGRATION

Most of the DG sources in an MG are inverter-based power sources (IBPS) such as solar and wind energy sources. Some of MG includes PV systems together with BESS. An inverter is a power converter device used as a link to connect an MG to the main grid network. According on the basis of PV module connection configurations, the classifications of PV inverters are PV module inverters or micro-inverters, multi-string inverters, string inverters, and central inverters. Depending on the control strategy used, three types of inverters are defined: grid-supporting inverters, grid-forming inverters, and grid-feeding inverters (David et al., 2017). In solar PV applications, the choice of the suitable inverter greatly influences the system's performance in meeting the requirement (Dogga & Pathak, 2019). Inverters used in solar PV applications are implemented by using different topologies such as multilevel inverters (David et al., 2017; Hasan et al., 2016; Mani et al., 2016; Odeh, 2016; Sezen et al., 2017), matrix inverters (David et al., 2017), two-level voltage source inverters (David et al., 2017), current source inverters (CSI) (David et al., 2017), and solid-state transformer (David et al., 2017). On the other hand, when integrated with BESS, the control strategy is in such a way to keep defined limit of the state SOC of the battery system.

## 6.1. Solar PV Inverter Configuration

Solar PV inverter configurations are classified according to several factors. Primarily, it represents the methods used to connect inverter with PV modules, and secondly, it represents the control method used for the PV system and electricity grid interconnection. According to the connection of PV modules, inverters are classified as central inverters, string inverters, multi-string inverters, and PV module inverters. Depending on control strategies, solar PV inverters are classified as grid-following inverters, grid-forming inverters, and grid-supporting inverters further classified as grid-support grid-following and grid-support grid-forming inverters (Vinayagam et al., 2017).

### 6.1.1. PV Inverters on the Basis of Modules Configuration

A PV system comprises PV modules connected in parallel and/or series (strings). On the other hand, the inverter is the link between the AC grid or AC load and PV modules. PV modules produce only DC power, that is why to convert that DC power to AC power an inverter is needed. The ways a group of modules are connected to a single or multiple inverter can be used to define an inverter configuration (Corba et al., 2012).

The central configuration, based on one centralized inverter for all modules of a solar PV plant, offers a cost-effective solution. PV modules are connected in series to form a string, and these strings are connected to each other through a diode. A single inverter is then used to convert the total DC power from all strings to AC power. The advantage of this configuration is the reduction in construction cost, making it an attractive option. However, it's important to be aware of the potential disadvantages, such as power losses due to common MPPT for all strings, module mismatch, and string diodes.

String inverter configuration is based on converting the DC power of each string separately. Inverter with MPPT is connected to each PV string. This configuration overcomes the advantages of a central inverter by reducing the power loss due to the individual MPPT for each string. However, the construction cost is high due to the use of many inverters.

The multi-string inverter configuration provides solution that combines central and string inverters advantages (low power loss and low cost). DC-DC converters with independent MPPT, unlike the string configuration, is connected to each string and then a common inverter is connected to all these converters. For the module inverter configuration, each individual module is connected to its own inverter. This design offers significant advantages, including a reduction in power loss as each module has its own MPPT, and the elimination of module mismatch. However, the production cost for this configuration is higher. Figure 6.1 shows different types of inverters configuration based on module configuration.

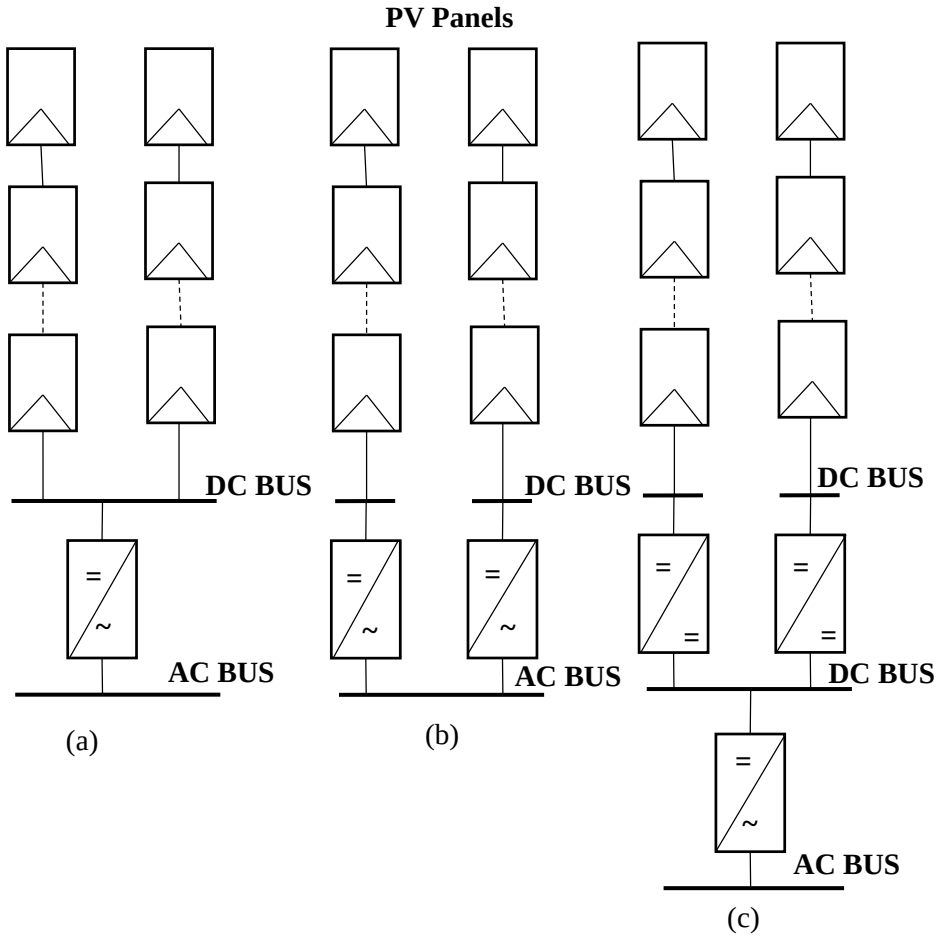


Figure 6.1. Solar inverter configuration: (a) central inverter, (b) string inverter, (c) multi-string inverter

### 6.1.2. PV Inverter Configuration on the Basis of Grid Connection

This classification of inverter mainly depends on the interconnection control of the inverter to the grid. More precisely, it defines the function of the inverter toward the grid or in a microgrid.

Grid-following inverters (GFL) are widely used to integrate solar PV and BESS into electric grids (Y. Li et al., 2021). In GFL, reactive power is injected into the grid and is controlled as current source inverter (CSI). GFL inverter feeds a controlled current into the grid and through phase-locked loop (PLL), follows phase angle of the grid voltage (Y. Li et al., 2021; Reichert et al., 2017).

During standalone or islanding mode of operation in MG system, GFL inverter cannot operate independently because it needs an external voltage signal for synchronization. Grid forming inverter (GFM) ensures the operation of MG in islanded mode by providing frequency and voltage references for electrical loads and DGs in MG network (Antunes et al., 2020). Achieving high penetration of RES, improved voltage harmonics, and the capability to replace synchronous generators for grid ancillary services are the advantages associated with grid-forming inverters.

The duality in the relationship between GFL and GFM can be re-classified as a voltage-following current-forming inverter and a current-following voltage-forming inverter (Y. Li et al., 2021). In MGs and grids dominated by IBPSs, inverters share active and reactive power and simultaneously form the grid voltage and current. This function cannot be achieved by a following inverter or grid-forming inverter. However, this task is achieved by grid-supporting inverters (Reichert et al., 2017).

To improve power quality, grid-supporting inverters can be used. In the literature, different control strategies are presented for inverter configurations in grid-connected and/or islanded modes of operations. Grid support grid forming allows the power inverter to operate in both grid-connected and islanded modes of operation of MG without changing control configuration (Vinayagam et al., 2017). As the increase of IBPS in a power system reduces the synchronous generators number that are the source of voltage inertia and frequency regulation in the grid, implementing grid-supporting PV system offers inertia and participation in regulation of frequency (Xu et al., 2018). Models for different inverter configurations (Du et al., 2021; Rahmoun et al., 2017), and sizing (Gouveia & Moreira, 2019) were presented. In the literature, control techniques are such as droop control for grid forming (David et al., 2017; Du et al., 2021; Y. Li et al., 2021; Rahmoun et al., 2017; Schömann et al., 2019), PLL control for grid following inverter (Du et al., 2021; Y. Li et al., 2021), droop control for grid supporting inverter (David et al., 2017; Xu et al., 2018), droop control and voltage control loop for grid support grid forming inverter (Vinayagam et al., 2017), virtual synchronous generator control for grid supporting inverter (Xu et al., 2018).

## 6.2. MPPT and Charge controller

Energy harvesting from solar energy sources by using solar PV material goes with the introduction of different techniques and control algorithms to increase energy production as much as possible. The maximum power point tracker (MPPT) is used to maintain PV modules maximum power point by matching the current and voltage operating points with the load characteristics. Furthermore, BESS integrated with PV systems are charged through battery chargers that need to be controlled. With a charger controller, the state of charge of batteries is controlled. Charger controllers analyze the conditions of the PV modules and load to decide whether batteries must be charged or discharged.

### 6.2.1. MPPT Algorithms

The output P-V and I-V characteristics of a solar cell show that, at given conditions, there is a current and voltage at maximum power. The maximum power can be attained by controlling the output voltage or current of PV panels. Various MPPT algorithms have been proposed. Although all MPPT algorithms have the same purposes, their functionalities differ according to efficiency, tracking speed, steady-state oscillations, hardware implementation, and cost (Mao et al., 2020; Motahhir et al., 2020). MPPT approaches are classified into three groups. The most popular is known as direct control techniques or the conventional MPPTs. It is based on specific observations by applying control signals to power converters. The conventional MPPTs are incremental conductance (INC), hill climbing (HC), and perturb and observe (P&O) methods. The second MPPT group tracks the characteristics of PV panels, also known as intelligent or indirect methods. The third group is based on soft computational techniques. Those techniques deal with approximate models to give optimum solutions, and are Artificial Neural Network (ANN), Kalman filter, and Fuzzy Logic Controller (FLC). The third method is known as the optimization method. Different methods for MPPT have been proposed or exist (Mao et al., 2020; Motahhir et al., 2020; Yap et al., 2020). During uniform solar radiation, conventional MPPT is preferred as there is only one maximum power point to track. During partial shading conditions, there are multiple maximum power points (MPP); one is called global MPP, and the others are local MPPTs. Hence, the MPPT methods based on tracking of PV characteristics and on approximate models are preferred to differentiate global MPP and local MPP (Bollipo et al., 2020).

The perturb & Observe (P&O) method uses the trial and error technique for MPP determination. The output voltage is updated by comparing the power from two points in a P-V characteristics curve. The algorithm calculates the power from the two points and compares the results. The flow chart algorithm representation of P&O technique is shown in Figure 6.2. This method continuously tracks the change of the power of PV module. The process consists of setting and comparing a reference power with the actual power. The results obtained help in deciding how to update the output voltage of PV module. In other words, the measured output power and previous power are compared. To cause power variation, a minor perturbation is introduced. The same process continues if the power increases. The perturbation is reversed, if the power decreases. From the P-V characteristics of a PV module, if the increase in voltage leads to an increase in the output power, this means that the MPP is located on the right-hand side of the operating point. Thus, a perturbation increases the output voltage and it is required to move the operation point toward the MPP. If the increase in the output voltage leads to a decrease in the output power, the MPP is be located on the left-hand side of the operating point. Thus, a negative perturbation is needed (Bollipo et al., 2020; Mao et al., 2020; Salman et al., 2018).

The Incremental Conductance (INC) algorithm acquires fixed and high potential step size to maintain the high accuracy rate. The INC algorithm uses the derivative of power with respect to the output voltage of a PV module ($dP/dV$) to track MPP. From the P-V characteristic, the power delivered by a PV panel is maximum when $dP/dV$ equals zero. Thus, the INC algorithm achieves the tracking process if $dP/dV$ is zero. The mechanism of INC is similar to the P&O algorithm. However, it uses the I-V relationship to track the MPP. Figure 6.3 shows the flow chart of the INC MPPT algorithm (Bollipo et al., 2020; Mao et al., 2020).

The Hill Climbing (HC) method Operates like P&O. The difference is that P&O perturbs the voltage or current, whereas HC perturbs the duty cycle. As for the other methods, the process starts by guessing the initial solution. With incremental steps, the search for the optimum solution is conducted. The limitations of MPPT methods lie in the oscillations around MPP and in differentiating the real cause of the power change (Bollipo et al.,

2021; Mao et al., 2020). MPPT is implemented in different configurations with a DC-DC converter or in an Inverter.

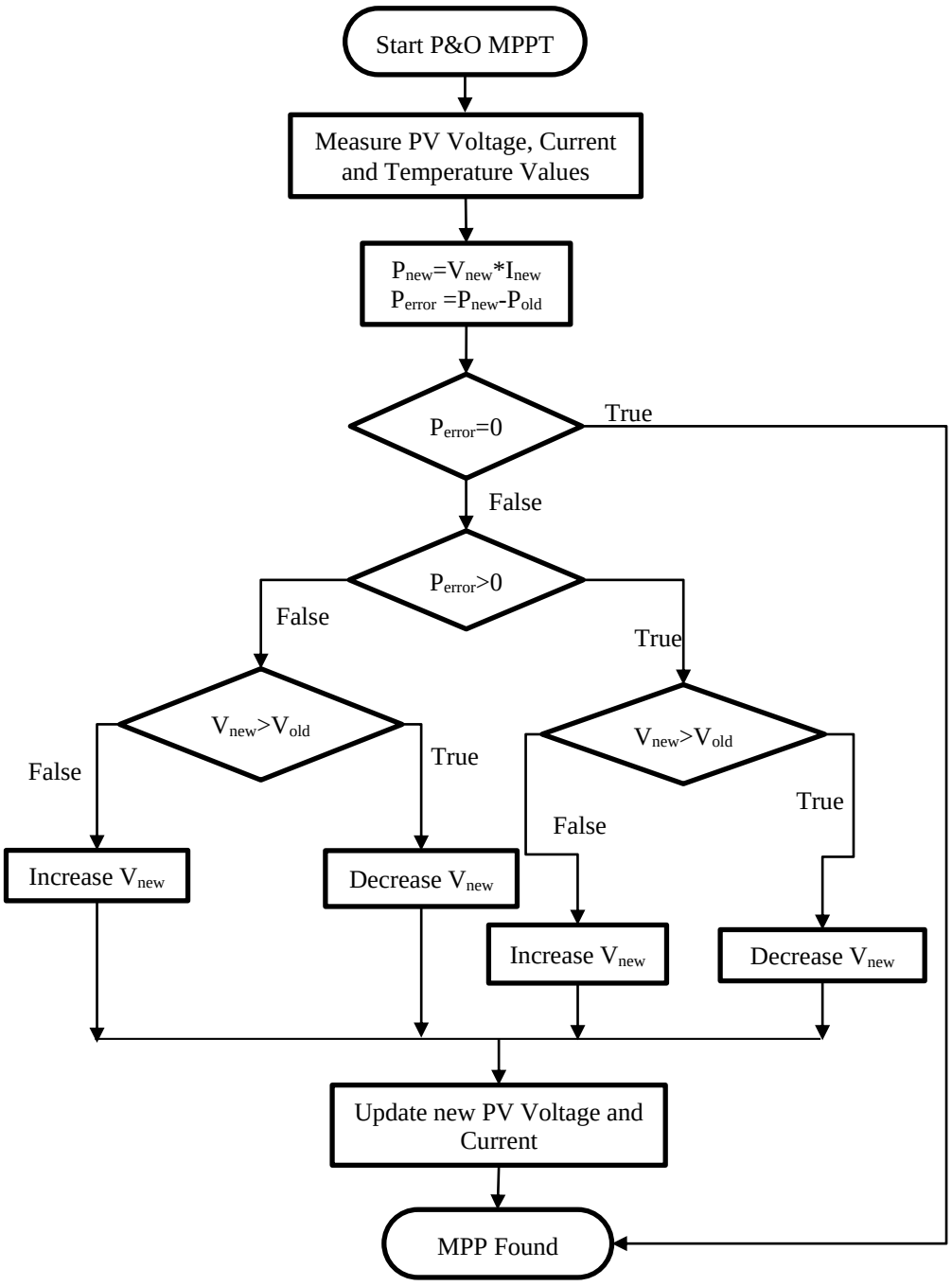


Figure 6.2. Flow chart representation of P&O algorithm

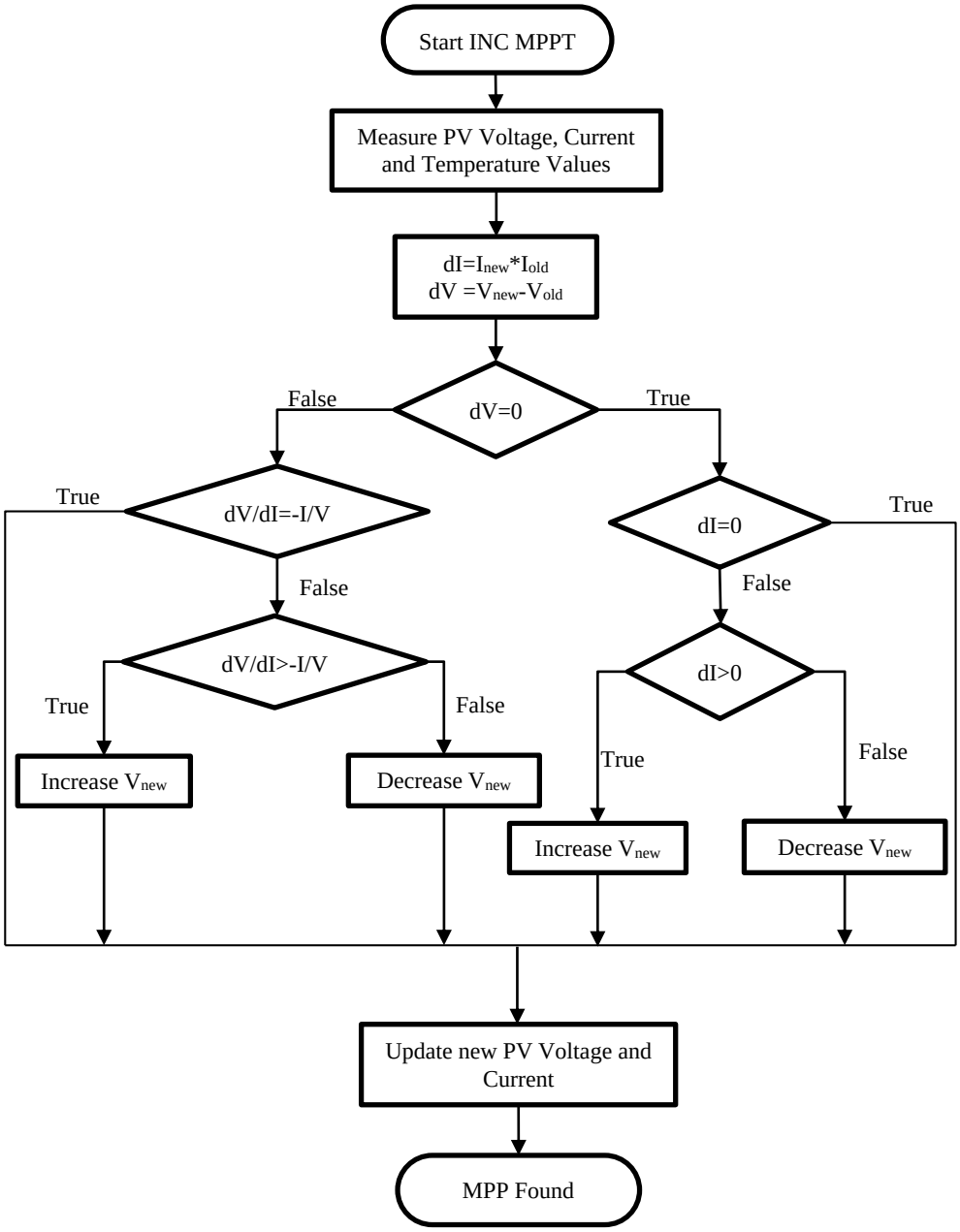


Figure 6.3. Flow chart representation of INC MPPT algorithm

### 6.2.2. Charger Controller

Batteries are usually used to store energy generated from a PV system. PV modules and batteries are connected by charger controllers. A solar charger controller, in a more simplified way, control the charging process between the solar panels and the battery. A DC-DC power converter is used to adjusting the operating duration of a boost converter by increasing the PV panel output voltage. In the charger controller, the input voltage from PV modules is controlled to match the battery charging voltage. Battery charging,

protecting the battery from overcharging, supplying DC load, and supplying DC power to DC-AC inverter for AC load or grid connection are the features that can be provided in a charger controller. Different studies on DC-DC converter topologies, such as isolated and non-isolated DC-DC converters, were conducted in the literature (Amir et al., 2019). A high voltage gain DC-DC converter topology is favorable for PV system applications for battery charging and other applications such as in multiple string inverters and modular inverters.

# 7. MODIFIED RBTS BUS-2 DISTRIBUTION NETWORKS RELIABILITY ANALYSIS

This study presents the integration at the distribution level of solar PV systems with BESS. The study focuses on the reliability evaluation of a modified Roy Billinton Test System (RBTS) Bus-2 distribution network integrated solar PV system and BESS by considering estimated load profiles (ELP). While considering varying load profiles, the results from the PV*SOL simulation tool indicated a reduction of 50.30% of the PV system required peak power.

In DigSILENT PowerFactory, quasi dynamic analysis revealed that while considering varying load profiles, the PV system with BESS can support the grid up to 39.98%. The reliability analysis also revealed the potential of PV system with BESS to improve system's reliability, with 29.75% for system interruption frequency, 43.4% for customer interruption frequency and duration, and 5.09% for system interruption duration.

## 7.1. Methodology

The reliability of the standard RBTS Bus-2 is compared with that of the modified RBTS Bus-2 integrated with a solar PV system and BESS.

DigSILENT PowerFactory is used for modeling and reliability simulations. PV*SOL is used to simulate data of solar PV systems. Solar PV systems and BESS are integrated into the standard RBTS Bus-2 at each load center, and their impact on the system's reliability is evaluated.

Integrating solar PV Systems with constant and varying load demand profiles are the considered scenarios. PV system and BESS power characteristic for each load point (LP) is determined using the PV*SOL simulation tool. The location considered during the simulation is Rwanda, with 50% and 100% desired ratios to consumption. As advised in PV*SOL, the BESS capacity is selected to meet the load demand during the night. It is important to consider load demand profiles when sizing the peak power of a Solar PV system and the capacity of BESS.

In the case of the modified RBTS Bus-2, load profiles are estimated using the Standard Load Profiles (SLP) provided by the Federal Association of the German Energy and Water Industries (BDEW) and can be accessed in DigSILENT PowerFactory.

### 7.1.1. RBTS Bus-2

RBTS Bus-2 is a standard distribution network used to assess reliability for the purposes of education. It comprises 56 bus bars of 400V, 11kV, and 33kV, together with 132kV bus bars connecting the incoming line. The load data, which includes the numbers of customers and active power demand, are provided in (Allan et al., 1991).

The standard RBTS Bus-2 data are provided in Table 7.1, while the circuit diagram of the standard RBTS Bus-2 is shown in Figure 7.1.

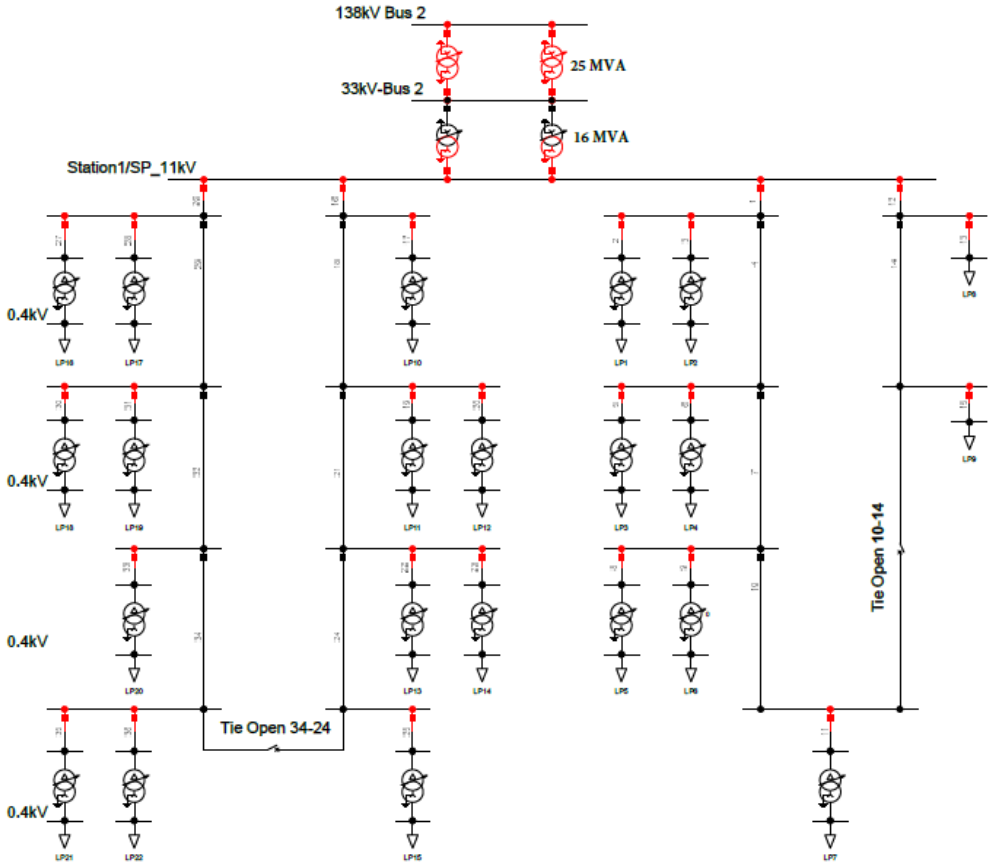


Figure 7.1. Electrical circuit diagram of RBTS Bus-2

Table 7.1. Standard RBTS Bus-2 input data (Allan et al., 1991)

| Load Data | | | Line Data | | | |
|---|---|---|---|---|---|---|
| Name | Number of Customers | Active Power [MW] | Line Length [km] | Name | Line Length [km] | Name |
| LP1 | 210 | 0.8668 | 0.75 | 1 | 0.8 | 23 |
| LP2 | 210 | 0.8668 | 0.6 | 2 | 0.75 | 24 |
| LP3 | 210 | 0.8668 | 0.8 | 3 | 0.6 | 25 |
| LP4 | 1 | 0.9167 | 0.75 | 4 | 0.8 | 26 |
| LP5 | 1 | 0.9167 | 0.8 | 5 | 0.75 | 27 |
| LP6 | 10 | 0.75 | 0.6 | 6 | 0.6 | 28 |
| LP7 | 10 | 0.75 | 0.75 | 7 | 0.75 | 29 |
| LP8 | 1 | 1.6279 | 0.8 | 8 | 0.6 | 30 |
| LP9 | 1 | 1.8721 | 0.75 | 9 | 0.8 | 31 |
| LP10 | 210 | 0.8668 | 0.6 | 10 | 0.75 | 32 |
| LP11 | 210 | 0.8668 | 0.8 | 11 | 0.8 | 33 |
| LP12 | 200 | 0.7291 | 0.75 | 12 | 0.6 | 34 |
| LP13 | 1 | 0.9167 | 0.8 | 13 | 0.75 | 35 |
| LP14 | 1 | 0.9167 | 0.6 | 14 | 0.8 | 36 |
| LP15 | 10 | 0.75 | 0.8 | 15 | | |
| LP16 | 10 | 0.75 | 0.75 | 16 | | |
| LP17 | 200 | 0.7291 | 0.6 | 17 | | |
| LP18 | 200 | 0.7291 | 0.8 | 18 | | |
| LP19 | 200 | 0.7291 | 0.75 | 19 | | |
| LP20 | 1 | 0.9167 | 0.8 | 20 | | |
| LP21 | 1 | 0.9167 | 0.6 | 21 | | |
| LP22 | 10 | 0.75 | 0.75 | 22 | | |

| Line and Transformer failure data | | |
|---|---|---|
| Name | Repair Duration [h] | Failure Frequency |
| 110kV Line | 5 | 0.065 [1/(a*km)] |
| 138/33kV - Transformer | 15 | 0.01[1/a] |
| 110/0.4kV - Transformer | 200 | 0.015 [1/a] |
| 33/11kV - Transformer | 15 | 0.015[1/a] |

### 7.1.2. Modified RBTS Bus-2

At each load point in the standard RBTS Bus-2 system, PV systems and BESSs are introduced, and Table 7.2 and Table 7.3 show the corresponding data, considering 50% and 100% desired ratio to consumption.

The diagram in Figure 7.4 illustrates the modified RBTS Bus-2 circuit diagram integrated with the PV system and BESS.

PV system and BESS Power profiles for the first seven days of the year for 0.75MW load are shown in Figure 7.2 and Figure 7.3, respectively. For BESS, positive values show the discharging power used to supply the load and negative values show the charging power.

Furthermore, Fault-clearing fuses are installed not only in the standard RBTS Bus-2 system, but also on each distribution line connected to the load point centers' bus bars. Additionally, fault-clearing fuses are added at the PV Systems and BESS' LV terminals and on the distribution lines linked to the load center bus bars that connect to the HV side of the step-up transformers of the PV System and BESS.

Table 7.2. Load center PV system installed capacity

| PV NAME | LOAD NAME | LOAD ACTIVE POWER [MW] | PV INSTALLED CAPACITY (kWp) | | | |
|---|---|---|---|---|---|---|
| | | | 50% Desired Ration to Consumption | | 100% Desired Ration to Consumption | |
| | | | With constant load | With varying load profile | With constant load | With varying load profile |
| PV-1 | LP1, LP2 | 1.7336 | 4658.4 | 2483.4 | 9316.8 | 4966.8 |
| PV-2 | LP3, LP4 | 1.7835 | 4792.4 | 2374.4 | 9585 | 4748.6 |
| PV-3 | LP5, PL6 | 1.6667 | 4478.6 | 2055 | 8957.2 | 4110 |
| PV-4 | LP7 | 0.75 | 2015.4 | 924.8 | 4030.6 | 1849.4 |
| PV-5 | LP8 | 1.6279 | 4374.4 | 2332 | 8748.8 | 4664 |
| PV-6 | LP9 | 1.8721 | 5030.6 | 2680.2 | 10061.2 | 5360.6 |
| PV-7 | LP10 | 0.8668 | 2329.2 | 1241.8 | 4658.4 | 2483.4 |
| PV-8 | LP11, LP12 | 1.5959 | 4288.4 | 2286.2 | 8576.8 | 4572.4 |
| PV-9 | LP13, LP14 | 1.8334 | 4926.6 | 2265.2 | 9853.2 | 4530.4 |
| PV-10 | LP15 | 0.75 | 2015.4 | 926.6 | 4030.6 | 1853.2 |
| PV-11 | LP16, LP17 | 1.4791 | 3974.6 | 1971 | 7949 | 3942.2 |
| PV-12 | LP18, LP19 | 1.4582 | 3918.4 | 2089 | 7836.8 | 4177.8 |
| PV-13 | LP20 | 0.9167 | 2463.2 | 1132.6 | 4926.6 | 2265.2 |
| PV-14 | LP21, LP22 | 1.6667 | 4478.6 | 2059.2 | 8957.2 | 4118.4 |

Table 7.3. Load center BESS capacity

| BESS NAME | LOAD NAME | LOAD ACTIVE POWER [MW] | BESS SYSTEM | | | |
|---|---|---|---|---|---|---|
| | | | With Constant Load | | With Varying Load Profile | |
| | | | No of battery | BESS capacity (kWh) | No of battery | BESS capacity (kWh) |
| BESS-1 | LP1, LP2 | 1.7336 | 14 | 15873.2 | 8 | 9070.4 |
| BESS-2 | LP3, LP4 | 1.7835 | 15 | 17007 | 7 | 7936.6 |
| BESS-3 | LP5, PL6 | 1.6667 | 14 | 15873.2 | 6 | 6802.8 |
| BESS-4 | LP7 | 0.75 | 6 | 6802.8 | 3 | 3401.4 |
| BESS-7 | LP10 | 0.8668 | 7 | 7936.6 | 4 | 4535.2 |
| BESS-8 | LP11, LP12 | 1.5959 | 13 | 14739.4 | 7 | 7936.6 |
| BESS-9 | LP13, LP14 | 1.8334 | 15 | 17007 | 7 | 7936.6 |
| BESS-10 | LP15 | 0.75 | 6 | 6802.8 | 3 | 3401.4 |
| BESS-11 | LP16, LP17 | 1.4791 | 12 | 13605.6 | 6 | 6802.8 |
| BESS-12 | LP18, LP19 | 1.4582 | 12 | 13605.6 | 6 | 6802.8 |
| BESS-13 | LP20 | 0.9167 | 8 | 9070.4 | 4 | 4535.2 |
| BESS-14 | LP21, LP22 | 1.6667 | 14 | 15873.2 | 6 | 6802.8 |

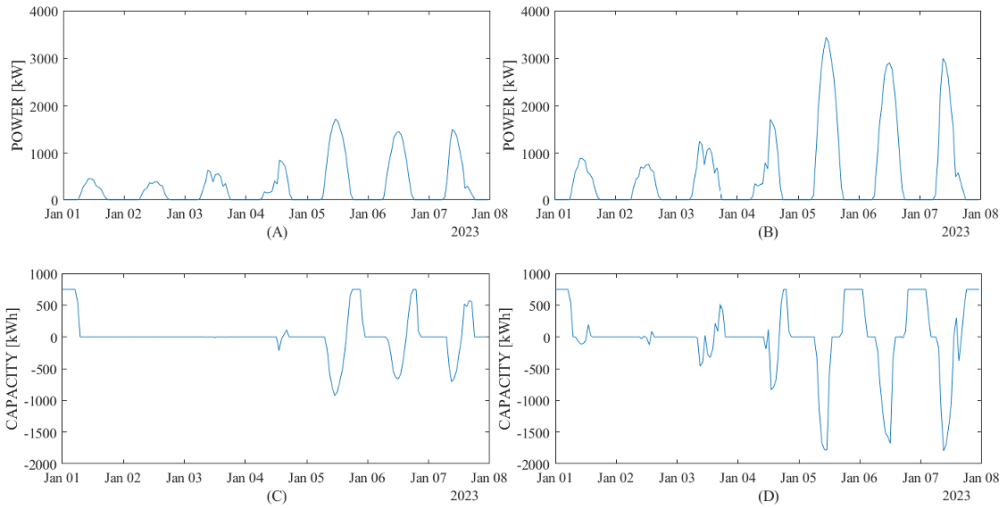


Figure 7.2. 0.75MW PV installed capacity with constant load point for 50% and 100% desired ratio to consumption: (A) and (B) PV system, (C) and (D) BESS charging and discharging capacity

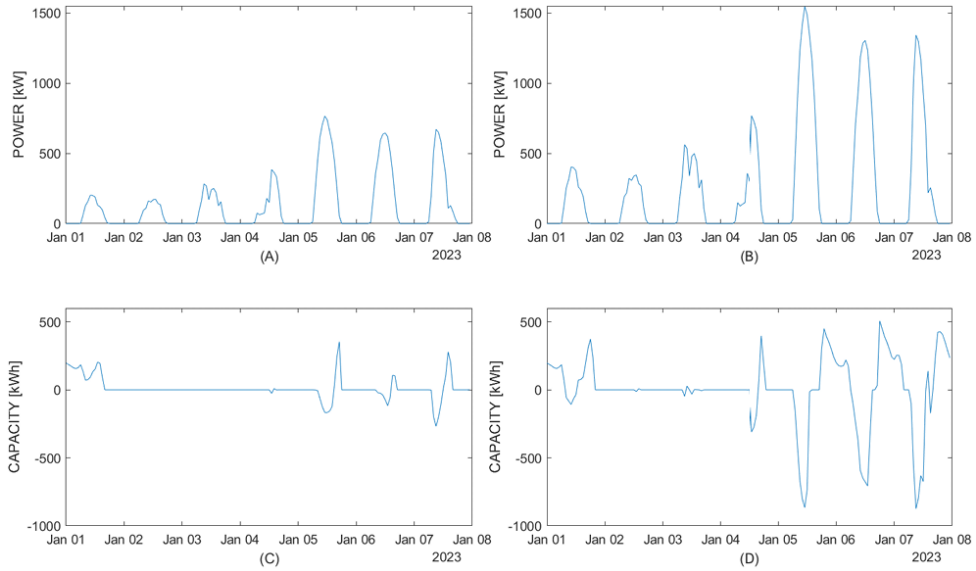


Figure 7.3. 0.75MW PV installed capacity with varying load profile for 50% and 100% desired ratio to consumption: (A) and (B) PV system, (C) and (D) BESS charging and discharging capacity

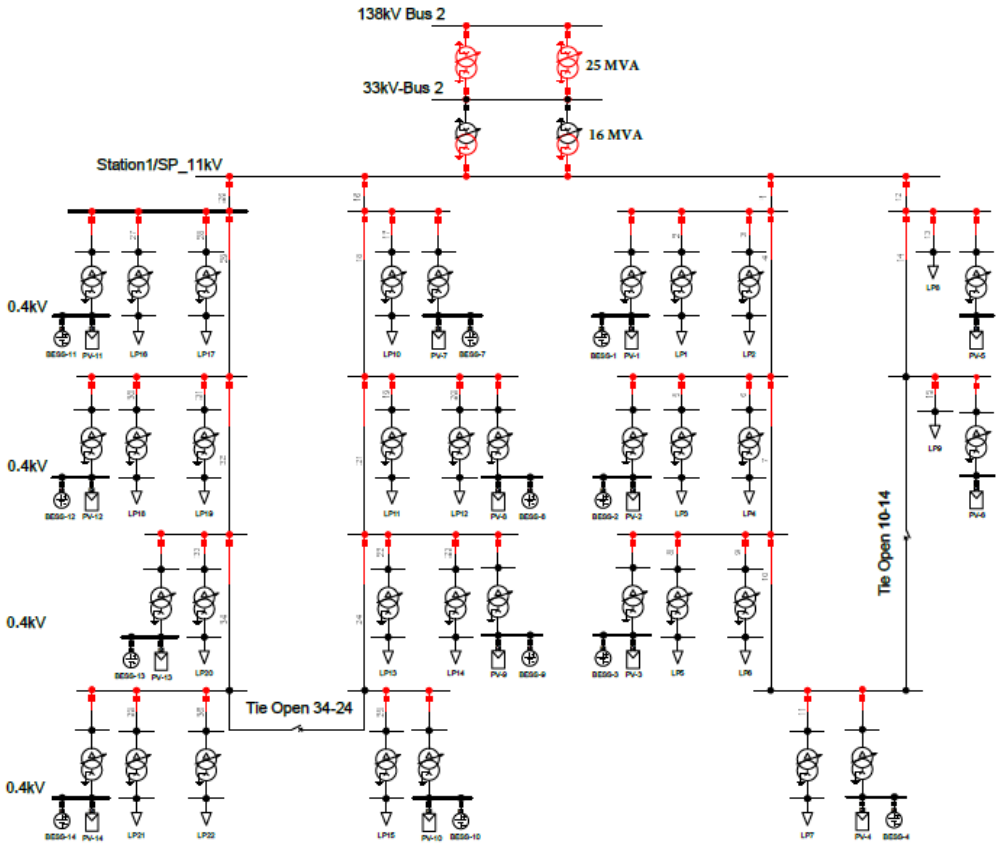


Figure 7.4. Modified RBTS Bus-2 single line diagram

## 7.2. Results and Discussions

### 7.2.1. Quasi-Dynamic Simulation

A load-flow analysis and quasi-dynamic simulation were conducted over the first seven days of the year and the performance of PV system generation profiles and the loading level of substation transformers in the RBTS Bus-2 system were assessed. The simulation results demonstrate the PV systems' ability to support the load demand. The substation transformer loading values in the modified RBTS Bus-2, integrated with only PV System and BESS, are shown in Figure 7.5 and Figure 7.6 for both constant and varying load profiles. In the case of constant load scenarios, for 50% desired ratio to consumption, the average values of distribution transformer loading are 27.24% with PV system and BESS and 31.8% with only PV system. For a 100% desired ratio to consumption, the average values of distribution transformer loading are 23.46% with PV system and BESS and 30.89% with only PV system. In scenarios with varying load profiles, for 50% desired ratio to consumption, the average values of substation transformer loading are 13.42% with PV system and BESS and 14.8% with only PV system. For the 100% desired ratio to consumption case, the average values of distribution transformer loading are 11.6% for the case with PV system and BESS and 14.37% with only PV system.

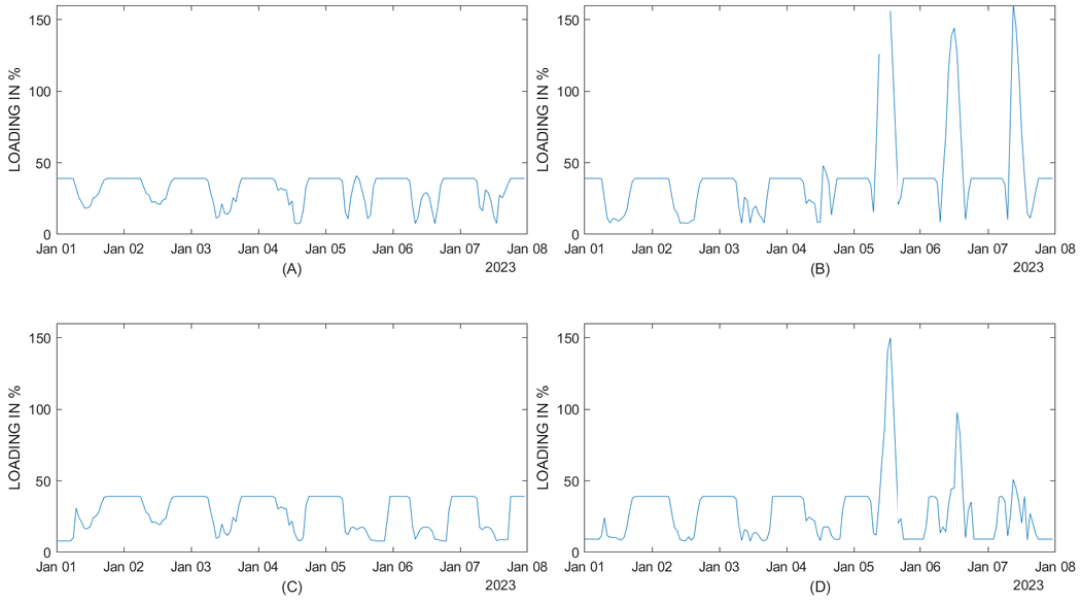


Figure 7.5. Loading of substation transformer for constant load with 50% and 100% desired ratio to consumption: (A) and (B) PV system, (C) and (D) PV system and BESS

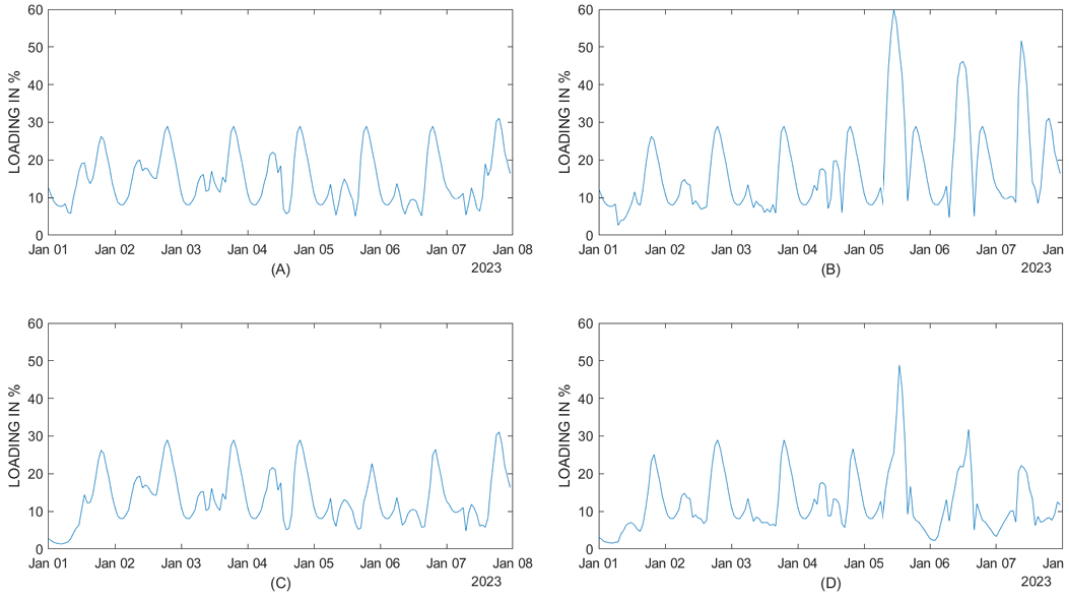


Figure 7.6. Loading of substation transformer for varying load with 50% and 100% desired ratio to consumption: (A) and (B) PV system, (C) and (D) PV system and BESS

### 7.2.2. Reliability Analysis Results

Two reliability analysis scenarios are considered under constant load profile and varying load profiles. Table 7.4 compares the reliability analysis results of the modified RBTS Bus-2 system for the reliability indices of the two scenarios with the standard RBTS Bus-2 system.

Table 7.4. Reliability indices comparison from simulation results

| Reliability index | Standard RBST Bus-2 | Modified RBTS Bus-2 with constant load profile | Modified RBTS Bus-2 with varying load profile |
|---|---|---|---|
| SAIFI [1/Ca] | 0.248211 | 0.140486 | 0.140486 |
| CAIFI [1/Ca] | 0.248211 | 0.140486 | 0.140486 |
| SAIDI [h/Ca] | 3.600 | 3.483 | 3.483 |
| CAIDI [h] | 14.502 | 24.792 | 24.792 |
| ASAI | 0.999589 | 0.999602 | 0.999602 |
| ASUI | 0.000411 | 0.000398 | 0.000397 |
| ENS [MWh/a] | 37.608 | 36.753 | 11.443 |
| AENS [MWh/Ca] | 0.020 | 0.019 | 0.006 |
| ACCI [MWh/Ca] | 0.110 | 0.179 | 0.056 |
| ASIFI [1/a] | 0.230444 | 0.168427 | 0.161874 |
| ASIDI [h/a] | 3.059892 | 2.990444 | 2.903902 |

For both scenarios, the reliability improvement is 3.23% for SAIDI, 43.4% for SAIFI and CAIFI, 3.24% for ASUI, and 0.001% for ASAI. The reliability improvement for the constant load profile scenario is 2.27% for ASIDI, 5% for AENS, 2.27% for ENS, and 26.91% for ASIFI. The reliability improvement for varying load profile scenario is 5.09% for ASIDI, 7% for AENS, 69.57% for ENS, 49% for ACCI, and 29.75% for ASIFI. The CAIDI index does not show improved reliability due to a 70.95% increase in interruption duration hours. Additionally, the ACCI has increased by 62.72% for the constant load scenario.

### 7.3. Conclusion

The results demonstrate the significance of considering load profiles when designing a solar PV system. As a result, the peak power needed for the PV system was decreased by 50.38% by considering the varying load profile. The quasi-dynamic analysis findings indicate that a PV system with BESS can contribute up to 39.98% support to the grid when taking into account varying load profiles. Furthermore, the reliability analysis results demonstrate that the PV system with BESS is capable of enhancing system reliability. Simulations reveal 29.75% enhancement in system interruption frequency, 43.4% improvement in customer interruption frequency and duration, and 5.09% reduction in system interruption duration.

# 8. RELIABILITY ANALYSIS AND LOAD FLOW CALCULATIONS OF RWANDA'S ELECTRICITY GRID ON DISTRIBUTION LEVEL AT NTONGWE AND GATUMBA FEEDERS INTEGRATED WITH PV SYSTEM AND BESS.

This study assesses how the integration of solar PV plants with BESS can improve the reliability of Rwanda's electricity grid, specifically at the distribution level of the Gatumba and Ntongwe feeders. It also examines the effects of integrating Solar PV power plants with BESS systems on Rwanda’s electricity grid from various perspectives. Gatumba and Ntongwe feeders are modelled in DigSILENT PowerFactory, and the Solar PV systems and BESS power flow profiles are simulated using PV*SOL software. For reliability enhancement of the grid to the feeders where solar PV system and BESS are connected, protection switches are configured so that the PV systems and BESS supply the load demand in the absence of the grid, thereby increasing the generation capacity and reducing interruption frequency and duration. Simulation results from DigSILENT and PV*SOL simulation tools showed that by integrating solar PV systems with BESS to Gatumba and Ntongwe feeders, the system reliability ameliorates by 71.6% and 95.5% for system average interruption frequency and duration, respectively.

## 8.1. Methodology

This study consists of the reliability analysis and load flow calculations of Rwanda’s electricity grid at distribution level on Gatumba and Ntongwe feeders integrated with PV system and BESS. Data are collected from Rwanda Energy Group. After data processing and load profile estimation, PV*SOL simulation tool is used for obtaining the generated PV system power profile and BESS for each load demand. In PV*SOL simulations, three scenarios were considered: 50%, 100%, and 150% as the desired ratio to consumption. The BESS capacity was chosen to match the nighttime load demand, based on PV*SOL's recommendation. The methodology for simulation in PV*SOL is explained in chapter 5. The modeling of Gatumba and Ntongwe feeders is done using DigSILENT PowerFactory. Load profiles, PV system, and BESS power profiles are added to the DigSILENT PowerFactory Model for all scenarios. After Quasi dynamic and Reliability simulations are performed. For Quasi dynamic and Reliability simulations 6 cases are considered as shown in Table 8.1.

The simulation steps include:

1. Estimating load profiles for Ntongwe and Gatumba Feeder's load points.
2. Performing PV*SOL simulations to size, analyze, and acquire the power characteristics of PV systems and BESS according to the scenarios specified in Table 8.1.
3. Modeling Ntongwe and Gatumba feeders in DigSILENT PowerFactory.
4. Importing load profiles, PV systems, and BESS power profiles into DigSILENT PowerFactory based on the cases in Table 8.1.
5. Performing quasi-dynamic and reliability analysis simulations in DigSILENT PowerFactory.

Table 8.1. Considered cases for reliability analysis

| **Scenario** | **Case** | **Scenario Description** | **Case Description** |
|---|---|---|---|
| | BASE CASE | | DigSILENT PowerFactory simulations without PV system and BESS |
| SCENARIO-1 | CASE-1 | PV system and BESS simulation in PV*SOL with 50% desired ratio to consumption | DigSILENT PowerFactory simulations with PV system (50% desired ratio to consumption) |
| | CASE-2 | | DigSILENT PowerFactory simulations with PV system and BESS (50% desired ratio to consumption) |
| SCENARIO-2 | CASE-3 | PV system and BESS simulation in PV*SOL with 100% desired ratio to consumption | DigSILENT PowerFactory simulations with PV system (100% desired ratio to consumption) |
| | CASE-4 | | DigSILENT PowerFactory simulations with PV system and BESS (100% desired ratio to consumption) |
| SCENARIO-3 | CASE-5 | PV system and BESS simulation in PV*SOL with 150% desired ratio to consumption | DigSILENT PowerFactory simulations with PV system (150% desired ratio to consumption) |
| | CASE-6 | | DigSILENT PowerFactory simulations with PV system and BESS (150% desired ratio to consumption) |

### 8.1.1. Ntongwe and Gatumba Feeders Configuration for Reliability Analysis

Compulsory and optional steps are configured in DigSILENT PowerFactory to complete the reliability assessment. The first step is to create failure stochastic models for lines, transformers, busbars, and switches. The second step is to define radial feeders. The third step is configuring switches for actuation time, switching stages, and power restoration. Finally, the number of connected customers, interruption cost, priority, and shedding load transfer are defined on the load side. In addition, optional steps are defining load characteristics, creating protection devices, creating maintenance plans, and specifying constraints. After configuration, the generation of reliability indices, with the help of the reliability analysis tool, consists of load modelling, failure modelling, failure effect analysis (FEA), system state creation, and statistical analysis. The failure models for Lines and transformers are configured according to the standard RBTS Bus-2 system, as the exact model data are unavailable, as shown in Table 8.2 (Allan et al., 1991). For PV system and BESS, availability data are calculated according to the power profile obtained from PV*SOL simulation.

Table 8.2. Failure data for lines and transformers

| **Element** | **Failure Frequency in [1/(a*km]** | **Repair Duration in h** |
|---|---|---|
| Line Failure Model | 0.065 | 5 |
| 110kV/30kV-Transformer Failures Model | 0.015 | 15 |
| 30kV/0.4kV-Transformer Failures Model | 0.015 | 200 |

### 8.1.2. Data Collection and Processing

Data Collection

A comprehensive set of data and information about the grid is essential for conducting a reliability analysis of an electricity grid. Those data are input into simulation software that performs the reliability calculations. The necessary collected data includes a single-line diagram of the national electricity network at Kigoma Substation for Gatumba and Ntongwe Feeders, the geographical locations of secondary substations, the rated power

of the transformers connected at Gatumba and Ntongwe Feeders, and the length of the distribution lines.

Data Processing

Load Point and Load Profile Estimation

In total, Gatumba and Ntongwe Feeders consist of 187 and 118 second distribution transformers, respectively. Distribution transformers in the same geographical location or on the same feeder branch are grouped together. The combined capacity of the grouped transformers is considered as the maximum load demand, and their number is considered as the number of connected customers. The load point location refers to the location of the distribution transformer with the highest capacity or the midpoint of all grouped distribution transformers. Figure 8.1 shows the geographical layout of Ntongwe and Gatumba feeders after the distribution transformers are grouped, along with a detailed connection of one PV system and BESS. The list of load points for Ntongwe and Gatumba feeders are given in Table 8.3 and Table 8.4, respectively. The loads are grouped as residential load (L-RES), commercial load (L-COM), industrial load (L-IND), and small industrial load (L-SIND).

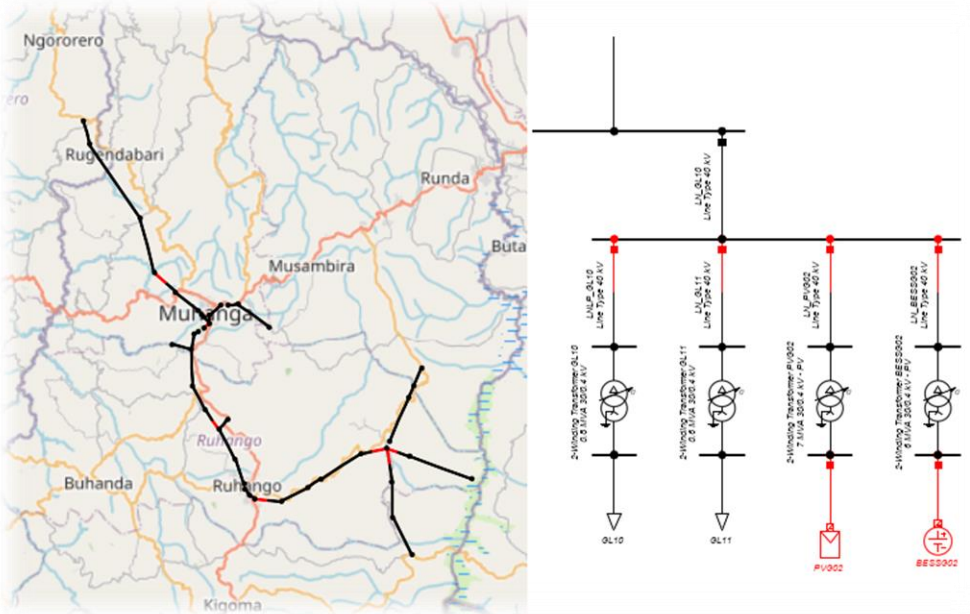


Figure 8.1. (A) Geographical representation of Ntongwe and Gatumba feeders, (B) detail connection of PV system, BESS and load connection at distribution

Table 8.3. Load points for Ntongwe feeder after data processing

| NTONGWE FEEDER | | | |
|---|---|---|---|
| **LOAD NAME** | **TOTAL TRANSFORMER CAPACITY [KVA]** | **NUMBER OF TRANSFORMER** | **TYPE OF LOAD** |
| N-L01 | 305 | 8 | L-RES |
| N-L02 | 550 | 12 | L-RES AND L-COM |
| N-L03 | 325 | 7 | L-RES |
| N-L04 | 235 | 8 | L-RES |
| N-L05 | 400 | 5 | L-RES AND L-COM |
| N-L06 | 400 | 1 | L-COM (HOSPITAL) |
| N-L07 | 360 | 5 | L-RES AND L-COM |
| N-L08 | 350 | 3 | L-RES AND L-SIND |
| N-L09 | 450 | 7 | L-RES AND L-SIND |
| N-L10 | 575 | 5 | L-RES AND L-COM |
| N-L11 | 310 | 5 | L-RES AND L-COM |
| N-L12 | 410 | 14 | L-RES |
| N-L13 | 315 | 1 | L-RES AND L-COM |
| N-L14 | 375 | 10 | L-RES |
| N-L15 | 425 | 12 | L-RES AND L-COM |
| N-L16 | 400 | 1 | L-IND |
| N-L17 | 290 | 14 | L-RES AND L-COM |

The load profile of each load point is estimated by taking into account the Maximum Load Demand (MLD) and load type and using Standard Load Profiles (SLP) from the Federal Association of the Germany Energy and Water Industries (BDEW). Eq. (1) provides the Estimated Load Profile (ELP);

$$ELP = \sum (MLD \quad * SLP \quad ) \tag{8.1}$$

Where:

*ELP* is the Estimated Load Profile, *MLD* is the Maximum Load Demand, and *SLP* is the BDEW Standard Load Profile.

Solar PV system and BESS Data

The Gatumba and Ntongwe feeders are integrated with solar PV systems and BESS at selected load points. The integration of the PV system has been analyzed in three different scenarios: 50%, 100%, and 150% of the desired ratio to consumption. Each scenario has

been thoroughly examined in two cases: one with just the PV system, and the other with the PV system in combination with BESS.

Table 8.5 shows the list of connected PV systems and BESS capacity and associated loads for each case.

Table 8.4. Load points for Gatumba feeder after data processing

| GATUMBA FEEDER | | | |
|---|---|---|---|
| **LOAD NAME** | **TOTAL TRANSFORMER CAPACITY [KVA]** | **NUMBER OF TRANSFORMER** | **TYPE OF LOAD** |
| G-L01 | 500 | 2 | L-RES AND L-COM |
| G-L02 | 625 | 4 | L-RES AND L-COM |
| G-L03 | 175 | 3 | L-RES AND L-COM |
| G-L04 | 450 | 6 | L-RES |
| G-L05 | 550 | 10 | L-RES AND L-COM |
| G-L06 | 800 | 5 | L-RES AND L-COM |
| G-L07 | 800 | 11 | L-RES AND L-COM |
| G-L08 | 240 | 7 | L-RES |
| G-L09 | 850 | 6 | L-RES AND L-COM |
| G-L10 | 650 | 2 | L-IND |
| G-L11 | 490 | 7 | L-RES AND L-COM |
| G-L12 | 1035 | 10 | L-RES AND L-COM |
| G-L13 | 400 | 1 | L-COM (HOSPITAL) |
| G-L14 | 880 | 2 | L-COM |
| G-L15 | 400 | 1 | L-COM |
| G-L16 | 630 | 1 | L-COM |
| G-L17 | 600 | 2 | L-SIND |
| G-L18 | 500 | 2 | L-RES AND L-COM |
| G-L19 | 675 | 5 | L-RES AND L-SIND |
| G-L20 | 350 | 7 | L-RES AND L-COM |
| G-L21 | 550 | 12 | L-RES |
| G-L22 | 640 | 11 | L-RES AND L-COM |
| G-L23 | 325 | 4 | L-RES AND L-COM |
| G-L24 | 450 | 23 | L-RES AND L-COM |
| G-L25 | 650 | 2 | L-IND |
| G-L26 | 740 | 10 | L-RES AND L-COM |
| G-L27 | 425 | 2 | L-RES AND L-COM |
| G-L28 | 750 | 3 | L-RES AND L-COM |
| G-L29 | 125 | 2 | L-RES |
| G-L30 | 550 | 4 | L-RES AND L-COM |
| G-L31 | 750 | 2 | L-RES AND L-COM |
| G-L32 | 365 | 9 | L-RES |
| G-L33 | 550 | 9 | L-RES AND L-COM |

Table 8.5. PV system and BESS capacity at each load center

| PV NAME | BESS NAME | LOAD NAME | LOCATION OF LP | PV PEAK POWER (MWp) FOR EACH CASE | | | BESS SYSTEM | | |
|---|---|---|---|---|---|---|---|---|---|
| | | | | 50% | 100% | 150% | No of Battery systems | Battery Inverter Nominal Output (kW) | Battery Capacity (kWh) |
| PV-G01 | BESS-G01 | G-L01, G-L02, G-L03, G-L04, G-L05, G-L06, G-L07 | G-L03 | 4.81 | 9.62 | 14.43 | 14 | 300 | 1133.8 |
| PV-G02 | BESS-G02 | G-L08, G-L09, G-L10 G-L11, G-L12, G-L13, G-L14 | G-L10 | 6.50 | 13.01 | 19.52 | 19 | 300 | 1133.8 |
| PV-G03 | BESS-G03 | G-L15, G-L16, G-L17 G-L19, G-L19 | G-L15 | 3.27 | 6.54 | 9.82 | 10 | 300 | 1133.8 |
| PV-G04 | BESS-G04 | G-L20, G-L21, G-L22 G-L23, G-L24, G-L25, G-L26 | G-L23 | 5.08 | 10.14 | 15.21 | 14 | 300 | 1133.8 |
| PV-G05 | BESS-G05 | G-L27, G-L28, G-L29 G-L30, G-L31, G-L32, G-L33 | G-L30 | 4.35 | 8.70 | 13.05 | 13 | 300 | 1133.8 |
| PV-N01 | BESS-N01 | N-L01, N-L02, N-L03, N-L04 | N-L04 | 1.93 | 3.86 | 5.80 | 6 | 300 | 1133.8 |
| PV-N02 | BESS-N02 | N-L05, N-L06, N-L07, N-L08, N-L09, N-L10 | N-L06 | 3.18 | 6.36 | 9.54 | 10 | 300 | 1133.8 |
| PV-N03 | BESS-N03 | N-L11, N-L12, N-L13, N-L14 | N-L12 | 1.63 | 3.26 | 4.89 | 5 | 300 | 1133.8 |
| PV-N04 | BESS-N04 | N-L15, N-L16, N-L17 | N-L16 | 1.56 | 3.12 | 4.68 | 5 | 300 | 1133.8 |

## 8.2. Simulation Results

### 8.2.1. PV*SOL Simulation

In the PV*SOL simulation tool, a simulation of a Grid-connected PV System with Electrical Appliances and Battery Systems was conducted to evaluate the performance of a Solar PV system and BESS.

The simulation results summary are presented in Figure 8.2 and Figure 8.3, and Table 8.6. Across all scenarios, the performance ratio exceeds 80%, demonstrating the high potential of solar energy in the installed locations. The desired ratio to consumption should be selected based on the level of self-sufficiency and own power consumption. For a 50% desired ratio to consumption, the level of self-sufficiency falls below 50%, indicating that the system is designed to meet only 50% of the load demand despite consuming 100% of its power.

On the other hand, for 100% and 150% design ratios to consumption, the self-sufficiencies are around 72% and 82%, respectively, while the own power consumptions are approximately 82% and 60%, respectively.

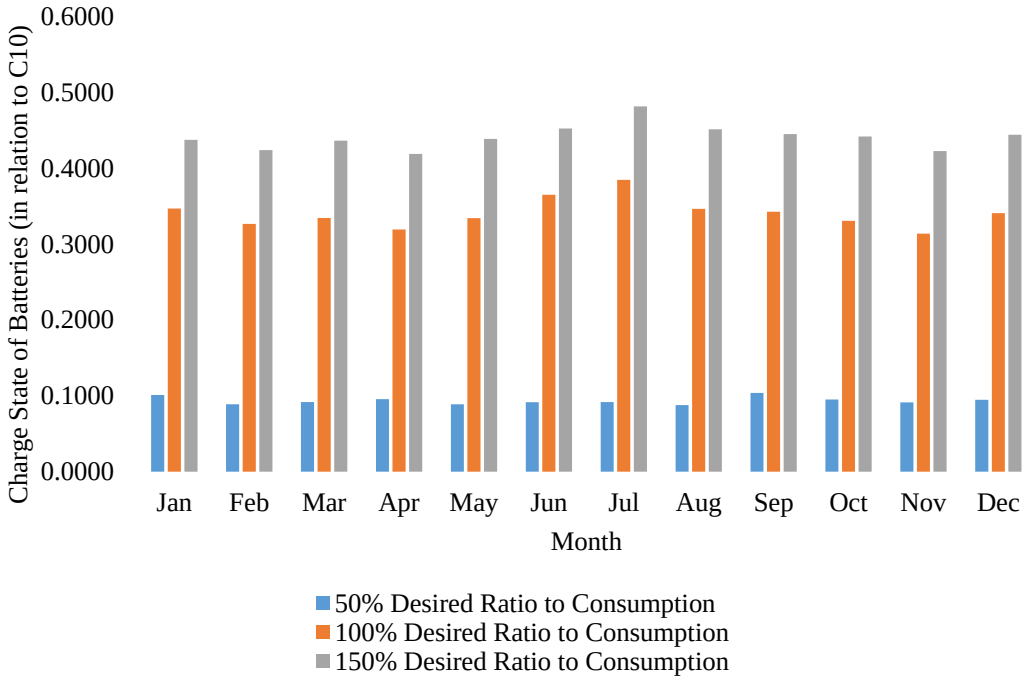


Figure 8.2. PV system monthly total energy generation

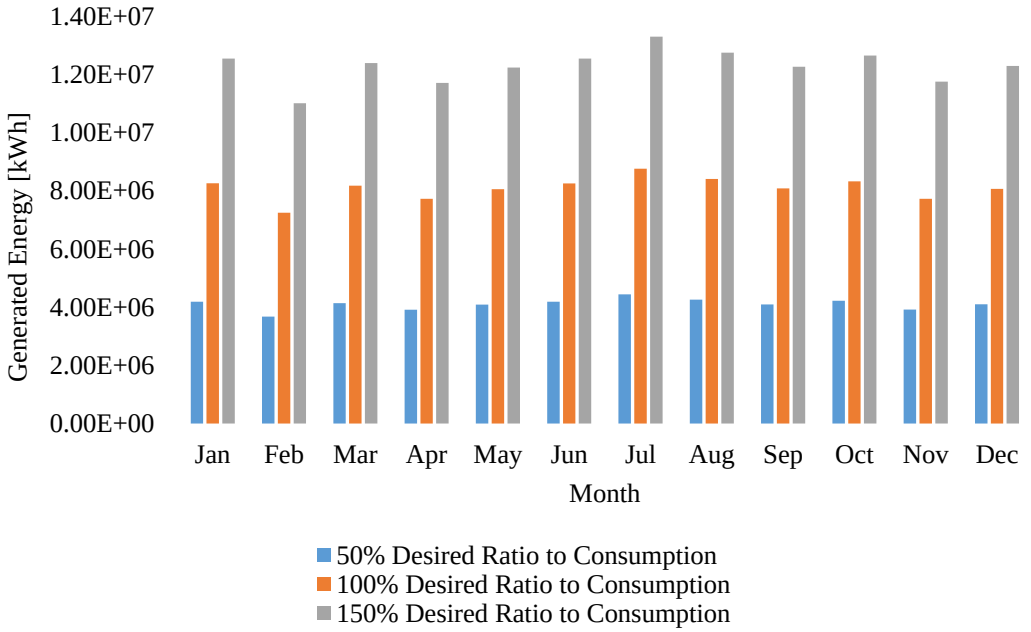


Figure 8.3. Average monthly charge state of BESS (in relation to C10)

Table 8.6. PV*SOL simulation results summary

| PV SYSTEM | DESIRED RATIO TO CONSUMPTION | PERFORMANCE RATIO | LEVEL OF SELF-SUFFICIENCY | OWN POWER CONSUMPTION | DIRECT OWN USE (kWh/Year) | GRID FEED-IN (kWh/Year) | BATTERY CHARGE BY PV SYSTEM (kWh/Year) | BATTERY CHARGE BY GRID (kWh/Year) | NET BATTERY FOR COVERING THE CONSUMPTION (kWh/Year) | NET GRID ENERGY FOR COVERING THE CONSUMPTION (kWh/Year) |
|---|---|---|---|---|---|---|---|---|---|---|
| PV-G01 | **50%** | 83.5% | 45.6% | 100% | 6067361 | 4 | 1389675 | 0 | 1150270 | 8609754 |
| | **100%** | 82.3% | 72.8% | 82.3% | 7405853 | 2598839 | 4684759 | 12588 | 41109935 | 4311662 |
| | **150%** | 83.8% | 81.5% | 60.4% | 7957978 | 8901142 | 5594451 | 14775 | 4948697 | 2927693 |
| PV-G02 | **50%** | 83.3% | 45.3% | 100% | 7805642 | 2547 | 2120069 | 983 | 1770365 | 11572580 |
| | **100%** | 81.9% | 71% | 80.8% | 9484787 | 3741958 | 6301360 | 19565 | 5522611 | 6141932 |
| | **150%** | 83% | 79.9% | 60% | 10280344 | 11890822 | 7532713 | 17902 | 6631554 | 4245836 |
| PV-G03 | **50%** | 83.2% | 45.4% | 99.9% | 4103242 | 3945 | 881521 | 3379 | 720629 | 5811304 |
| | **100%** | 83.5% | 73.2% | 83.5% | 5111494 | 1628343 | 3108681 | 8572 | 2670448 | 2853278 |
| | **150%** | 83.1% | 82.2% | 62.2% | 5595844 | 5647152 | 3699541 | 7183 | 3192011 | 1898375 |
| PV-G04 | **50%** | 82.8% | 45.2% | 100% | 5921109 | 4 | 1451594 | 0 | 1209816 | 8634685 |
| | **100%** | 81.8% | 71.4% | 81.1% | 7236744 | 2749410 | 4581295 | 12333 | 4027329 | 4502062 |
| | **150%** | 82.8% | 80% | 60.1% | 7836015 | 8831413 | 5452889 | 6026 | 4815980 | 3156122 |
| PV-G05 | **50%** | 83.7% | 45.7% | 100% | 5396359 | 4 | 1283542 | 0 | 1063096 | 7679129 |
| | **100%** | 82.2% | 73.1% | 82.8% | 6638176 | 2254827 | 4229009 | 9367 | 3690506 | 3809913 |
| | **150%** | 83.1% | 81.7% | 61.3% | 7165299 | 7699104 | 5037519 | 10830 | 4416037 | 2594496 |
| PV-N01 | **50%** | 83.8% | 45.5% | 100% | 2356413 | 2 | 649188 | 0 | 538484 | 3462065 |
| | **100%** | 82.3% | 72.5% | 82.4% | 2839366 | 1040245 | 2020942 | 6860 | 1769254 | 1748364 |
| | **150%** | 82.9% | 80.9% | 61% | 3040399 | 3484528 | 2395951 | 7305 | 2118310 | 1214513 |
| PV-N02 | **50%** | 83.3% | 45.4% | 100% | 3974345 | 46 | 938808 | 457 | 770001 | 5713780 |
| | **100%** | 82.8% | 74.5% | 84.4% | 4847541 | 1525987 | 3386564 | 10190 | 2948074 | 2662572 |
| | **150%** | 83.2% | 83.3% | 62.9% | 5198657 | 5461323 | 4064365 | 12996 | 3557728 | 1751073 |
| PV-N03 | **50%** | 83% | 45.4% | 100% | 2102264 | 1 | 409606 | 0 | 333506 | 2923464 |
| | **100%** | 82.4% | 75.4% | 85.3% | 2587602 | 731402 | 1668102 | 4016 | 1452101 | 1319555 |
| | **150%** | 83.8% | 84% | 62.8% | 2778566 | 2834916 | 1995118 | 3510 | 1747365 | 859615 |
| PV-N04 | **50%** | 83.1% | 45.3% | 100% | 1892249 | 1 | 522250 | 0 | 432537 | 2811485 |
| | **100%** | 82.1% | 72.6% | 82.5% | 2285719 | 832446 | 1648183 | 5031 | 1442098 | 1408476 |
| | **150%** | 82.6% | 81.2% | 61.4% | 2440938 | 2779419 | 1976844 | 5026 | 1740693 | 967677 |

### 8.2.2. Quasi-Dynamic Simulation

During the first week of the year, quasi-dynamic simulations and load-flow calculations are conducted to analyze the generation profiles of photovoltaic (PV) systems and the power flow from the external grid and it involves examining the behavior of the PV systems' energy generation and studying how the power is distributed and flows within the grid. Figure 8.4 shows the power flow from external grid to Ntongwe and Gatumba feeders integrated with PV System and BESS for all cases.

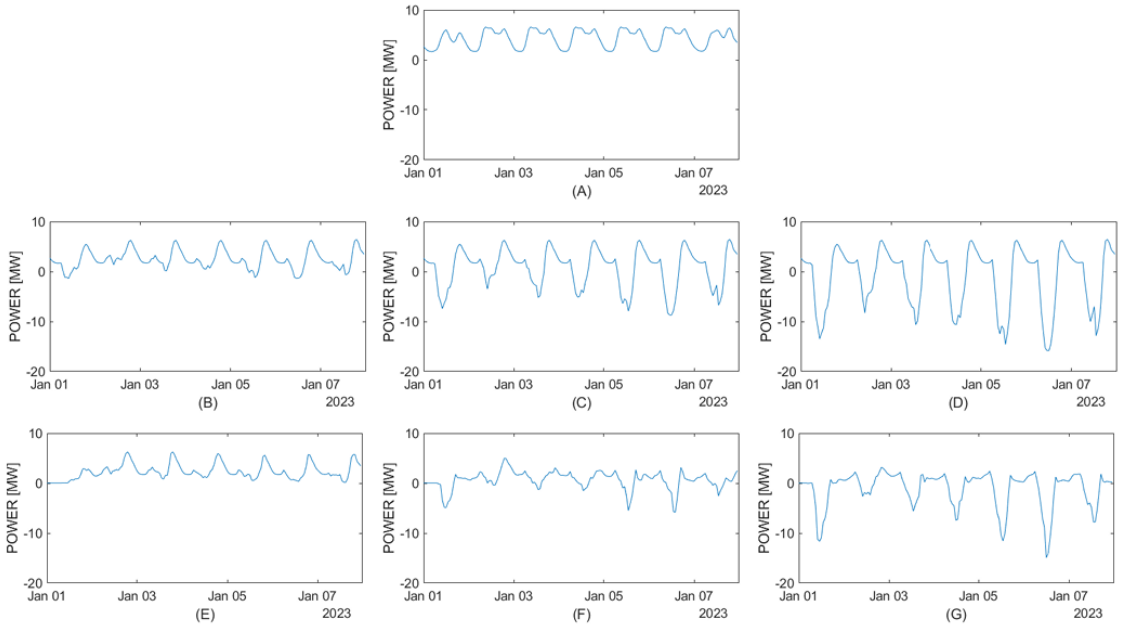


Figure 8.4. Power supply from external grid to Ntongwe and Gatumba feeders with 50%, 100%, and 150% desired ratio to consumption: (A) without PV system, (B), (C) and (D) PV system, (E), (F), and (G) PV system and BESS

### 8.2.3. Reliability Analysis Results

The reliability analysis considers three different scenarios. Two cases are examined for each scenario: one with only a PV system and the other with a PV system and a BESS. The reliability indices are compared in Table 8.7. The indices are SAIFI, CAIFI, SAIDI, CAIDI, ASAI, ASUI, ENS, AENS, ACCI, ASIFI, and ASIDI.

The simulation results from Table 8.7 show that integrating PV systems or PV systems with BESS leads to improved reliability at Gatumba and Ntongwe feeders. Integration with a PV system and BESS results in a 71.6% improvement in both SAIFI and CAIFI.

The reliability improves by 94% for SAIDI with the integration of the PV system alone and by 95.5% when BESS is added. For CAIDI, the reliability improves by 75% with integrating a PV system alone and reaches 84.3% by adding BESS. When only the PV system is integrated, the reliability improvements are 92.9% for ENS, 93.3% for AENS, 74.7% for ASIFI, and 92.9% for ASIDI. Integrating the PV system and BESS results in a 95.3% improvement for ENS, 95.2% for AENS, 74.7% for ASIFI, and 95.3% for ASIDI.

Table 8.7. Comparison of reliability indices from simulation results

| **Reliability** | **BASE CASE** | **50% RATIO TO CONSUMPTION** | | **100% RATIO TO CONSUMPTION** | | **150% RATIO TO CONSUMPTION** | |
|---|---|---|---|---|---|---|---|
| | | **PV ONLY** | **PV AND BESS** | **PV ONLY** | **PV AND BESS** | **PV ONLY** | **PV AND BESS** |
| SAIFI [1/Ca] | 3.494631 | 0.990686 | 0.990686 | 0.990686 | 0.990686 | 0.990686 | 0.990686 |
| CAIFI [1/Ca] | 3.494631 | 0.990686 | 0.990686 | 0.990686 | 0.990686 | 0.990686 | 0.990686 |
| SAIDI [h/Ca] | 12.699 | 0.888 | 0.565 | 0.884 | 0.646 | 0.888 | 0.664 |
| CAIDI [h] | 3.634 | 0.897 | 0.57 | 0.892 | 0.652 | 0.897 | 0.67 |
| ASAI | 0.998550 | 0.999898 | 0.999935 | 0.999899 | 0.999926 | 0.999899 | 0.999924 |
| ASUI | 0.001450 | 0.000101 | 0.0000645 | 0.000101 | 0.000074 | 0.000101 | 0.000075 |
| ENS [MWh/a] | 31.891 | 2.253 | 1.498 | 2.243 | 1.687 | 2.253 | 1.729 |
| AENS [MWh/Ca] | 0.105 | 0.007 | 0.005 | 0.007 | 0.006 | 0.007 | 0.006 |
| ACCI [MWh/Ca] | 1.676 | 0.035 | 0.023 | 0.035 | 0.026 | 0.035 | 0.027 |
| ASIFI [1/a] | 3.522847 | 0.887972 | 0.887972 | 0.887972 | 0.887972 | 0.887972 | 0.887972 |
| ASIDI [h/a] | 12.17744 | 0.860373 | 0.572025 | 0.856508 | 0.644141 | 0.860165 | 0.660365 |

## 8.3. Conclusion

This study aims to evaluate the impact of integrating Solar PV and Battery Energy Storage Systems (BESS) at the distribution level to improve the reliability of the Gatumba and Ntongwe feeders. According to the simulation results from PV*SOL, the solar energy performance ratio is 80%, indicating a high potential for solar energy in the installed locations. The level of self-sufficiency varies based on the desired consumption ratio and can reach up to 82%. For a photovoltaic system with BESS, the system needs to produce enough power to meet the load and also recharge the BESS by enhancing the targeted

consumption ratio. Based on the simulation results from PV*SOL, the annual average charge state of the Battery Energy Storage System (BESS) in relation to C10 was 0.0935 with a 50% desired consumption ratio, 0.3405 with a 100% desired consumption ratio, and 0.4412 with a 150% desired consumption ratio. The analysis results from DigSILENT PowerFactory demonstrate that integrating a PV system with BESS to the electric grid can significantly improve system reliability. The simulations show a 71.6% improvement in average interruption frequency for both customers and the system, a 95.5% improvement in system average interruption duration, and an 84.3% improvement in customer average interruption duration.

# 9. CONCLUSIONS AND RECOMMENDATIONS

This thesis was dedicated to investigate the capability of solar Energy system with BESS to improve grid network reliability.

During this thesis; the literature review, distributed generation, modelling of solar PV panel, techno-economic analysis of PV system with BESS for small household, inverter configuration and charger controller for solar PV and BESS integration, reliability improvement of standard RBTS Bus-2 by integration of PV Systems and BESS, and the reliability improvement of Rwanda Electricity grid by integration of PV system and BESS at Gatumba and Ntongwe feeders, researches activities were conducted. The conducted studies were in the line to investigate the impact of Solar PV system with BESS on the reliability of electricity grid.

Solar PV panels can be modelled by using the information provided by the manufacturer such as open-circuit voltage, short circuit current, voltage and current at the maximum point at standard test conditions ($25^{o}C$, $1000W/m^2$). The five reference parameters of the model equation of a solar PV panel are obtained by solving five equations obtained by using the mathematical model of solar PV panel at different conditions as provided by the manufacturer at standard condition. Solar PV together with BESS mitigate the negative effect associated with the intermittent of solar energy thereby ensuring the continuity of the supply of electricity. The DC output power from the PV panel need to be converted into AC power to supply AC appliances. Inverter are used as a link between PV panel and AC load or for AC grid. The power from PV modules can be maximized by using different techniques called MPPT algorithm. To ensure the continuity and to increase the reliability of PV system, BESS are used to store electricity from PV modules. Charger controllers are used to control the charge and discharge process of BESS. MPPT algorithms can be implemented in charger controllers or in inverter.

From techno-economic analysis of PV system with BESS for small household study, by using PV*SOL software, a PV system with BESS is designed and simulated to supply a community located in Rwanda, Muhanga district, Shyogwe sector with annual consumption of 82.34MWh with a peak load demand of 30.4kW. The simulation results showed that the load is successfully supplied from the PV system with 68.65% direct

power consumption, 64.38% level of self-sufficiency, and 86.05% performance ratio. The results showed that PV system integrated with BESS can be used to supply the load for local communities in developing countries. Even if the access to the grid is available, still the importance of PV system is impressive.

The results from the study of integration of PV System and BESS to the standard RBTS Bus-2 showed that Solar PV system can be integrated with grid at the distribution level to improve the electricity network reliability. It was shown that SAIFI and CAIFI indices are improved by 43.4%, SAIDI index by 3.40%, ENS by 2.45% and ASAI index by 0.0023%.

From the detailed study about the reliability improvement of Rwanda electricity grid by integration of PV system and BESS at Gatumba and Ntongwe feeders, the simulation results from PV*SOL show that the solar energy performance ratio is 80% and the level of self-sufficiency varies according to desired ration to consumption and can reach up to 82%. For PV system with BESS, by adjusting the desired ratio to consumption, PV system can produce sufficient power to meet the load demand and charge BESS. Simulation results in PV*SOL, for 50%,100%, and 150% desired ratio to consumptions, show that the yearly average Charge State of BESS (in relation to C10) were 0.0935, 0.3405, and 0.4412, respectively. The DigSILENT PowerFactory reliability analysis results show the ability of PV system with BESS to improve the system reliability with 71.6% for customer and system average interruption frequency, 95.5% for system average interruption duration, and 84.3% for customer average interruption duration.

It is suggested that future research should further investigate the impact of solar PV systems with BESS on enhancing the reliability of electricity grids. This could be achieved by exploring the following areas of study:

- A similar research study should be conducted for other substation feeders within Rwanda's electricity grid.
- It is recommended to assess the reliability improvement resulting from the integration of solar PV and BESS on the transmission network within Rwanda's electricity grid.
- Similar studies should be conducted on well-established electricity grids with high reliability to evaluate the impact of solar PV systems with BESS.

## REFERENCES


Abdin, G. C., Noussan, M. (2018). Electricity storage compared to net metering in residential PV applications. *Journal of Cleaner Production*, *176*, 175–186.

Adefarati, T., Bansal, R. C. (2017a). Reliability and economic assessment of a microgrid power system with the integration of renewable energy resources. *Applied Energy*, *206*, 911–933.

Adefarati, T., Bansal, R. C. (2017b). Reliability assessment of distribution system with the integration of renewable distributed generation. *Applied Energy*, *185*, 158–171.

Ahmad, L., Khordehgah, N., Malinauskaite, J., Jouhara, H. (2020). Recent advances and applications of solar photovoltaics and thermal technologies. *Energy*, *207*, 118254.

Al, H. Z., Awasthi, A., Ramli, M. A. M. (2018). Optimal design and analysis of grid-connected photovoltaic under di ff erent tracking systems using HOMER. *Energy Conversion and Management*, *155*, 42–57.

Ali Kadhem, A., Abdul Wahab, N. I., Aris, I., Jasni, J., Abdalla, A. N. (2017). Computational techniques for assessing the reliability and sustainability of electrical power systems: A review. *Renewable and Sustainable Energy Reviews*, *80*, 1175–1186.

Allan, R. N., Billinton, R., Sjarief, I., Goel, L., So, K. S. (1991). A Reliability Test System For Educational Purposes - Basic Distribution System Data and Results. *IEEE Transactions on Power Systems*, *6*(2), 813–820.

Alnoosani, A., Oreijah, M., Alhazmi, M., Samkari, Y., Faqeha, H. (2018). Design of 100MW Solar PV on-Grid Connected Power Plant Using (PVsyst) in Umm Al-Qura University. *International Journal of Science and Research*, *8*(11), 356–363.

Alsadi, S., Khatib, T. (2018). Photovoltaic power systems optimization research status: A review of criteria, constrains, models, techniques, and software tools. *Applied Sciences (Switzerland)*, *8*(10).

Amir, A., Amir, A., Seng, H., Elkhateb, A., Abd, N. (2019). Comparative analysis of high voltage gain DC-DC converter topologies for photovoltaic systems. *Renewable Energy*, *136*, 1147–1163.

Antunes, H. M. A., Silva, S. M., Brandao, D. I., Machado, A. A. P., Ferreira, R. V. (2020). A fault-tolerant grid-forming converter applied to AC microgrids. *International Journal of Electrical Power and Energy Systems*, *121*.

Bellia, H. (2019). A detailed modeling of photovoltaic module using MATLAB A detailed modeling of photovoltaic module using MATLAB. *NRIAG Journal of Astronomy and Geophysics*, *3*(1), 53–61.

Bimenyimana, S., Asemota, G. N. O., Li, L. (2018). The state of the power sector in Rwanda: A progressive sector with ambitious targets. *Frontiers in Energy Research*, *6*.

Bollipo, R. B., Mikkili, S., Bonthagorla, P. K. (2020). Critical Review on PV MPPT Techniques: Classical, Intelligent and Optimisation. *IET Renewable Power Generation*, *14*(9), 1433–1452.

Bollipo, R. B., Mikkili, S., Bonthagorla, P. K. (2021). Hybrid, optimal, intelligent and classical PV MPPT techniques: A review. *CSEE Journal of Power and Energy Systems*, *7*(1), 9–33.

Bolson, N., Yutkin, M., Patzek, T. (2021). Energy efficiency and sustainability assessment for methane harvesting from Lake Kivu. *Energy*, *225*, 120215.

Bousshoua, B., Elmaouhab, A. (2019). Smart grid reliability using reliable block diagram case study: Adrar's isolated network of Algeria. *5th International Conference on Power Generation Systems and Renewable Energy Technologies, PGSRET 2019*, 26–27.

Cao, Y., Taslimi, M. S., Dastjerdi, S. M., Ahmadi, P., Ashjaee, M. (2022). Design, dynamic simulation, and optimal size selection of a hybrid solar/wind and battery-based system for off-grid energy supply. *Renewable Energy*, *187*, 1082–1099.

Chennaif, M., Maaouane, M., Zahboune, H., Elhafyani, M. (2022). Tri-objective techno-economic sizing optimization of Off-grid and On-grid renewable energy systems using Electric system Cascade Extended analysis and system Advisor Model. *Applied Energy*, *305*, 117844.

Corba, Z., Katic, V. A., Dumnic, B., Milicevic, D. (2012). In-grid solar-to-electrical energy conversion system modeling and testing. *Thermal Science, 16*, 159-171.

Cui, W. H., Wang, J. S., Chen, Y. Y. (2018). Equivalent Circuit Model of Lead-acid Battery in Energy Storage Power Station and Its State-of-Charge Estimation Based on Extended Kalman Filtering Method. *Engineering Letters, 26*(4).

Dadfar, S., Marzban, M. M., Ghafouri, M. S. (2017). Reliability evaluation of 20 kW solar power station in grid-connected mode (a case study). *2017 25th Iranian Conference on Electrical Engineering, ICEE 2017*, 1343–1348.

David, J., Bastidas-rodríguez, J. D., Ramos-paja, C. (2017). Types of inverters and topologies for microgrid applications Types of inverters and topologies for microgrid applications. *Revista UIS Ingenierías, 16*(1), 7-14.

De Soto, W., Klein, S. A., Beckman, W. A. (2006). Improvement and validation of a model for photovoltaic array performance. *Solar energy*, *80*(1), 78-88.

Dogga, R., Pathak, M. K. (2019). Recent trends in solar PV inverter topologies. *Solar*

*Energy*, *183*, 57–73.

Dondariya, C., Porwal, D., Awasthi, A., Shukla, A. K., Sudhakar, K., Murali, M. M., Bhimte, A. (2018). Performance simulation of grid-connected rooftop solar PV system for small households: A case study of Ujjain, India. *Energy Reports*, *4*, 546–553.

Dongmei, Z., Wenhao, S., Xu, Z. (2014). Reliability evaluation for Mudanjiang regional power grid. *POWERCON 2014 - 2014 International Conference on Power System Technology: Towards Green, Efficient and Smart Power System, Proceedings*, *Powercon*, 746–751.

Dorahaki, S., Rashidinejad, M., Fatemi Ardestani, S. F., Abdollahi, A., Salehizadeh, M. R. (2022). A home energy management model considering energy storage and smart flexible appliances: A modified time-driven prospect theory approach. *Journal of Energy Storage*, *48*, 104049.

Du, W., Tuffner, F. K., Member, S., Schneider, K. P., Lasseter, R. H., Fellow, L., Xie, J., Chen, Z., Member, S. (2021). *Modeling of Grid-Forming and Grid-Following Inverters for Dynamic Simulation of Large-Scale Distribution Systems*. *36*(4), 2035–2045.

Ehsan, A., Yang, Q. (2018). Optimal integration and planning of renewable distributed generation in the power distribution networks: A review of analytical techniques. *Applied Energy*, *210*, 44–59.

Elma, O., Selamogullari, U. S. (2012). A comparative sizing analysis of a renewable energy supplied stand-alone house considering both demand side and source side dynamics. *Applied Energy*, *96*, 400–408.

Garip, S., Özdemir, Ş., Altın, N. (2022). Power System Reliability Assessment - A Review on Analysis and Evaluation Methods. *Journal of Energy Systems*, 401–419).

Gasore, G., Ahlborg, H., Ntagwirumugara, E., Zimmerle, D. (2021). Progress for on-grid renewable energy systems: Identification of sustainability factors for small-scale hydropower in rwanda. *Energies*, *14*(4).

Gautam, P. (2018). Reliability studies of distribution systems integrated with energy storage. Doctoral dissertation, University of Saskatchewan, Saskatchewan.

Gouveia, J., Moreira, C. L., Lopes, J. P. (2019, September). Grid-forming inverters sizing in islanded power systems–a stability perspective. *2019 International Conference on Smart Energy Systems and Technologies*, 1-6.

Guo-hua, Y., Yi, L., Qi, Y., Rong, Y. (2011). Study of Reliability of Grid Connected Photovoltaic Power Based on Monte Carlo Method. *Power Engineering and Automation Conference (PEAM), 2011 IEEE*, *1*, 92–95.

Hakizimana, E., Sandoval, D., Wali, U. G., Venant, K. (2020). Inventory Analysis Of Power Plants In Rwanda And Estimated Generation Capacities. *IJSTR. 9* (12).

Hakizimana, J. de D. K., Yoon, S. P., Kang, T. J., Kim, H. T., Jeon, Y. S., Choi, Y. C. (2016). Potential for peat-to-power usage in Rwanda and associated implications. *Energy Strategy Reviews*, *13–14*, 222–235.

Hargreaves, J. J., Jones, R. A. (2020). Long Term Energy Storage in Highly Renewable Systems. *Frontiers in Energy Research*, *8*, 1–10.

Harker Steele, A. J., Burnett, J. W., Bergstrom, J. C. (2021). The impact of variable renewable energy resources on power system reliability. *Energy Policy*, *151*, 111947.

Hasan, M. M., Mekhilef, S., Messikh, T., Ahmed, M. (2016). Three-phase multilevel inverter with high value of resolution per switch employing a space vector modulation control scheme. *Turkish Journal of Electrical Engineering and Computer Sciences*, *24*(4), 1993–2009.

Hashish, M. S., Hasanien, H. M., Ji, H., Alkuhayli, A., Alharbi, M., Akmaral, T., Turky, R. A., Jurado, F., Badr, A. O. (2023). Monte Carlo Simulation and a Clustering Technique for Solving the Probabilistic Optimal Power Flow Problem for Hybrid Renewable Energy Systems. *Sustainability (Switzerland)*, 15(1).

Heidari, A. (2015). Reliability analysis of power distribution system in presence of distributed generation units. Doctoral dissertation, University of New South Wales, Sydney.

Ituze, G., Mwongereza, J. d'Amour, Abimana, C., Rwema, M., Chisale, P. (2017). Energy Landscape of Rwanda and Institutional Framework. *Science Research*, *5*(3), 16.

Jagadale, P. R., Choudhari, A. B., Jadhav, S. S. (2022). Design and simulation of grid connected solar Si-poly photovoltaic plant using PVsyst for Pune, India location. *Renewable Energy Research and Applications, 3*(1), 41-49.

Jasuan, A., Nawawi, Z., Samaulah, H. (2018). Comparative analysis of applications off-grid PV system and on-grid PV system for households in Indonesia. *2018 international conference on electrical engineering and computer science (ICECOS)*, 253-258.

Jena, D., Ramana, V. V. (2015). Modeling of photovoltaic system for uniform and non-uniform irradiance: A critical review. *Renewable and Sustainable Energy Reviews, 52*, 400-417.

Jiang, Y., Kang, L., Liu, Y. (2021). Multi-objective design optimization of a multi-type battery energy storage in photovoltaic systems. *Journal of Energy Storage, 39.*

Kayhan, V. A., Ulker, F., Elma, O. (2015). Photovoltaic system design, feasibility and

financial outcomes for different regions in Turkey. *2015 4th International Conference on Electric Power and Energy Conversion Systems (EPECS)*, 1-6.

Khalil, L., Liaquat, K., Iqbal, M. A., Riaz, M., Khalil, K. (2021). Materials Today : Proceedings Optimization and designing of hybrid power system using HOMER pro. *Materials Today: Proceedings*, *47*, 110–S115.

Kim, D. K., Yoneoka, S., Banatwala, A. Z., Kim, Y. T., Nam, K. Y. (2018). Handbook on battery energy storage system. *Asian Development Bank: Manila, Philippines*, 1-6.

Koyi, O. O. (2019). Improving the reliability of Nigeria's electricity grid with renewable energy microgrids. M. Sc. thesis, Karadeniz technical university, Graduate school of natural and applied sciences, Trabzon, 607042.

Kumar, R., Rajoria, C. S., Sharma, A., Suhag, S. (2020). Design and simulation of standalone solar PV system using PVsyst Software: A case study. *Materials Today: Proceedings*, *46*, 5322–5328.

Lee, K. W., Lee, H. M., Lee, R. Da, Kim, D. S., Yoon, J. H. (2021). The impact of cracks in BIPV modules on power outputs: A case study based on measured and simulated data. *Energies*, *14*(4).

Li, W., Sun, L., Zou, W., Luo, C. (2014). Power system reliability analysis system based on PSASP and fault enumeration method and applications. *China International Conference on Electricity Distribution, CICED*, 1323–1326.

Li, Y., Feng, B., Li, G., Qi, J., Zhao, D., Mu, Y. (2018). Optimal distributed generation planning in active distribution networks considering integration of energy storage. *Applied Energy*, *210*, 1073–1081).

Li, Y., Gu, Y., Green, T. C. (2022). Revisiting grid-forming and grid-following inverters: A duality theory. *IEEE Transactions on Power Systems*, *37*(6), 4541-4554.

Luo, L., Gu, W., Zhang, X. P., Cao, G., Wang, W., Zhu, G., You, D., Wu, Z. (2018). Optimal siting and sizing of distributed generation in distribution systems with PV solar farm utilized as STATCOM (PV-STATCOM). *Applied Energy*, 210, 1092–1100.

Mani, V., Ramachandran, R., Nanjundappan, D. (2016). Implementation of a modified SVPWM-based three-phase inverter with reduced switches using a single DC source for a grid-connected PV system. *Turkish Journal of Electrical Engineering and Computer Sciences*, *24*(4), 3023–3035.

Mao, M., Cui, L., Zhang, Q., Guo, K., Zhou, L., Huang, H. (2020). Classification and summarization of solar photovoltaic MPPT techniques: A review based on traditional and intelligent control strategies. *Energy Reports*, *6*(174), 1312–1327.

Mbungu, N. T., Naidoo, R. M., Bansal, R. C., Siti, M. W., Tungadio, D. H. (2020). An overview of renewable energy resources and grid integration for commercial building applications. *Journal of Energy Storage*, *29*, 101385.

Mohamed, A. T., Helal, A. A., El Safty, S. M. (2019). Distribution system reliability evaluation in presence of DG. *2019 IEEE International Conference on Environment and Electrical Engineering and 2019 IEEE Industrial and Commercial Power Systems Europe (EEEIC/I&CPS Europe)*, 1-6).

Morad, M., Nayel, M., Elbaset, A. A., Galal, A. I. A. (2018). Sizing and analysis of grid-connected microgrid system for Assiut University using HOMER software. *2018 twentieth international middle east power systems conference (MEPCON)*, 694-699).

Motahhir, S., El, A., El, A. (2020). The most used MPPT algorithms : Review and the suitable low-cost embedded board for each algorithm. *Journal of Cleaner Production*, *246*, 118983.

Mrehel, O. G., Albgar, K. A. (2018). Design and simulation of a large-scale PV power generation in ben-walid city. *Libyan international conference on electrical engineering and technologies (LICEET2018)*, 3-7.

Narayanan, V., Kewat, S., Singh, B. (2020). Solar PV-BES Based Microgrid System with Multifunctional VSC. *IEEE Transactions on Industry Applications*, *56*(3), 2957–2967.

Nhau, N., Li, J., Wang, W., Yu, W., Zhao, C., Liu, Y. (2021). Simulation and analysis of economic benefits of different types of PV systems in shanghai. *2021 Power System and Green Energy Conference (PSGEC)*, 291-295).

Nigam, A., Sharma, K. K. (2020). Performance evaluation/analysis of distributed generation system. *European Journal of Molecular and Clinical Medicine*, *7*(7), 4638–4650.

Nwaigwe, K. N., Mutabilwa, P., Dintwa, E. (2019). An overview of solar power (PV systems) integration into electricity grids. *Materials Science for Energy Technologies*, *2*(3), 629–633.

Odeh, C. I. (2016). Cascaded half-full-bridge PWM multilevel inverter configuration. *Turkish Journal of Electrical Engineering and Computer Sciences*, *24*(4), 2071–2083.

Ostovar, S., Esmaeili-Nezhad, A., Moeini-Aghtaie, M., Fotuhi-Firuzabad, M. (2021). Reliability assessment of distribution system with the integration of photovoltaic and energy storage systems. *Sustainable Energy, Grids and Networks*, *28*.

Panigrahi, R., Mishra, S. K., Srivastava, S. C., Srivastava, A. K., Schulz, N. N. (2020). Grid Integration of Small-Scale Photovoltaic Systems in Secondary Distribution

Network - A Review. *IEEE Transactions on Industry Applications*, *56*(3), 3178–3195.

Panjwani, M. K., Kumar, J., Parhyar, N. R., Khan, D. (2021). Design and performance analysis of PV grid-tied system with energy storage system. *International Journal of Electrical and Computer Engineering*, *11*(2), 1077.

Pol, J. C., Kindermann, P., Van Der Krogt, M. G., Van Bergeijk, V. M., Remmerswaal, G., Kanning, W., ... Kok, M. (2023). The effect of interactions between failure mechanisms on the reliability of flood defenses. *Reliability Engineering & System Safety*, *231*, 108987.

Pushpavalli, M., Abirami, P., Sivagami, P., Geetha, V. (2021). Investigation of grid connected PV system with electrial appliances, electric vehicles and battery systems using PVsol software. *Proceedings of the First International Conference on Advanced Scientific Innovation in Science, Engineering and Technology, ICASISET 2020,* Chennai, India, 16-17 May 2020.

Rafał, F., Maciej, Ż., Wojciech, G. (2020). Dynamic Simulation and Energy Economic Analysis of a Household Hybrid Ground-Solar-Wind System Using TRNSYS Software. *Energies*, *13*(14), 3523.

Rahmoun, A., Armstorfer, A., Biechl, H., Rosin, A. (2017). Mathematical modeling of a battery energy storage system in grid forming mode. *2017 IEEE 58th International Scientific Conference on Power and Electrical Engineering of Riga Technical University (RTUCON)*, 1-6.

Ram, K., Swain, P. K., Vallabhaneni, R., Kumar, A. (2022). Critical assessment on application of software for designing hybrid energy systems. *Materials Today: Proceedings*, *49*, 425–432.

Razavi, S. E., Rahimi, E., Javadi, M. S., Nezhad, A. E., Lotfi, M., Shafie-khah, M., Catalão, J. P. S. (2019). Impact of distributed generation on protection and voltage regulation of distribution systems: A review. *Renewable and Sustainable Energy Reviews,105*, 157–167.

Reichert, S., Griepentrog, G., Stickan, B. (2017). Comparison between grid-feeding and grid-supporting inverters regarding power quality. *2017 IEEE 8th International Symposium on Power Electronics for Distributed Generation Systems, PEDG 2017*, 1–4.

Rosewater, D. M., Copp, D. A., Nguyen, T. A., Byrne, R. H., Santoso, S. (2019). Battery Energy Storage Models for Optimal Control. *IEEE Access*, *7*, 178357–178391.

Rout, K. C., Kulkarni, P. S. (2020, February). Design and performance evaluation of proposed 2 kW solar PV rooftop on grid system in Odisha using PVsyst. In *2020 IEEE International Students' Conference on Electrical, Electronics and Computer Science (SCEECS)*,1-6).

Saeedi, S. (2016). Impacts of distributed generations on distribution system reliability. M. Sc. thesis, Istanbul technical university, Graduate school of natural and applied sciences, Trabzon, 438153.

Salman, S., Ai, X., Wu, Z. (2018). Design of a P-&-O algorithm based MPPT charge controller for a stand-alone 200W PV system. *Protection and Control of Modern Power Systems, 3*(1).

Schömann, O., Sadri, H., Krüger, W., Bülo, T., Hardt, C., Hesse, R., Falk, A., Stankat, P. R. (2019). Experience with Large Grid-Forming Inverters on Various Island and Microgrid Projects. *4th International Hybrid Power Systems Workshop*, 0–4.

Segundo Sevilla, F. R., Parra, D., Wyrsch, N., Patel, M. K., Kienzle, F., Korba, P. (2018). Techno-economic analysis of battery storage and curtailment in a distribution grid with high PV penetration. *Journal of Energy Storage*, *17*, 73–83.

Sekhar, Y. R., Ganesh, D., Kumar, A. S., Abraham, R., Padmanathan, P. (2017). Performance simulation of a grid connected photovoltaic power system using TRNSYS 17. *IOP Conference Series: Materials Science and Engineering*, *263*(6), 4218–4229.

Sezen, S., Aktaş, A., Uçar, M., Özdemir, E. (2017). Design and operation of a multifunction photovoltaic power system with shunt active filtering using a single-stage three-phase multilevel inverter. *Turkish Journal of Electrical Engineering and Computer Sciences*, *25*(2), 1412–1425.

Shafiullah, M., Ahmed, S. D., Al-Sulaiman, F. A. (2022). Grid Integration Challenges and Solution Strategies for Solar PV Systems: A Review. *IEEE Access*, *10*, 52233–52257).

Shahzad, U., Asgarpoor, S. (2017). A Comprehensive Review of Protection Schemes for Distributed Generation. *Energy and Power Engineering*, *9*(8), 430–463.

Tercan, S. M., Elma, O., Gokalp, E., Cali, U. (2022). An expansion planning method for extending distributed energy system lifespan with energy storage systems. *Energy Exploration & Exploitation*, *40*(2), 599-618.

Teshome, A. D. (2016). Study of Distributed Generation in Improving Power System Reliability (Case Study: Addis Center Substation). Addis Ababa University, School of Graduate Studies, Addis Ababa Institute of Technology, Addis Ababa.

Tian, H., Mancilla-david, F., Ellis, K., Muljadi, E., Jenkins, P. (2012). A cell-to-module-to-array detailed model for photovoltaic panels. *Solar Energy*, *86*(9), 2695–2706.

Umar, N. H., Bora, B., Banerjee, C., Umar, N., Panwar, B. S. 'Study of different PV Technologies under Composite Climates using test beds at NISE View project Solar Photovoltaic Hub at BESU View project Comparison of different PV power simulation software: Case study on performance analysis of 1-MW gridconnected.

2018; 11-24.

URL-1. https://www.reg.rw/fileadmin/user_upload/REG_ANNUAL_REPORT_2022-2023.pdf (Access date: 1 September 2024).

URL-2. https://www.reg.rw/fileadmin/user_upload/Rwanda_Electricity_Distribution_Master_Plan_-_updated_June_2022.pdf (Access date: 1 September 2024).

URL-3. https://www.mininfra.gov.rw/digital-transformation-1-1 (Access date: 1 September 2024).

URL-4. https://www.hsdl.org/?abstract&did= (Access date: 1 September 2024).

URL-5. https://valentin-software.com/en/products/pvsol-premium/ (Access date: 1 September 2024).

URL-6. https://help.valentin-software.com/pvsol/en/calculation/irradiation/climate-data/ (Access date: 1 September 2024).

Valencia, A., Hincapie, R. A., Gallego, R. A. (2021). Optimal location, selection, and operation of battery energy storage systems and renewable distributed generation in medium–low voltage distribution networks. *Journal of Energy Storage*, *34*, 102158.

Vinayagam, A., Swarna, K. S. V., Khoo, S. Y., Oo, A. T., Stojcevski, A. (2017). PV Based Microgrid with Grid-Support Grid-Forming Inverter Control-(Simulation and Analysis). *Smart Grid and Renewable Energy*, *08*(01), 1–30.

Wadi, M., Baysal, M., Shobole, A., Tur, M. R. (2018, October). Reliability evaluation in smart grids via modified Monte Carlo simulation method. *2018 7th International Conference on Renewable Energy Research and Applications (ICRERA)*, 841-845.

Wadi, M. J. (2017). Reliability assessment of closed ring power distribution systems, Doctoral dissertation, Yıldız technical university, Graduate school of natural and applied sciences, Isyanbul, 478602.

Wang, H., Meng, Z., Guo, Y., Yao, Y., Xi, X. (2014). Analysis of Micro-grid power supply reliability. *2014 China International Conference on Electricity Distribution (CICED)*,107-110).

Wei, H., Zijun, H., Fengli, Hongliang, T., Li, Z. (2011). Reliability evaluation of microgrid with PV-WG hybrid system. *DRPT 2011 - 2011 4th International Conference on Electric Utility Deregulation and Restructuring and Power Technologies*, 1629–1632.

Wu, L., Wen, C., Ren, H. (2017). Reliability evaluation of the solar power system based on the Markov chain method. *International Journal of Energy Research*, *41*(15), 2509–2516.

Xu, H., Su, J., Liu, N., Shi, Y. (2018). A grid-supporting photovoltaic system implemented by a VSG with energy storage. *Energies*, *11*(11), 1–19.

Yang, Y., Bremner, S., Menictas, C., Kay, M. (2018). Battery energy storage system size determination in renewable energy systems: A review. *Renewable and Sustainable Energy Reviews*, *91*, 109–125.

Yap, K. Y., Sarimuthu, C. R., Lim, J. M. Y. (2020). Artificial Intelligence Based MPPT Techniques for Solar Power System: A review. *Journal of Modern Power Systems and Clean Energy*, *8*(6), 1043–1059.

Yuan, X., Xiang, Y., He, Y. (2014). Parameter extraction of solar cell models using mutative-scale parallel chaos optimization algorithm. *Solar Energy*, *108*, 238–251.

## PUBLICATIONS AND WORKS

**Nkuriyingoma, O.**, Özdemir, E., Sezen, S. (2022). Techno-economic analysis of a PV system with a battery energy storage system for small households: A case study in Rwanda. *Frontiers in Energy Research, 10*, 957564.

**Nkuriyingoma, O.,** Özdemir, E. (2023). Reliability analysis of modified RBST BUS-2 distribution networks including solar PV system and BESS. In International Marmara Sciences Congress IMASCON 2023-Autumn (p. 129).

## BIOGRAPHY

Obed NKURIYINGOMA began primary school in 1994. He began his university education at College of Science and Technology, University of Rwanda (Former Kigali Institute of Technology) in 2008. He received bachelor's degree in Electrical Engineering from the faculty of Engineering in 2012. He was admitted to Erciyes University for master education in 2013. His MSc. Thesis was entitled "Solar power plant electricity generation forecasting planning: a case study in Kayseri". He was awarded master's degree in Energy Systems Engineering from the Graduate School of Natural and Applied Sciences in 2018. He was accepted into a doctoral program at Kocaeli University in Energy Systems Engineering and began his studies in September 2019.